Design and Analysis of Linear Quadratic Optimal and Proportional Resonant Controllers for a Single Phase Two Level Pulse Width Modulated Grid Connected Inverters

By

Gussan Maaz Mufti

Reg# NUST2012MS-ESE-60726

Session 2012-14

Supervised by

Asst. Prof. Dr. Adeel Waqas

&

Asst. Prof. Dr. Mohsin Jamil

A Thesis Submitted to the Centre for Energy Systems in partial fulfillment of the requirements for the degree of MASTERS of SCIENCE in ENERGY SYSTEMS ENGINEERING

Centre for Energy Systems (CES)

National University of Sciences and Technology (NUST)

H-12, Islamabad 44000, Pakistan

January 2015

Design and Analysis of Linear Quadratic Optimal and Proportional Resonant Controllers for a Single Phase Two Level Pulse Width Modulated Grid Connected Inverters

By

Gussan Maaz Mufti

Reg# NUST2012MS-ESE-60726

Session 2012-14

Supervised by

Asst. Prof. Dr. Adeel Waqas

&

Asst. Prof. Dr. Mohsin Jamil

A Thesis Submitted to the Centre for Energy Systems in partial fulfillment of the requirements for the degree of MASTERS of SCIENCE in ENERGY SYSTEMS ENGINEERING

Centre for Energy Systems (CES)

National University of Sciences and Technology (NUST)

H-12, Islamabad 44000, Pakistan

January 2015

Certificate

This is to certify that work in this thesis has been carried out by **Mr. Gussan Maaz Mufti** and completed under my supervision in Advance Control Laboratory, Centre for Energy Systems, National University of Sciences and Technology, H-12, Islamabad, Pakistan.

Supervisor: _____

Dr. Adeel Waqas
Centre for Energy Systems
NUST, Islamabad

GEC member # 1: _____

(Co- Supervisor)

Dr. Mohsin Jamil
School of Mechanical and
Mechatronics Engineering
NUST, Islamabad

GEC member # 2: _____

Dr. Syed Omer Gilani
School of Mechanical and
Mechatronics Engineering
NUST, Islamabad

GEC member # 3: _____

Engr. Shahid Hussain Ansari
Centre for Energy Systems
NUST, Islamabad

HoD-CES _____

Dr. Zuhair S Khan
Centre for Energy Systems
NUST, Islamabad

Principal/ Dean _____

Dr. M. Bilal Khan
Centre for Energy Systems
NUST, Islamabad

Dedication

To my family and friends who have been standing with me through thick and thin.

Acknowledgements

To successfully complete the Masters of Science involves the direct and indirect support and help of many people. During my M.Sc. at the Advance Controls Laboratory (ACL), I benefitted from lot of such support and help, which tremendously encouraged me and motivated me in various ways. I am truly indebted to all people who provided me with all this support and helped me during my M.Sc. and in the following; I would try to mention them all, although it is inevitable not to pretermit some of them.

I would like to first express my sincere gratitude to my supervisors, Dr. Adeel Waqas and Dr. Mohsin Jamil for their invaluable help, support and guidance. They were giving me the liberty to take decisions during my research project while guiding me into the right directions. I am extremely blessed to have completed my Master thesis under their supervision, which was a great experience.

I would also like to thank my master's examination committee members, Dr. Syed Omer Gilani and Engr. Shahid Hussain Ansari for their constructive comments and discussions.

I would like to extend my appreciation to all members of the Advance Controls Laboratory who provided an extraordinary, delightful and charming atmosphere, which indeed enormously helped me during my master studies.

I cannot end without thanking my dear family, on whose unconditional love, support and encouragement, I have relied throughout my studies.

Abstract

The conventional generating stations using fossil fuels produce harmful emissions and greenhouse gases. These generating stations are also inefficient, with significant energy lost as heat. Distributed generations, including micro grids using renewable energy sources having inverters as an interfacing device can help to overcome power capacity limitations and reduce greenhouse gas emissions.

This thesis investigates the performance of the current controllers under utility harmonic distortions for a two level Pulse Width Modulated (PWM) grid connected inverters. The research is primarily motivated by the fact that classical controllers fail to perform well under the utility harmonics. The classical controllers failed to limit the Total Harmonic Distortion values according to the ANSI IEEE standard value of 5%. This is because of the inherent limitations of the classical controllers which limit them to provide higher gains at the selected harmonic frequencies.

In order to provide satisfactory performance, according to the standards of ANSI-IEEE under utility harmonic conditions optimal controllers (LQR) and Proportional Resonant (PR) controllers were being investigated. The simulation results show that the designed controllers were able to successfully limit the Total Harmonic Distortion values to 4.96% and 4.51% for Proportional Resonant (PR) controller and Linear Quadratic controller respectively.

Keywords: Grid Connected Inverter, Total Harmonic Distortion, Current Controller, Optimal Controller and LCL filter.

Table of Contents

List of Figures

List of Tables

List of journals/conference papers from this work

Conference Papers

1. **Gussan Maaz Mufti**,Dr. Mohsin Jamil and Dr. Adeel Waqas

Issues Challenges and Solutions for the Energy Crisis of Pakistan.[1]

2015 International Conference on Alternative Energy in Developing Countries and Emerging Economies (2015 AEDCEE), May 28-29, 2015**,** Sheraton Grande Sukhumvit Hotel, Bangkok, Thailand

2. **Gussan Maaz Mufti**,Dr. Mohsin Jamil and Dr. Adeel Waqas

Design and Analysis of Optimal Controllers for Grid Connected Inverters for Photo Voltaic Applications.[2]

2015 International Conference on Alternative Energy in Developing Countries and Emerging Economies (2015 AEDCEE), May 28-29, 2015**,** Sheraton Grande Sukhumvit Hotel, Bangkok, Thailand

[1]Attached as Annexure I.

[2]Attached as Annexure II.

List of Abbreviations

Renewable Energy System (RES)

Grid Connected Inverter (GCI)

Proportional Resonant (PR)

Linear Quadratic Regulator (LQR)

Photo Voltaic (PV)

Total Harmonic Distortion (THD)

Point Of Common Coupling (POCC)

Fast Fourier Transform (FFT)

Static Synchronous Compensator (STATCOM)

Demand Side Management System (DSMS)

Proportional Integral (PI)

Proportional Integral Derivative (PID)

Dynamic Voltage Regulators (DVR)

Unified Power Quality Conditioners (UPQC)

Chapter 1
Introduction

1.1. Motivation and System Description

The increasing industrial development of the world is making the growing demand for energy which gives rise to important problems such as system instability and in many cases the insufficient amount of energy available resulting in power outages. Therefore, there is a general need for increasing production of the energy. The depletion of fossil fuels, the heating losses associated with the systems running on the fossil fuels and their ever increasing costs have forced the authorities to turn towards more sustainable energy resources such as solar, wind and other forms of renewable energy resources. With the protection of the global environment, a growing concern, the need for the production of green energy having no pollution, such as solar energy has attracted wide attention as an alternative source for the future energy since it is clean, environmentally friendly and also inexhaustible. A number of incentives in this regard are being offered by some governments as well as world organizations to increase the trend of renewable energy. The high up front cost of the renewable energy systems, though, remains the main hurdle in its widespread.

1.2. Grid Connected Systems

There are basically two modes of operation for the renewable energy setups. They can either be stand-alone systems or grid connected systems. Stand-alone systems are mostly used to provide energy to the remote areas which are isolated from the main grid and the connecting them to the grid in the form of transmission lines is cost ineffective. The other widely operated scheme is grid connected systems. In this type renewable energy systems work in combination with existing electrical networks. However, their requirements vary and depend upon the standard being followed by the utility. These standards are followed to ensure the safety of both the user as well the utility. The technical requirements like grid interconnection, total harmonic distortion levels and electromagnetic interferences are thus needed to be taken care off before installing a grid connected system. The various factors affecting the energy production from grid tied or grid connected system are geographical location of the installed system, the system designing, the surroundings and the quality of the components being used. The classification of the components thus plays an important role [1] on deciding the components used [2]–[4].

In the analysis of the grid connected systems, utility supply is considered to be producing a pure sinusoidal waveform without any distortions. However, the operation of the renewable energy system is affected due to any distortion related to the Point Of Common Coupling (POCC)[5][6].

Several hybrid renewable energy systems are also getting popularity and many different optimization techniques for these hybrid renewable energy systems have also been developed[7]–[9]. Figure 1.1 shows the block diagram representation of the commonly used renewable energy systems, whereas figure 2.2 represents the grid connected renewable energy system.

The pivotal component of the system is inverter which converts the D.C. power produced by renewable systems to A.C. A safe and reliable operation of the inverter would in turn ensure the constant and reliable power production. Research is being done on the control strategies of inverters to further improve its operation. The operation of the inverter depends upon the frequency and voltage of the grid. The more efficient the operation of the inverter the better the power produced having minimum losses and low total harmonic distortion. There are still challenges that needs to be addressed [9], [10], [11].

However some recent semi-conductor technologies and the ever growing demand of inverters in the Renewable Energy Systems (RES) have diversified their applications [13]–[17]. Due to the unpredictable nature of the RES most of the systems are being provided by energy storage devices most commonly in the form of Lead acid batteries.

1.3. Solar Photo Voltaic Systems

Solar Photo Voltaic (PV) has been a major portion in the energy mix of European nations for over a decade. Italy, Greece and Germany meet more than 5 percent of the annual electricity generated by solar PV but most of the European countries have reached their peaks for the production of the solar PV. Asian countries on the other hand have started investing in solar PV. A total of 36.9 GW of solar capacity of the whole world was added in 2013 in which china's share was 31 percent.

In 2011, after the nuclear disaster in Fukushima, Japan, the emphasis has shifted to the development of solar PV projects. According to estimates, Japan would install 9 GW of solar power by 2014.

Most of the PV systems are first being simulated which gives the designer the liberty

to study the PV system under different load characteristics, simulate the real time conditions, employ different experimentations and estimate the financial aspects of the system[18].

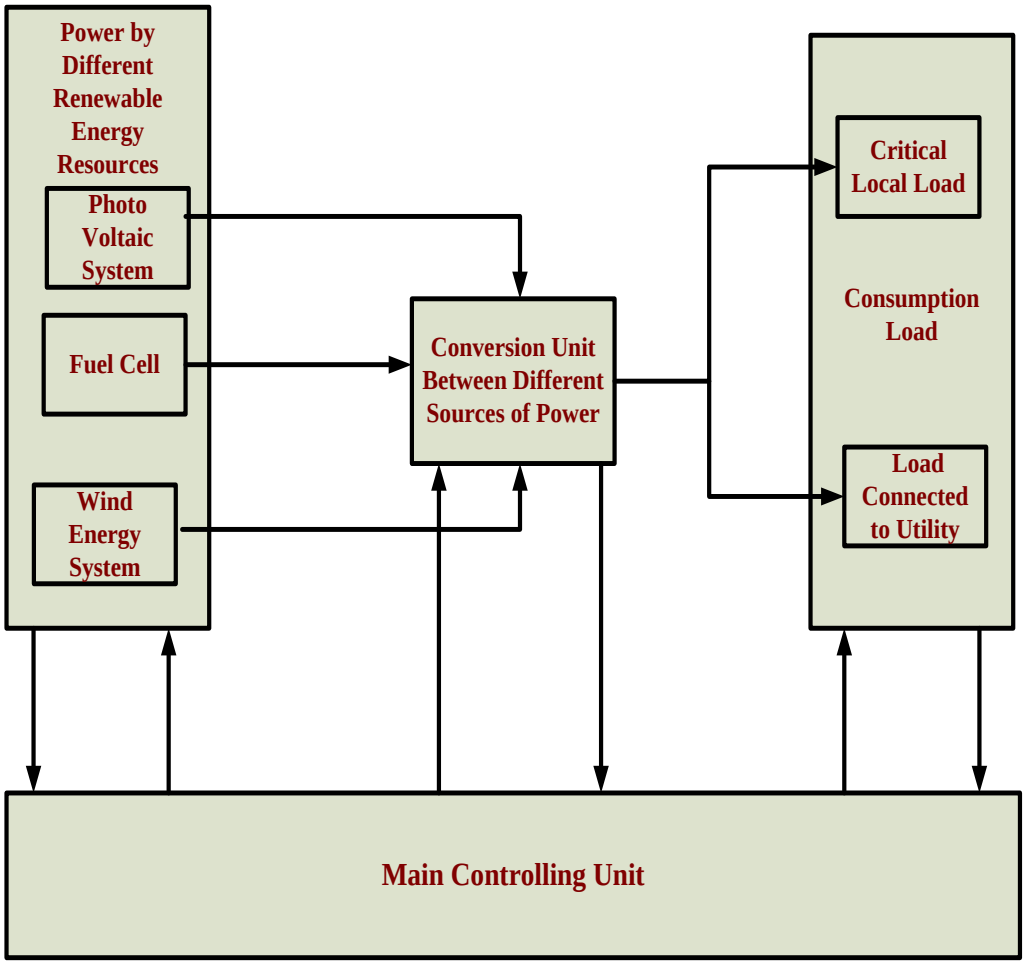

Figure 1.1. Block diagram representation of the Renewable Energy System

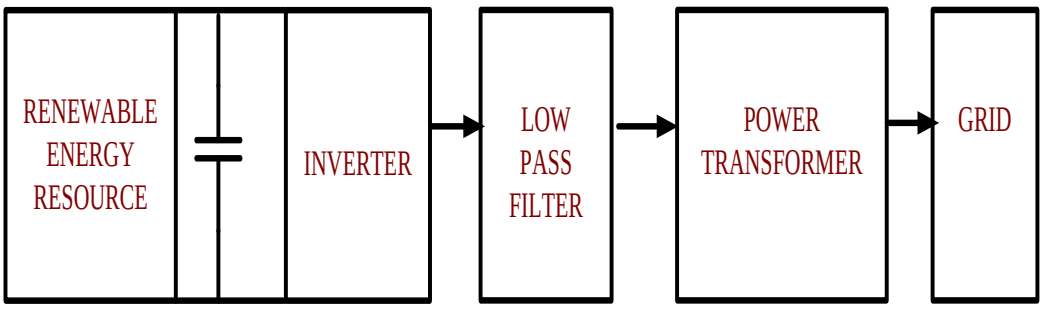

Figure 1.2. Block diagram representation of the Grid tied system

Most of the PV systems are first being simulated which gives the designer the liberty to study the PV system under different load characteristics, simulate the real time conditions, employ different experimentations and estimate the financial aspects of the system[18].

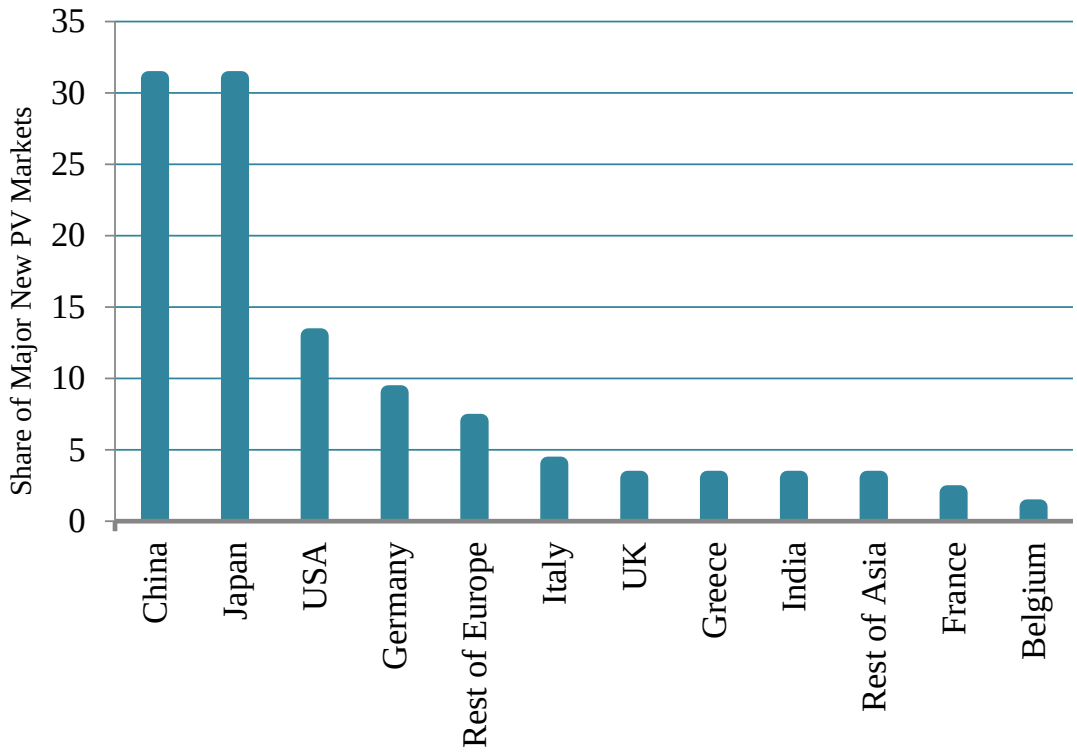

Figure 1.3. Share of major PV markets for new installations in 2013 [1]

1.4. Problem Description

Harmonics are part and parcel of power systems since the inception of non-linear load because most of these loads produce harmonics. Potential sources of these harmonics are; switched mode power supplies, current regulators, frequency converters, inverters with pulse width modulated converters, low power consumption lights, electrical arc-furnaces and induction motors with irregular magnetizing current associated with saturation of the iron etc.

Importantly, the power quality is assessed by the amount of harmonic distortion. Generally, to quantify this distortion, Total Harmonic Distortion (THD) is obtained which represents the distortion as a percentage of the fundamental frequency (pure sine) of voltage and current waveforms. These harmonics present in the main supply are a problem because they may cause increased losses in the utility power system equipment of customers. The problem is even worse for transformers because the saturated transformer can produce high current harmonics.

The power quality, importance increases in Renewable Energy Systems (RES) especially PhotoVoltaic (PV) systems. The increase in the number of the Photovoltaic systems connected to the grid has increased the importance for the implementation of a unified standard for these installations. In this regard, the standards followed are IEEE 1547 and IEEE929 along with IEC 612727.According

to these standards, the overall allowable limit of the Total Harmonic Distortion (THD) is 5%. The odd harmonics from 3rd to 9th should be under 4% each and allowable limit of the odd harmonics from 11th to 15th must be 2%. Another requirement for the reliable operation of the Photovoltaic system has been stated that the average lagging power factor of the operating PV system must be 0.9 when the output power has a value greater than 50% of the rated power.

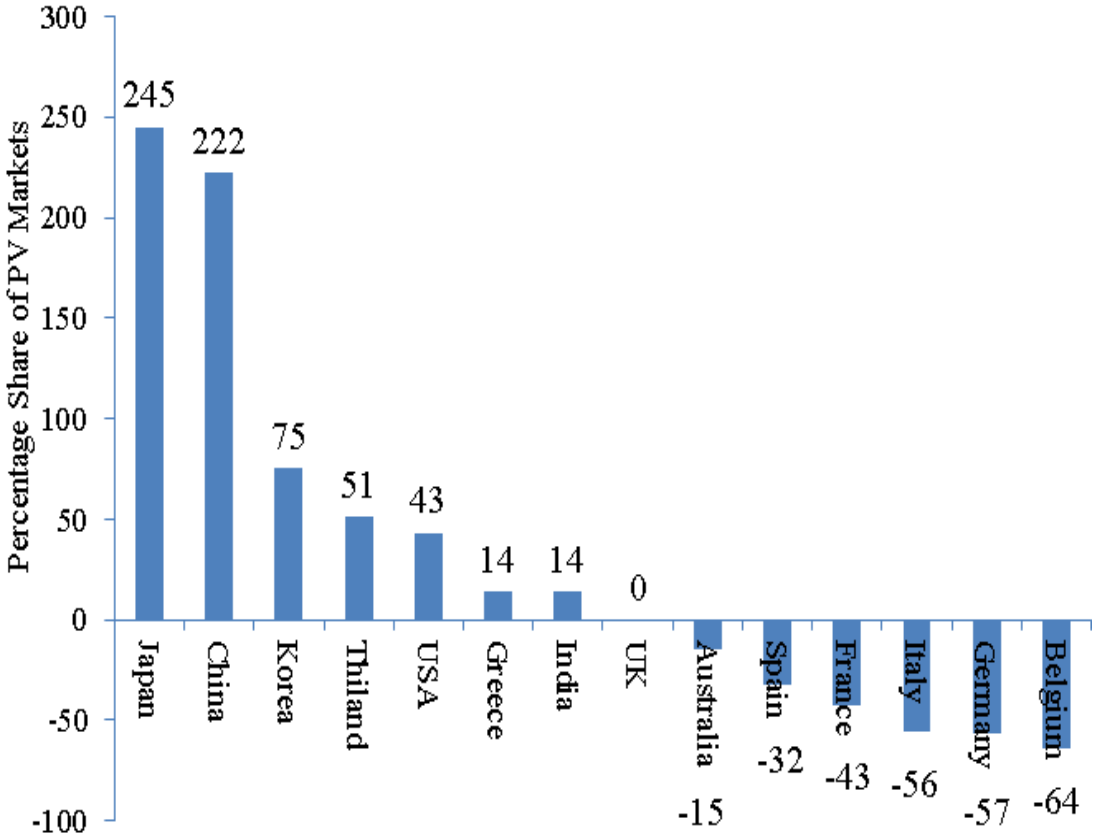

Figure 1.4. PV markets growth in 2013[1]

These standards present a challenge to the design engineers to develop current control systems that is able to not only meet these requirements, but is also capable of rejection of the grid variation in order to ensure a reliable operation of the installed PV system according to the prescribed standards of IEEE. Figure 1.5 shows a sinusoidal waveform with the fundamental frequency of 50 Hz and a distorted wave. The distortions of 3rd harmonics, 5th harmonics and 7th harmonics have been included in the sinusoidal waveform. As seen from the figure that the presence of harmonics can result in a reduction of the power quality as seen from figure. The conventional controllers fail to mitigate the harmonics and thus there rises a need to adopt advance current controllers that can effectively remove the harmonics.

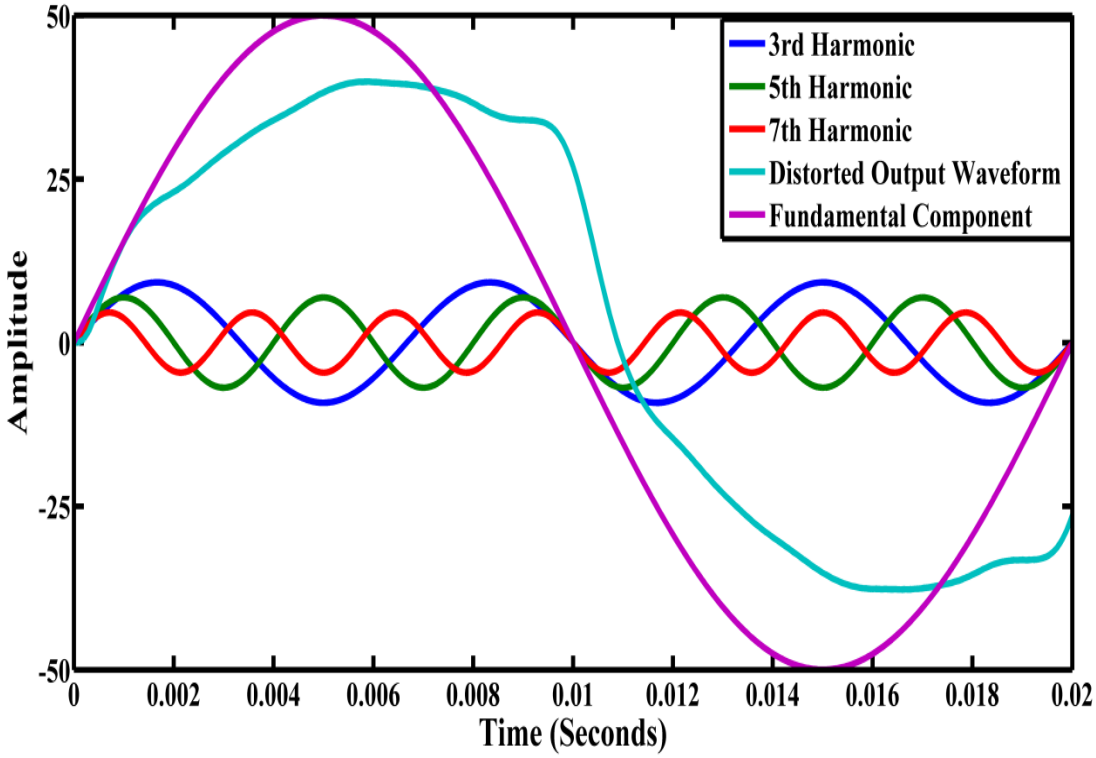

Figure 1.5. Current Waveform under Harmonics

1.5. Objectives

- Develop a linear transfer function model for the computer simulation of a two level grid connected inverter using Matlab Simulink.
- Investigate the effect of the gain by root locus plots on the open loop response of the linear transfer function model and find the stability constraints for the selected values of the LCL filter.
- Investigate the performance of the classical controllers P/PI/PID in terms of steady state error, robustness and performance under high utility harmonics of the simulation model developed.
- Design and analyze optimal control schemes (LQR) and Proportional Resonant (PR) and analyze their performance under high utility harmonics.
- Investigate the performance of the PR controller and tradeoffs between stability constraints and high harmonic compensation.

1.6. Thesis Organization

Chapter 2 presents the literature review of the different control schemes of the grid connected inverters. Different control schemes are critically reviewed and their limitations are discussed in context to the available controllers. A brief overview to the challenging power quality issues are also being discussed with special focus given to the effects of the Total Harmonic Distortion (THD).

Chapter 3 derives the Matlab/Simulink model that is used to analyze the performance of the current controllers and a subsequent single phase equivalent model is derived. The model and the transfer function developed is used to analyze the performance of the voltage source grid connected inverter.

Chapter 4 investigates the design and analysis of the classical controllers P/PI/PID for a two level voltage source grid connected inverter connected via LCL filter. The performance of the designed controllers was analyzed in terms of the step responses, robustness by changing the LCL filter parameters and effects on the system by changing the utility impedance. A further investigation was performed by analyzing the frequency spectrum of the designed current controllers under high utility harmonics.

Chapter 5 discusses the design and analysis of optimal controllers (LQR) and Proportional Resonant controllers and their performance under high utility harmonics. The frequency spectrum analysis was analyzed and compared to the classical controllers. It also presents the conclusion of the research work and the future recommendations.

References

[1] M. a. Eltawil and Z. Zhao, “Grid-connected photovoltaic power systems: Technical and potential problems—A review,” *Renew. Sustain. Energy Rev.*, vol. 14, no. 1, pp. 112–129, Jan. 2013.

[2] H. Keyhani, M. Johnson, and H. a. Toliyat, “A soft-switched highly reliable grid-tied inverter for PV applications,” *2014 IEEE Appl. Power Electron. Conf. Expo. - APEC 2014*, pp. 1725–1732, Mar. 2014.

[3] T. G. Module, “Design and Implementation of Three-Phase Integrated Converter,” vol. 29, no. 8, pp. 3881–3892, 2014.

[4] E. . Spooner and G. Harbidge, “Review of international standards for grid connected photovoltaic systems,” *Renew. Energy*, vol. 22, no. 1–3, pp. 235–239, Jan. 2001.

[5] G. Inverters, H. Wang, F. Blaabjerg, D. Wang, S. Member, and B. Zhang, “Frequency Adaptive Selective Harmonic Control for Inverters,” vol. 8993, no. c, pp. 1–13, 2014.

[6] J. Wiley, “Photovoltaic Inverters and its applications,” no. June, pp. 300–309, 1999.

[7] B. S. Borowy and Z. M. Salameh, “Methodology for optimally sizing the combination of a battery bank and PV array in a wind/PV hybrid system,” *IEEE Trans. Energy Convers.*, vol. 11, no. 2, pp. 367–375, Jun. 1996.

[8] W. Kellogg, G. Venkataramanan, and V. Gerez, “generating system,” vol. 39, pp. 35–38, 1996.

[9] S. H. Karaki, R. B. Chedid, and R. Ramadan, “Probabilistic performance assessment of autonomous solar-wind energy conversion systems,” *IEEE Trans. Energy Convers.*, vol. 14, no. 3, pp. 766–772, 1999.

[10] A. B. Maish, C. Atcitty, S. Hester, D. Greenberg, D. Osborn, D. Collier, and M. Brine, “Photovoltaic system reliability,” *Conf. Rec. Twenty Sixth IEEE Photovolt. Spec. Conf. - 1997*, vol. 3, pp. 1049–1054, 1997.

[11] Preglej.A. and Begovic.M, “Impact Of Inverter Configuration On Pv System Reliability,” *Conf. Rec. IEEE Photovolt. Spec. Conf.* pp. 1388–1391,2002

[12] S. Issue, “Millennium Special Issue,” vol. 126, no. June 1999, pp. 113–126, 2000.

[13] L. M. Tolbert and F. Hall, “Multilevel Converters as a Utility In ’ terface for Renewable Energy Systems,” vol. 00, no. c, pp. 1271–1274, 2009.

[14] H. Ertl, J. W. Kolar, and F. C. Zach, “A novel multicell DC-AC converter for applications in renewable energy systems,” *IEEE Trans. Ind. Electron.*, vol. 49, no. 5, pp. 1048–1057, Oct. 2002.

[15] J. M. Carrasco, L. G. Franquelo, J. T. Bialasiewicz, S. Member, E. Galván, R. C. P. Guisado, S. Member, M. Ángeles, M. Prats, J. I. León, and N. Moreno-alfonso, “Power-Electronic Systems for the Grid Integration of Renewable Energy Sources : A Survey,” vol. 53, no. 4, pp. 1002–1016, 2006.

[16] S. Alepuz, S. Busquets-monge, S. Member, J. Bordonau, J. Gago, D. González, and J. Balcells, “Interfacing Renewable Energy Sources to the Utility Grid Using a Three-Level Inverter,” vol. 53, no. 5, pp. 1504–1511, 2006.

[17] G. M. Martins, J. A. Pomilio, S. Member, S. Buso, and G. Spiazzi, “Three-Phase Low-Frequency Commutation Inverter for Renewable Energy Systems,” vol. 53, no. 5, pp. 1522–1528, 2006.

[18] A. Trejos, D. Gonzalez, and C. A. Ramos-Paja, “Modeling of Step-up Grid-Connected Photovoltaic Systems for Control Purposes,” *Energies*, vol. 5, no. 12, pp. 1900–1926, Jun. 2012.

[19] P. Thummala, Z. Zhang, M. A. E. Andersen, and D.-K. Lyngby, “Design of a High Voltage Bidirectional DC-DC Converter for Driving Capacitive Incremental Actuators Usable in Electric Vehicles (EVs),” 2014.

[20] P. Thummala, S. M. Ieee, H. Schneider, and Z. Zhang, “Efficiency Optimization by Considering the High Voltage Flyback Transformer Parasitics using an Automatic Winding Layout Technique,” vol. 8993, no. c, 2014.

[21] K. Zhou, Y. Yang, F. Blaabjerg, W. Lu, and D. Wang, “Selective Harmonic Control for Power Converters,” no. 2, pp. 4–8, 2014.

[22] S. Member, F. Blaabjerg, H. Wang, S. Member, P. D. P. Rimmen, and I. Engineering, “Special Issue on Robust Design and Reliability in Power Electronics , 2015 Reliability Oriented Design Tool For the New Generation of Grid Connected PV - Inverters,” pp. 1–22, 2015.

[23] N. Sintamarean, S. Member, and F. Blaabjerg, “Real Field Mission Profile Oriented Design of a SiC-Based PV-Inverter Application,” vol. 50, no. 6, pp. 4082–4089, 2014.

[24] Y. P. Siwakoti, P. C. Loh, F. Blaabjerg, and G. E. Town, “Magnetically coupled high-gain Y-source isolated DC / DC converter,” no. April, pp. 2817–2824, 2014.

[25] Y. P. Siwakoti, P. C. Loh, F. Blaabjerg, S. J. Andreasen, and G. E. Town, “Y - Source Boost DC / DC Converter for Distributed Generation,” no. c, 2014.

[26] Y. P. Siwakoti, S. Member, F. Z. Peng, F. Blaabjerg, P. C. Loh, S. Member, G. E. Town, and S. Yang, "Impedance-Source Networks for Electric Power Conversion Part II : Review of Control and Modulation Techniques," vol. 30, no. 4, pp. 1887–1906, 2015.

[27] R. Beres, X. Wang, F. Blaabjerg, C. L. Bak, and M. Liserre, "Comparative analysis of the selective resonant LCL and LCL plus trap filters," pp. 740–747, 2014.

[28] X. Wang, M. Liserre, H. S. H. Chung, W. Wu, Y. Sun, M. Huang, H. Wang, and F. Blaabjerg, "A Robust Passive Damping Method for LLCL -Filter-Based Grid-Tied Inverters to Minimize," vol. 29, no. 7, pp. 3279–3289, 2014.

[29] S. Chen, X. Wang, C. Su, and Z. Chen, "An Improved Power Flow Method Based on Extended Chain-table Storage Structure for Distribution Network with PV Nodes," pp. 892–896, 2014.

[30] P. Chioncel, E. Spunei, and C. P. Chioncel, "Calculation of Control Circuits in Frequency Domain using Scilab Environment," no. 3, pp. 303–308, 2014.

[31] I. U. Nutkani, P. C. Loh, and F. Blaabjerg, "Cost-based droop scheme with lower generation costs for microgrids," no. April 2013, pp. 1171–1180, 2014.

[32] X. Wang and P. C. Loh, "Design-Oriented Analysis of Resonance Damping and Harmonic Compensation for LCL-Filtered Voltage Source Converters," pp. 216–223, 2014.

[33] J. Kwon, X. Wang, and F. Blaabjerg, "Impedance Based Analysis and Design of Harmonic Resonant Controller for a Wide Range of Grid Impedance," 2014.

[34] I. Ullah, P. Chiang, P. Wang, T. King, and F. Blaabjerg, "Electrical Power and Energy Systems Intertied ac – ac microgrids with autonomous power import and export," *Int. J. Electr. POWER ENERGY Syst.*, vol. 65, pp. 385–393, 2015.

[35] R. Peña-alzola, M. Liserre, F. Blaabjerg, M. Ordonez, and A. Grid-connected, "LCL -Filter Design for Robust Active Damping in Grid-Connected Converters," vol. 10, no. 4, pp. 2192–2203, 2014.

Chapter 2

Literature Review

2.1. International Standards for the Grid Interconnection

With the increase in the development of renewable energy systems and PV in particular the size of the systems installed is rapidly increasing. To ensure the reliable and safe operation of the grid connected PV systems, it is important that the systems installed follow the grid interconnection codes.

The codes may vary from region to region, but an effort is put to come up with unified standards that are applicable and followed worldwide. Some of the organizations formulating the grid codes are in the following table

Table 2.1. Official Bodies for Making Grid Codes

S.No.	Name of the body	Abbreviation meaning	Country
1.	IEEE	Institute of Electrical and Electronics Engineering	U.S.A.
2.	DKE	German commission for Electrical, Electronic and Information technology	Germany
3.	IEC	International Electro technical Commission	France

These rules and regulations greatly impact the PV products that are being produced in the regions specified. The PV industry thus reflects back the grid codes that are prevalent in a particular region and worldwide in particular.

This chapter thus introduces the requirements of the grid connected system in the form of different international codes. It is tried that first important and standard regulations are discussed. Next associated grid connections are discussed with a comparison of the different standards is done.

2.2. Introduction to IEC 61000

IEC 61000-3-12 is for the systems with the equipment's having currents higher than 16 A and lower than 75 A. Currents having values lower than 16 A is dealt with IEC 61000-3-2. It also deals with the harmonic currents of both the input current of the equipment tested as well as the harmonic current injected to the grid. The voltage fluctuations are addressed by IEC 61000-3-11 having testing equipment current greater than 16 A and less than 75 A. IEC 61000-3-3 is for the testing equipment that

has phase current less than 16 A or is equal to 16 A, primarily in the low distribution network.

2.3. Codes for the Abnormal Grid conditions

The system reliability and safety depend upon the disconnection of the PV inverters when an abnormal grid condition arises. It is therefore important that the grid disconnects itself before some damage is reflected back to the total system. This also ensures the safety of the personnel doing the maintenance.

The time in the table gives the disconnection time defined as the time interval between the occurrence of the abnormal/faulty condition of the grid and the time the inverter ceases to power the line. The inverter actually remains connected to the line and does not disconnect completely from the grid. This allows the inverter to sense the prevailing conditions of the grid and reconnects/powers the line as soon as the conditions for the reconnection are satisfied. These conditions vary for different standards are given in the table by the name of trip reconnection conditions. IEC-61727 ensures that an extra delay is given to ensure that the grid is resynchronized before reconnection.

The delay time also ensures that the small disturbances in the grid are ignored and the grid always disconnects to ensure the safety of the equipment. The value of the voltage is the value of the nominal system (local) voltage. Their values are Root Mean Square values. They are measured at the common point of connection where the grid connects to the utility. The low frequency values for VDE 0126-1-1 require synchronization in the form of adaptive frequency as compared to the other two standards.

2.4. Codes for Anti islanding:

Islanding in grid connected PV systems is defined as the condition in which the grid trips but the inverters continue to supply power to the local loads that are connected to it. It is one of the most important conditions and poses a security threat to the maintenance staff that thinks that the line is not active. Therefore, for the safety measures it is ensured that the same standards are defined.

In IEEE 1547 an islanding in which is unintentional should disconnect the grid within 2 sec. The U.S. standard UL 1741 also follows the same criteria as IEEE 1547. This standard is much easier to achieve and measurable as compared to IEEE 929-2000.

The trip time in IEC 61727 is same as of IEEE 1547. No special anti-islanding requirements are stated in IEC 61727 but a reference to IEC 62116 is given.

Table 2.2. Comparison of Grid Codes

S. No.	Parameter	IEEE 1547		IEC 61727		VDE 0126-1-1	
		Values	Time in sec	Values	Time in sec	Values	Time in sec
1.	Voltage Variation	V<50 (%)	0.16	V<50 (%)	0.10	110<= V<85 (%)	0.2
		50<=V <88 (%)	2.00	50<=V<85 (%)	2.00	N/A	N/A
		110<V <120 (%)	1.00	110<V<135 (%)	2.00	N/A	N/A
		V>120 (%)	0.16	V>=135(%)	0.05	N/A	N/A
2.	Frequency Variation	59.3< f <60.5 (Hz)	0.16	$f_n - 1 < f < f_n + 1$ (Hz)	0.2	47.5< f <50.2	0.2
3.	Trip Reconnection conditions	88<V< 110(%) & 59.3< f <60.5 (Hz)		88<V<110 (%) & $f_n - 1 < f < f_n + 1$ (Hz) & Delay of three minutes		N/A	N/A

2.5. Codes for the Power Quality

Power quality is determined by the different parameters like voltage, frequency and current harmonics. The power quality standards ensures that the power fed to the grid are according to the international standards and failing to meet those imply that the power is cut off until its quality is improved again.

The renewable sources produce D.C. that are rectified to A.C. are fed to the grid. The power fed to the grid must contain a small portion of D.C. otherwise it would result in the overheating of the transformer due to the saturation. The D.C. current injection was not a big problem in the traditional PV systems due to the galvanic isolation, but the modern systems with the transformer less inverters have increased this problem.

The table gives the acceptable limits of the D.C. currents. IEEE 1547 and IEC 61727 does not require a tripping time. They can be measured by Fourier transforms. A trip time is required for VDE 0126-1-1 and it requires special current sensors that disconnect the system within the time limit.

Table 2.3. D.C. Current Injection Standards

S.N.	Parameter	IEEE 1547	IEC 61727	VDE 0126-1-1
1.	D.C. Current Injection	Idc < 0.5(%) of the Root Mean Square Values of the rated current	Idc < 1(%) of the Root Mean Square of the rated current	Idc < 1A with the trip time having a maximum value of 0.2 sec
2.	Average Power Factor	No requirement	Inverter having power factor greater than 0.9 lagging for output greater than 50 %	No requirement

PV inverters are designed for a good power factor they usually operate near the ideal power factor of unity. IEEE 1547 and VE 0126-1-1 have no requirement in this regard. The power factor for the inverter is only required in IEC 61727.

The current harmonics also determine the quality of the power that is fed to the grid. It is ensured that the current harmonics are limited to a minimum level so that it does not damage the system and equipment that are connected with the system. The current harmonics are specified for IEEE 1547 and IEC 61727. Even harmonics should be less than 25% of the odd harmonics and the total harmonic distortions should be 5%. The table gives the odd harmonic order for the IEEE 1547 and IEC 61727.

Table 2.4. Harmonics Limits for IEEE 1547 and IEC 61727

S.No.	Odd Harmonics	Limits in IEEE 1547 and IEC 61727
1.	n < 11	4 %
2.	11 <= n < 17	2 %
3.	17 <= n < 23	1.5 %
4.	23 <= n < 35	0.6 %
5.	35 <= n	0.3 %

2.6. Control Structures of Renewable Energy Systems:

Increased use of renewable energy sources connected to the grid has a direct impact on the power quality of the grid. The system network operator controls the power flow running on the systems. In case of a running maintenance in a system, the dispatched generation to other systems can be reduced to meet the power requirements of the local system. Similarly, the operator can increase the outflow power to other systems if the power generated in the local system is lower than the load of the system [1].The control system forms an integral part of the renewable energy system[2]–[4]. The control of the renewable energy system has two main parts. The grid side control and the input power control. The grid side control mainly handles the power flow and its control from the grid side. It may include control of active and reactive power, synchronizing the grid and quality of the power. The input power control ensures that maximum power is extracted from the renewable energy systems, keeping in view the safety and reliability of the whole system. Figure 2.1 shows the block diagram for the control of the renewable energy systems.

The most common control scheme that is applied to control the converter of the grid side in the renewable energy systems has two interlinked control loop [5]–[10]. The inner current loop has a faster response and it controls the grid current. It is the main loop for the quality of power that is fed to the utility. It also ensures the protection of the equipment by controlling the current. The external voltage loop is responsible for controlling the voltage across the capacitor that serves as the D.C. link. One of the main aims of this loop design is to ensure the system stability, which is achieved by keeping its dynamics slow. Several different control strategies for the renewable energy systems are also available. Instead of having an inner current loop, there can be a power loop[11]. This power loop ensures an indirect control of current. The opposite of this control scheme is also available in which there is an inner current loop linked with an outer power loop[12].

A classification of the various control structures is made depending upon the reference frames in which they are implemented.

2.6.1. Synchronous Reference Frame Control

The dq control is shown in Figure 2.3.This frame uses abc to dq transformation block to change the main as well as the reference values of the voltages to the values that are synchronously rotating. The rotating frequency is equal to the frequency of the generator. This converts the control variables to the D.C. values that are

synchronously rotating which enable both easier controls as well as the implementation. The filtering can also be easily achieved by employing this technique.

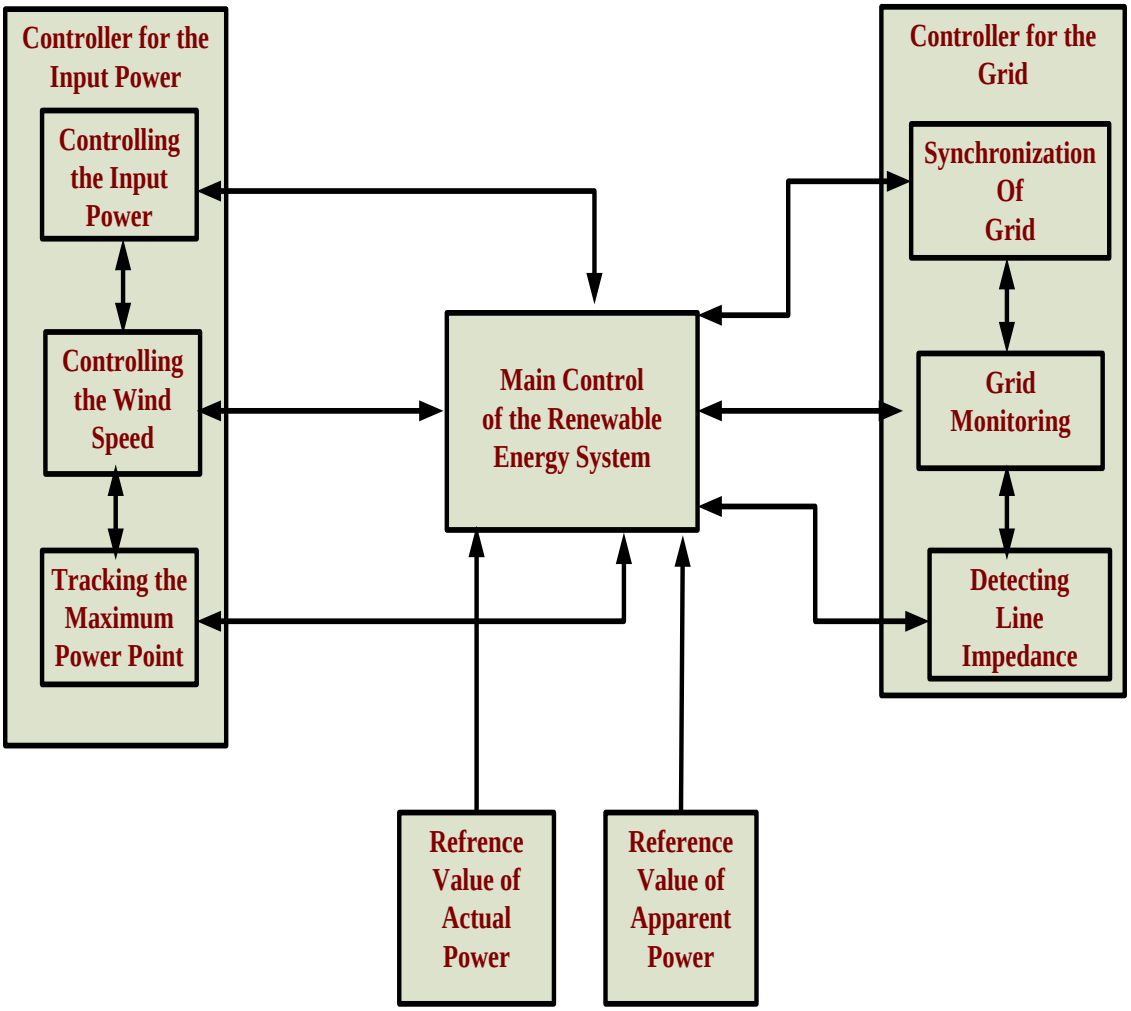

Figure 2.1. Block Diagram of the Control Structure of the Renewable Energy System

In this type of control the link voltage is varied according to the output power which is required. Its output is fed as a reference value to the current controller associated with the active component. The control of the reactive component of the current can also be done by associating a suitable reference value.

Proportional integral controllers are used with the dq control as they have shown good performance. The transfer function of the proportional integral controllers in dq control is given by equation 2.1. where K_p and K_i stands for the proportional and integral gain for the controller respectively. The phase lock loop gives the phase of the grid system and they are necessary to keep the controlling current synchronized with the whole system. Another technique is to filter the grid voltages and then use

an inverse tangent function which also gives the phase angle of the grid [13]–[15].However, phase locked loop is the technique that is mostly employed.

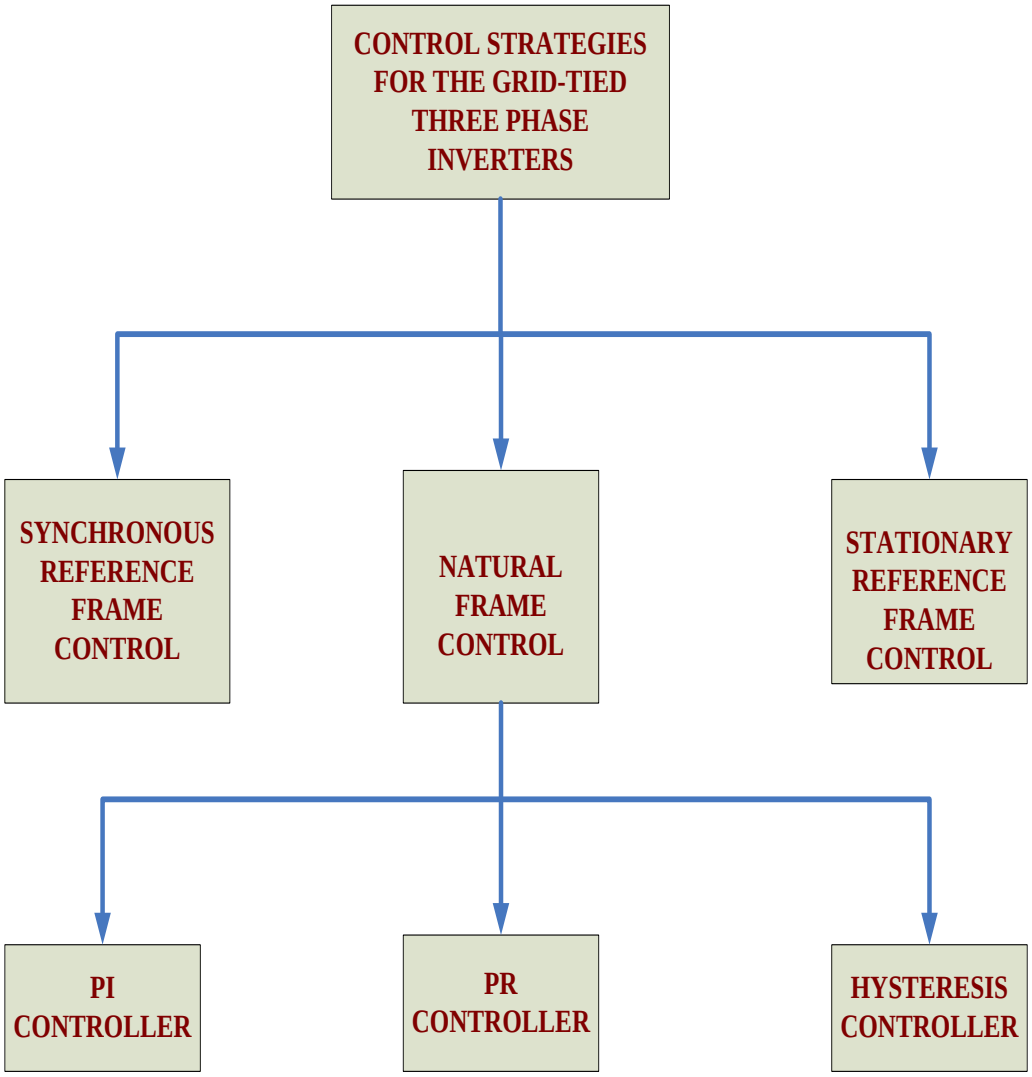

Figure 2.2. Control Strategies of Three Phase Grid Tied Inverters

$$G_{PI(dq)}(s) = \begin{pmatrix} K_p + \frac{K_i}{s} & 0 \\ 0 & K_p + \frac{K_i}{s} \end{pmatrix} \qquad (2.1)$$

The performance of the PI controllers could be improved by using voltage feed forward [10], [16]–[18]. One of their major drawbacks arises when dealing with harmonics of low order. They are unable to mitigate the harmonics of low order and thus fail to produce output according to prescribed limits of IEEE. Some of their drawbacks however are being addressed by using stationary frame of reference as compared to synchronous frame.

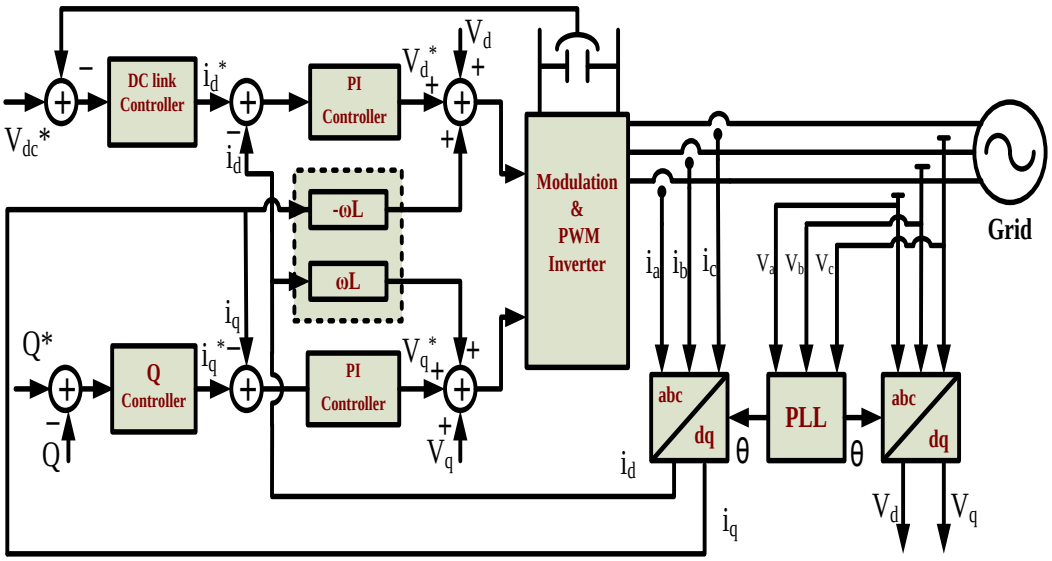

Figure 2.3. Equivalent Structure for Synchronous Reference Frame Control

2.6.2. Stationary Reference Frame Control

For stationary reference control scheme, three phase grid currents are converted to the stationary frame by using abc to alpha beta transformation. The implementation of the PI controller in this case is not suitable because of the inherit inability of the PI controller to remove the steady state error. The Proportional Resonant controllers have become a popular choice in the last years for the grid connected systems[19]–[22].

The proportional resonant controllers have a high gain at the natural resonant frequency which is given by

$$G(s) = K_{p+}\frac{K_i s}{s^2 + w^2} \tag{2.2}$$

Where

w = Resonant frequency of the proportional resonant controller.

K_p =Proportional gain of the proportional resonant controller.

K_i = Integral gain of the proportional resonant controller.

The transfer function for the proportional resonant controllers in *dq* control is given

$$G_{PR(\alpha\beta)}(s) = \begin{pmatrix} K_p + \frac{K_i s}{s^2 + w^2} & 0 \\ 0 & K_p + \frac{K_i s}{s^2 + w^2} \end{pmatrix} \tag{2.3}$$

They are widely used in the *abc* reference frame such that the control variables are

sinusoidal [19],[23]. As it has very high frequency at the resonant frequency, it can neglect the static error between the desired value and the controlled signal.

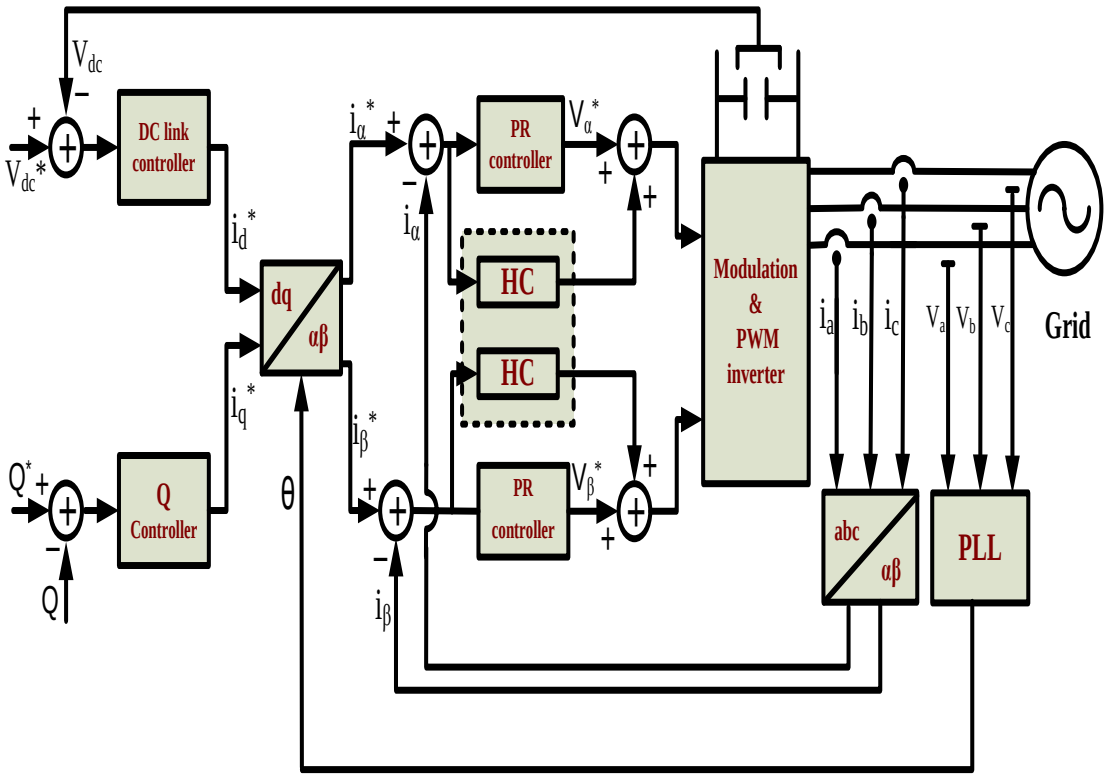

Figure 2.4. Equivalent Structure for Stationary Reference Frame Control

A Lower K_i can result in a narrow band, and higher K_i causes higher band. Harmonic compensation of proportional resonant controller can be achieved by cascading many generalized integrators that are set to achieve resonance at a certain frequency. In this way certain frequencies are compensated. Typically, harmonic compensators are introduced for the odd harmonics[24][25]. The transfer function is

$$G_{harmonic}(s) = \sum_{h=3,5,7} K_{i(h)} \left(\frac{s}{s^2 + (hw)^2} \right) \qquad (2.4)$$

2.6.3. Natural Frame Control

In natural frame control each current is treated differently and a controller is designed for each current. Thus, for a three phase circuit each phase has an individual controller. The controller design varies as there are numerous ways to connect a three phase circuit, e.g. a three phase system can be star connected or delta connected. Therefore the circuit connections play a pivotal role in designing a controller. The design is however getting simpler for an isolated neutral system in which the design is restricted to only two controllers, as the third current can be

computed by Kirchhoff current law. The three independent controllers can be designed if the design considerations are considered independently. *abc* frame is used with the nonlinear controllers. The aggressive performance of the nonlinear controllers is the reason behind their usage in this frame. Sampling frequency greatly affects the *p*erformance of these controllers. The greater the sampling frequency the better is the performance of the controllers. It was due to this fact that these controllers failed to perform well in the past and were not generally implemented. The advancements in the digital signal processors and the inclusion of other devices such as programmable logic array have proved to be highly beneficial for these controllers.

The following controllers can be used with abc frame control.

2.6.3.1. PI Controller:

PI controllers are mostly used with *dq* control. However, they could also be used and implemented in *abc* frame[16].Due to many non-diagonal terms the complexity of the control matrix is increased immensely.

2.6.3.2. 4.3.2. PR Controller:

The implementation of Proportional Resonant controller becomes easier because it is in stationary frame and it could be implemented by three controllers. Only two controllers are required if the three phase circuit has an isolated neutral. The complexity of the controller is much less as compared to PI controllers.

2.6.3.3. Hysteresis Controller:

The hysteresis controller implementation requires a controller having an adaptive band, so that it can have a fixed frequency. Many methods exist for obtaining a fixed frequency[26]–[29]. The circuit hierarchy also has the effect on the controller design. An a term was introduced in [27].A similar approach was also found in [30].

The implementation for the *abc* control is shown in Figure 18. The transfer function for the proportional resonant controllers in *abc* control is given by equation 2.5.

The phase angle φ is provided by the help of phase locked loop. The active current reference values are generated with the help of monitoring the output of the voltage of the d.c. link. This helps to create the three reference currents. These reference currents are then compared to the actual values and the error values are obtained. The error values are fed to the controller. The controller changes the switching values of the power converters accordingly. The requirement of the modulators depends upon the type of the controller which is used. For dead beat and hysteresis controller, the

For Proportional integral controllers and proportional resonant controllers modulators are required as they vary the PWM switching functions by having different duty cycles.

$$G_{PR(\mathrm{abc})}(\mathrm{s}) = \begin{pmatrix} K_p + \dfrac{K_i s}{s^2 + w^2} & 0 & 0 \\ 0 & K_p + \dfrac{K_i s}{s^2 + w^2} & 0 \\ 0 & 0 & K_p + \dfrac{K_i s}{s^2 + w^2} \end{pmatrix} \tag{2.5}$$

2.7. Power Quality Issues of PV Systems

Power quality issues can be broadly classified into two types that is, quality issues arising from the utility side and quality issues arising from the consumer's side. Installing line conditioning systems by the utilities that suppress or counteracts the power system disturbances helps to address the power quality issues arising from the utility side. Load conditioning from the consumer's side by having equipment that are less sensitive to power disturbances, which can even operate under significant voltage distortions, helps to mitigate problems arising from the consumer side[31].

The main issues of the power quality in a grid connected networks are voltage fluctuations, frequency fluctuations and phase synchronization issues etc. These issues are being discussed and a solution to these problems is also being presented at the end of this section.

2.7.1. Intermittent Effect of PV Systems:

The intermittent nature of the solar energy systems has an impact on the power quality of the network. An accurate forecasting and planning of solar radiations helps to rectify this problem and bring more predictability in the amount of the power that is produced by the renewable energy systems. Several statistical forecasting and regression analysis methods and algorithms are being used for weather pattern forecasting. These method help to forecast wind speeds and solar radiation that helps to make future decisions and planning [32].

Different models for weather forecasting have different strengths and weaknesses. Therefore a combination of these weather models are used that help to improve the accuracy of weather forecasts thus enhancing the accuracy of the forecasted conditions[33].

2.7.2. Voltage Variations:

Voltage variations may be due to the differences in irregular solar radiation and wind speeds with time. These intermittent nature of solar and wind energy systems can cause variations in the voltage due to the sudden changes in the reactive power. The characteristic of the voltage variation is mainly dependent on the type and size of the load in addition to the robustness of the connected system and its size. Shunt active power filters also known as Static Synchronous Compensators (STATCOMS), series active power filters or Dynamic Voltage Regulators (DVRs) and a combination of series and shunt active power filters also known as Unified Power Quality Conditioners (UPQCs) are the latest interfacing devices between grids and consumer appliances that can be used to resolve the issue of voltage fluctuation[31].

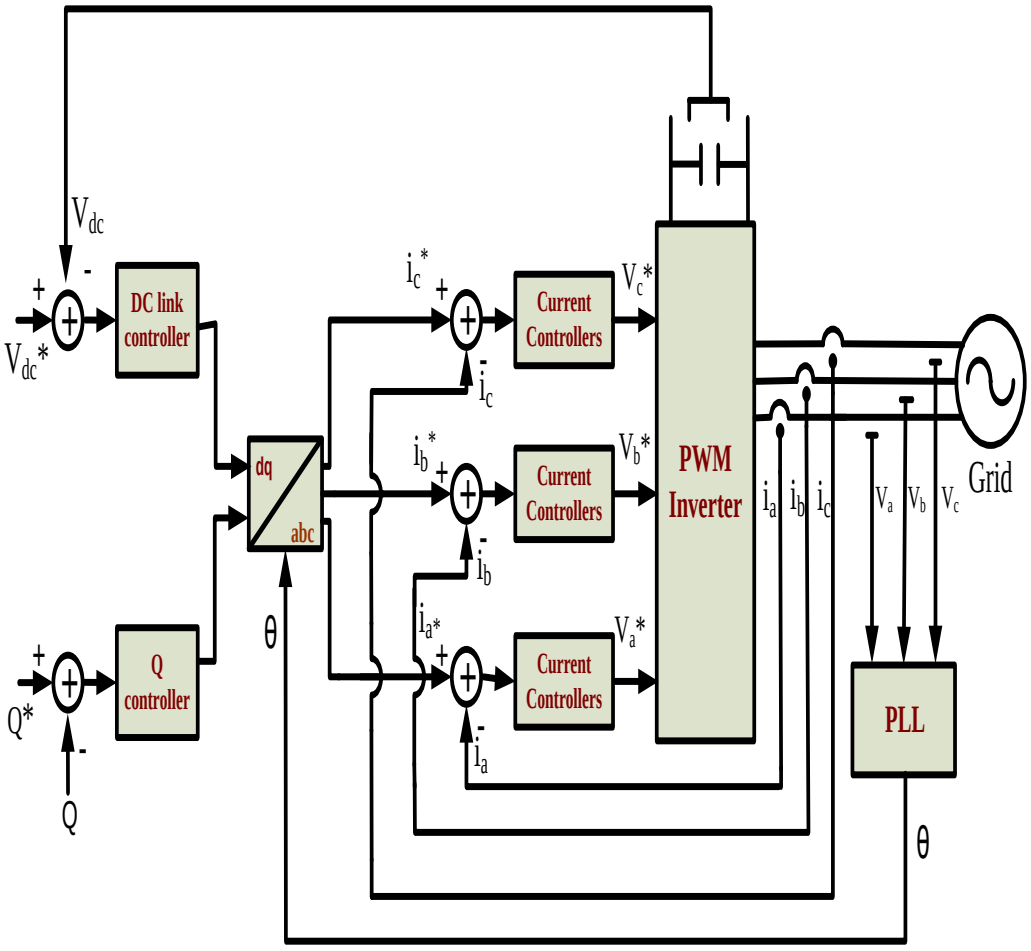

Figure 2.5. Equivalent Structure for Natural Frame Control

A good predicting technique of renewable energy's generated output can provide a good solution for this issue where the voltage fluctuation can be generally measured with lighting flicker level[34]. Power compensators such as switched capacitor, fixed capacitor or static compensator can be used to solve reactive power issue.

Table 2.5. .Comparison of Different Frame of Controls for Grid Tied Three Phase Inverters

S.No.	Control Schemes	Controller Type	Advantages	Disadvantages
1.	Synchronous Frame Control	Proportional Integral	Simple Control is Easy Filtering can be done Easily	Non Removal of Steady State Error and Poor Compensation Capability at Low Order Harmonics
2.	Stationary Frame Control	Proportional Resonant	High Dynamic Performance Complete Removal of Steady State Error	Complex Hardware Implementation and Lack of Power Factor Control
3.	Natural Frame Control	Proportional Integral	Small steady state error	Complex transfer function due to non-diagonal terms
		Proportional Resonant	Simpler transfer function due to the cancellation of non-diagonal terms	Increased Complexity as Compared to Hysteresis and Dead Beat Controller
		Dead Beat	Highly Dynamic Simpler Control for Current Regulation	Implementation complexities for high frequency micro-controllers
		Hysteresis	Highly Dynamic	Complexity in Control for Current Monitoring and Regulation

2.7.3. Phase Synchronization:

The most popular grid synchronization technique is based on phase-locked loop. It is a control system that generates an output signal whose phase is related to the phase of an input signal. Other techniques for synchronization include the detection of zero crossing of the grid voltages or using combinations of filters coupled with a non-linear transformation. The following four conditions must be met for synchronization between RES and grid[35]:

i) Phase sequences of both three-phase voltages must be the same.

ii) Terminal-voltage magnitude must match with grid's magnitude, preferably a few percentages higher.

iii) Frequency must be as close as possible to the grid frequency.

iv) Phase angle between two voltages must be ≤ 5 degrees.

2.7.4. Frequency fluctuation:

System frequency fluctuation in AC grids represents an unbalance situation between load and generation which is mainly a result of sudden changes in active power drawn by a load. Hence, it is important to design control loops for power and frequency control[36]. Bae and Kwasinski[37] highlighted that a primary goal of a PWM inverter controller was to regulate three-phase local ac bus voltage and frequency in a micro grid and to dispatch target active power to a distribution grid, which may be set by users or grid operators.

2.7.5. Energy management Systems:

Reaction to the imbalance of power in the power system is made in the form of the reduction or an increase in the energy demand of the system. This process is known as the Demand-Side Management System *DSMS*. However, the DSMS is used less frequently. The most commonly used practice is the adjustment in the generation levels of the renewable energy system. This solution depends on the possibilities of the load management and economic benefits resulting due to the provision of the loads having flexible contracts[36]. Energy Management Systems *EMSs* use Supervisory Control and Data Acquisition *SCADA* at higher transmissions levels by employing advance analytical tools for data collection in order to create a safe and generally acceptable economic operating conditions for the overall power system. At consumer end, EMSs can control the overall electricity consumption of the consumer, on site generation as well as storage, with the potential for electric vehicle charging[38]. Demand side management and batteries of electric vehicles could play roles in energy storages, for both vehicles and power grids[39].

2.7.6. Energy Storage Devices:

Energy storage devices can provide power when there is energy deficiency and store excess energy when external power supply is adequate[40]. Existing energy storage technologies such as battery, flywheels, super conducting magnetic energy storage and super-capacitors could greatly reduce or balance fluctuations in outputs of renewable generations by their energy storage and fast response functions[39]. The

use of Uninterruptable Power Supply UPS and batteries can save surplus energy produced and provide it to the grid during peak consumption periods[41]. Mixture of renewable energy systems and having a large-scale storage technology can be an efficient powerful scheduling tool for power generation. Intelligent scheduling along with the technical support system having real-time data acquisition and monitoring, network security analysis and dynamic stability warning[40] can help to ensure smooth running of the renewable energy systems

Specific power quality problems can be solved by several devices such as isolation transformers, super-capacitors, flywheels, constant voltage transformers, noise filters, transient voltage surge suppresses and harmonic filters, etc. On the other hand, custom power devices such as dynamic voltage regulators, shunt active power filters commonly known as Static Synchronous Compensators STATCOMs and a combination of series and shunt active power filters also known as Unified Power Quality Conditioners UPQCs are capable to solve multiple power quality problems[31].

The use of fast response control facilities such as flexible alternating current transmission systems and automatic generation control systems helps to alleviate the transient response impacts on the hybrid energy network. The demands of the response abilities of the overall system and the real time management[39] are a core issues that must be considered in long term planning of the overall system [38].One solution to avoid such problems is to distribute small units of renewable energy systems to a larger geographical area instead of large units installed and concentrated in a single area. This practice also can control the intermittent effect of the power generation from the hybrid energy network[42].

2.8. Summary:

A brief introduction to the PV grid connected system is given to familiarize with the standards prevailing in the world. With increasing renewable energy in the recent years especially PV systems, efforts are made to regularize the systems that are installed. Efforts are also made that the major countries having the PV installations have the codes and standards that are flexible and related to each other which can lead to encourage masses /governments to install renewable energy technologies. IEEE 1547 is made as a standard and different standards of the other countries like UL 1471 in case of U.S. and VDE 0126-1-1 in case of Germany are tailored to be similar with the IEEE standard.

References

[1] D. A. Halamay, S. Member, T. K. A. Brekken, A. Simmons, and S. Mcarthur, "Reserve Requirement Impacts of Large-Scale Integration of Wind , Solar , and Ocean Wave Power Generation," vol. 2, no. 3, pp. 321–328, 2011.

[2] F. Ferri, S. Ambühl, B. Fischer, and J. Kofoed, "Balancing Power Output and Structural Fatigue of Wave Energy Converters by Means of Control Strategies," *Energies*, vol. 7, no. 4, pp. 2246–2273, Apr. 2014.

[3] J. Pascual, P. Sanchis, and L. Marroyo, "Implementation and Control of a Residential Electrothermal Microgrid Based on Renewable Energies, a Hybrid Storage System and Demand Side Management," *Energies*, vol. 7, no. 1, pp. 210–237, Jan. 2014.

[4] H. G. Jeong, R. H. Seung, and K. B. Lee, "An Improved Maximum Power Point Tracking Method for Wind Power Systems," *Energies*, vol. 5, no. 12, pp. 1339–1354, May 2012.

[5] G. Mode, R. Teodorescu, S. Member, and F. Blaabjerg, "Flexible Control of Small Wind Turbines With Grid Failure Detection Operating in," vol. 19, no. 5, pp. 1323–1332, 2004.

[6] R. Teodorescu and F. Blaabjerg, "A New Control Structure for Grid-Connected LCL PV Inverters with Zero Steady-State Error and Selective Harmonic Compensation," vol. 00, no. C, pp. 580–586, 2004.

[7] H. Zhu, B. Arnet, L. Haines, and E. Shaffer, "Grid Synchronization Control without AC Voltage Sensors," vol. 00, no. C, pp. 172–178, 2003.

[8] I. Agirman, V. Blasko, and S. Member, "A Novel Control Method of a VSC Without AC Line Voltage Sensors," vol. 39, no. 2, pp. 519–524, 2003.

[9] S. Song, S. Kang, and A. W. P. Characteristics, "Implementation and Control of Grid Connected AC-DC-AC Power Converter for Variable Speed Wind Energy Conversion System," vol. 00, no. C, 2003.

[10] G. Saccomando and J. Svensson, "Transient operation of grid-connected voltage source converter under unbalanced voltage conditions," *Conf. Rec. 2001 IEEE Ind. Appl. Conf. 36th IAS Annu. Meet. (Cat. No.01CH37248)*, vol. 4, pp. 2419–2424.

[11] C. J. Ramos, A. P. Martins, A. S. Araujo, and A. S. Carvalho, "Line AC supply," pp. 0–5.

[12] D. Candusso, I. Valero, A. Walter, S. Bacha, E. Rullitre, and B. Raison, "Modelling, Control and Simulation of a Fuel Cell Based Power Supply System with Energy Management."

[13] J. Svensson, “Synchronisation methods for grid-connected voltage source converters,” *IEE Proc. - Gener. Transm. Distrib.*, vol. 148, no. 3, p. 229, 2001.

[14] S.-J. Lee, H. Kim, S.-K. Sul, and F. Blaabjerg, “A Novel Control Algorithm for Static Series Compensators by Use of PQR Instantaneous Power Theory,” *IEEE Trans. Power Electron.*, vol. 19, no. 3, pp. 814–827, May 2004.

[15] H. Kim, S. Lee, S. Sul, and A. P. Q. R. Transformation, “Reference Wave Generation in Dynamic Voltage Restorers by use of PQR Power Theory,” vol. 00, no. C, pp. 1452–1457, 2004.

[16] E. Twining and D. G. Holmes, “Grid current regulation of a three-phase voltage source inverter with an LCL input filter,” *2002 IEEE 33rd Annu. IEEE Power Electron. Spec. Conf. Proc. (Cat. No.02CH37289)*, pp. 1189–1194, 2002.

[17] L. N. Arruda and S. M. Silva, “PLL Structures for Utility Connected Systems,” vol. 00, no. C, pp. 2655–2660, 2001.

[18] Y. Hong, R. Waters, C. Boström, M. Eriksson, J. Engström, and M. Leijon, “Review on electrical control strategies for wave energy converting systems,” *Renew. Sustain. Energy Rev.*, vol. 31, pp. 329–342, Mar. 2014.

[19] D. N. Zmood, S. Member, and D. G. Holmes, “Stationary Frame Current Regulation of PWM Inverters With Zero Steady-State Error,” vol. 18, no. 3, pp. 814–822, 2003.

[20] S. Fukuda, S. Member, and T. Yoda, “A Novel Current-Tracking Method for Active Filters Based on a Sinusoidal Internal Model,” vol. 37, no. 3, pp. 888–895, 2001.

[21] R. Teodorescu, F. Blaabjerg, M. Liserre, and P. C. Loh, “Proportional-resonant controllers and filters for grid-connected voltage-source converters,” vol. 153, no. 5, 2006.

[22] X. Yuan, J. Allmeling, W. Merk, and H. Stemmier, “Stationary Frame Generalized Integrators for Current Control of Active Power Filters with Zero Steady State Error for Current Harmonics of Concern under Unbalanced and Distorted Operation Conditions,” pp. 2143–2150, 2000.

[23] M. Ciobotaru, R. Teodorescu, and F. Blaabjerg, “Control of single-stage single-phase PV inverter Keywords,” pp. 1–10, 2005.

[24] H.-G. Jeong, G.-S. Kim, and K.-B. Lee, “Second-Order Harmonic Reduction Technique for Photovoltaic Power Conditioning Systems Using a Proportional-Resonant Controller,” *Energies*, vol. 6, no. 1, pp. 79–96, Jan. 2013.

[25] K. Zhou, Y. Yang, F. Blaabjerg, W. Lu, and D. Wang, “Selective Harmonic Control for Power Converters,” no. 2, pp. 4–8, 2014.

[26] L. Malesani, P. Mattavelli, A. Member, and P. Tomasin, “Improved Constant-Frequency Hysteresis Current Control of VSI Inverters with Simple Feedforward Bandwidth Prediction,” vol. 33, no. 5, pp. 1194–1202, 1997.

[27] A. Society and A. Meeting, “A Novel Hysteresis Control Method for PWM Inverters with Constant Modulation Frequency,” vol. 26, no. I, pp. 88–92, 1990.

[28] L. Sonaglioni, “Predictive digital hysteresis current control,” *IAS ’95. Conf. Rec. 1995 IEEE Ind. Appl. Conf. Thirtieth IAS Annu. Meet.*, vol. 3, pp. 1879–1886, 1995.

[29] I. Transactions and O. N. Industrial, “An Adaptive Hy steresis-Band Current Control Technique of a Voltage-Fed PWM Inverter for Machine Drive System,” vol. 31, no. 5, pp. 402–408, 1990.

[30] Q. Yao and D. G. Holmes, “A simple, novel method for variable-hysteresis-band current control of a three phase inverter with constant switching frequency,” *Conf. Rec. 1993 IEEE Ind. Appl. Conf. Twenty-Eighth IAS Annu. Meet.*, pp. 1122–1129.

[31] S. K. Khadem, M. Basu, and M. F. Conlon, “Power Quality in Grid connected Renewable Energy Systems : Role of Custom Power Devices 3 . Grid integration of Renewable Energy,” 2010.

[32] G. M. Shafiullah, A. M. T. Oo, D. Jarvis, A. B. M. S. Ali, and P. Wolfs, “Potential Challenges : Integrating Renewable Energy with the Smart Grid,” pp. 1–6.

[33] B. Ernst, F. Reyer, and J. Vanzetta, “TSOs,” pp. 1–9, 2009.

[34] P. Dalwadi, V. Shrinet, C. R. Mehta, and P. Shah, “Optimization of solar-wind hybrid system for distributed generation,” *2011 Nirma Univ. Int. Conf. Eng.*, pp. 1–4, Dec. 2011.

[35] F. Group, “Wind and Solar Power Systems: Design, Analysis, and Operation, Second Edition,” 2006.

[36] F. O. Resende, J. A. P. Lopes, and S. Member, “Management and Control Systems for Large Scale Integration of Renewable Energy Sources into the Electrical Networks,” pp. 1–6.

[37] S. Bae, S. Member, and A. Kwasinski, “Dynamic Modeling and Operation Strategy for a Microgrid With Wind and Photovoltaic Resources,” vol. 3, no. 4, pp. 1867–1876, 2012.

[38] E. F. Camacho, T. Samad, M. Garcia-sanz, and I. Hiskens, “Control for Renewable Energy and Smart Grids,” 2011.

[39] Y. Liu and C. Jiang, “A Review on Technologies and Methods of Mitigating Impacts of Large - Scale Intermittent Renewable Generations on Power System,” vol. 5, no. 9, pp. 2765–2770, 2013.

[40] M. Zeng, L. Huang, F. Yan, and D. Jiang, “Research of the Problems of Renewable Energy Orderly Combined to the Grid in Smart Grid,” *2010 Asia-Pacific Power Energy Eng. Conf.*, pp. 1–4, 2010.

[41] E. Systems, “Grid Integration of Wind-Solar Hybrid Renewables Using AC / DC Converters as DG Power Sources,” pp. 171–177, 2011.

Chapter 3

Methodology

3.1. Single Phase Equivalent Model:

A single phase equivalent model of the converter is derived for the design and analysis of the current controllers which is given by fig 3.1.

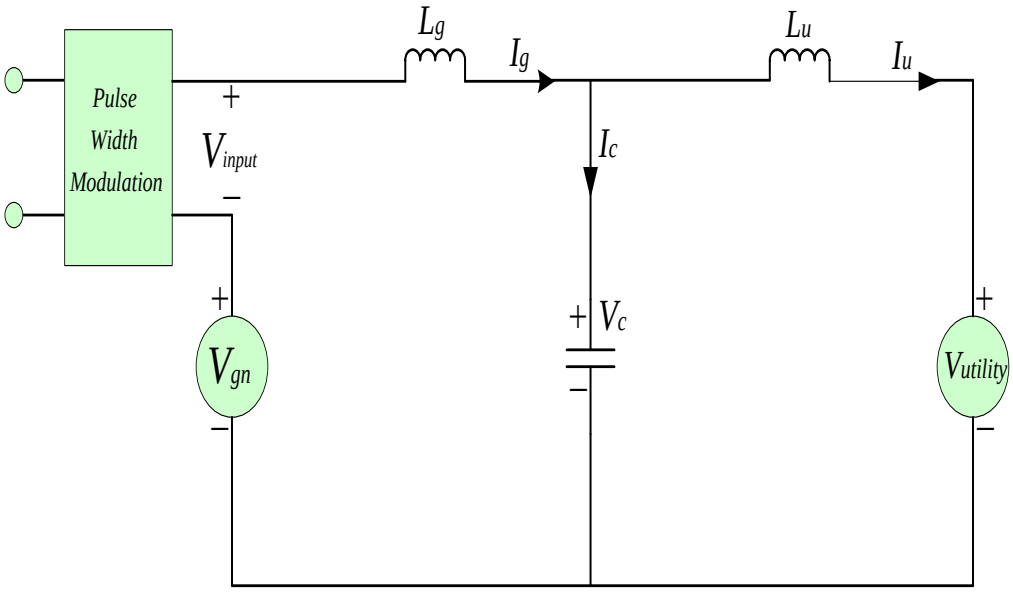

Figure 3.1. Linear Model of Two Level Converter

The disturbance Vgn can be given by the following equation;

$$Vgn = \frac{Vag + Vbg + Vcg}{3} \tag{3.1}$$

Vag = Phase of voltage a with respect to the ground

Vbg = Phase of voltage b with respect to the ground

Vcg = Phase of voltage c with respect to the ground

Vgn = Phase coupling voltage.

It depends upon the switching states of the three phases and it is negligible when capacitors are connected to the d.c. link.

The following analysis of the single phase linear model of the converter is given by assuming that the system is balanced and there exists no phase interaction between the phases.

$$V_{input} - Vc = Lg \frac{dIg}{dt} \tag{3.2}$$

$$Ic = C\frac{dV_C}{dt} \tag{3.3}$$

$$Ic = Ig - Iu \tag{3.4}$$

$$Vc - Vu = L_2\frac{dIu}{dt} \tag{3.5}$$

The expression for the output current can be derived by using the above equations as shown below;

Putting (3.3) in (3.4)

$$C\frac{dV_C}{dt} = Ig - Iu \tag{3.6}$$

$$Ig = \frac{dV_C}{dt} + Iu \tag{3.7}$$

Differentiating (3.7)

$$\frac{dIg}{dt} = \frac{d}{dt}[C\frac{dV_C}{dt}] + \frac{dIu}{dt} \tag{3.8}$$

Putting (3.8) in (3.2)

$$Vinput - Vc = Lg\left[\frac{d}{dt}C\frac{dV_C}{dt} + \frac{dIu}{dt}\right] \tag{3.9}$$

$$Vinput - Vc = LgC\frac{d^2V_C}{dt^2} + Lg\frac{dIu}{dt} \tag{3.10}$$

$$Vinput = LgC\frac{d^2V_C}{dt^2} + Lg\frac{dIu}{dt} + Vc \tag{3.11}$$

Subsitute the value $of\ Vc = Lu\frac{dIu}{dt} + Vutility\ in$ (3.11)

$$Vinput = LgC\frac{d^2}{dt^2}(Lu\frac{dIu}{dt} + Vutility) + Lg\frac{dIu}{dt} + Vc \tag{3.12}$$

$$Vinput = Lg\left[\frac{d^2C}{dt^2}(Lu\frac{dIu}{dt} + Vutility) + \frac{dIu}{dt}\right] + Vc \tag{3.13}$$

$$Vinput = Lg\left[\frac{d^2C}{dt^2}(Lu\frac{dIu}{dt}+Vutility)+\frac{dIu}{dt}\right]+Lu\frac{dIu}{dt}+Vu \quad (3.14)$$

$$Vinput = Lg\left[\frac{d^2}{dt^2}CVutility+CLu\frac{d^3Iu}{dt^3}+\frac{dIu}{dt}\right]+Lu\frac{dIu}{dt}+Vutility \quad (3.15)$$

Applying Laplace Transform

$$Vinput = Lg\left[s^2CVutility+LuCs^3Iu+sIu\right]+LusIu+Vutility \quad (3.16)$$

$$Vinput = Lgs^2CVutility+LgLuCs^3Iu+LgsIu+LusIu+Vutility \quad (3.17)$$

$$Vinput = Lgs^2CVutility+(LgLuCs^3+Lgs+Lus)Iu+Vutility \quad (3.18)$$

$$Vinput = Vutility(Lgs^2C+1)+Iu(LgLuCs^3+Lgs+Lus) \quad (3.19)$$

$$Iu(LgLuCs^3+Lgs+Lus) = Vinput-Vutility(Lgs^2C+1) \quad (3.20)$$

$$Iu(LgLuCs^3+(Lg+Lu)s) = Vinput-Vutility(Lgs^2C+1) \quad (3.21)$$

$$Iu = \frac{1}{(LgLuCs^3+(Lg+Lu)s)}Vinput-\frac{(Lgs^2C+1)}{(LgLuCs^3+(Lg+Lu)s)}Vutility \quad (3.22)$$

The two loop structure is developed using this equation as shown in figure 3.2. The figure 3.3 further simplifies figure 3.2 in which the error is fed up to the controller.

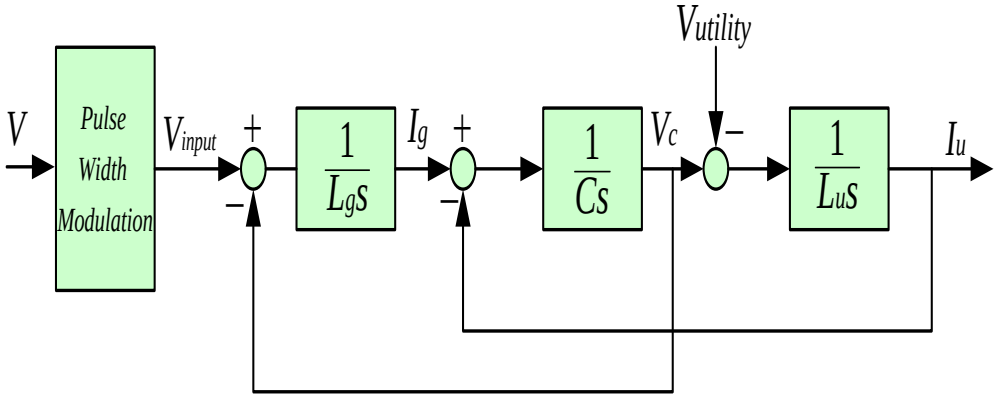

Figure 3.2. Block Diagram of Single Phase Equivalent Circuit

Wide research has already been done on the passive as well active methods of the damping[1]–[3].The most widely used damping which is easy is active based damping by feed backing the capacitor current[4]–[7]. The gain of the capacitor thus acts as a virtual resistance connected parallel to the capacitor. The main feedback signal Iu is subtracted from reference current and the error is fed to the controller.

The expression for the output current is now given by the equation 3.23 as shown in the figure 3.3. The open loop transfer function of the two level converter as shown in figure 3.3 is given by equation 3.24.

$$Iu = \frac{K_{gain}}{(LgLuCs^3 + (Lg + Lu)s) + K_{gain}} Iref - \frac{(Lgs^2C + 1)}{(LgLuCs^3 + (Lg + Lu)s)} Vutility \quad (3.23)$$

$$G_{plant(s)} = \frac{1}{CLgLus^3 + (Lg + Lu)s} \quad (3.24)$$

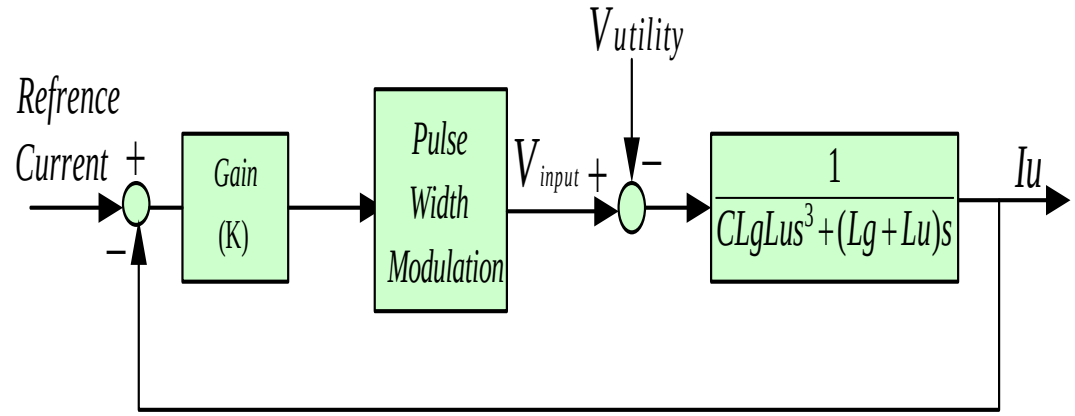

Figure 3.3. Single Feedback Loop of Current

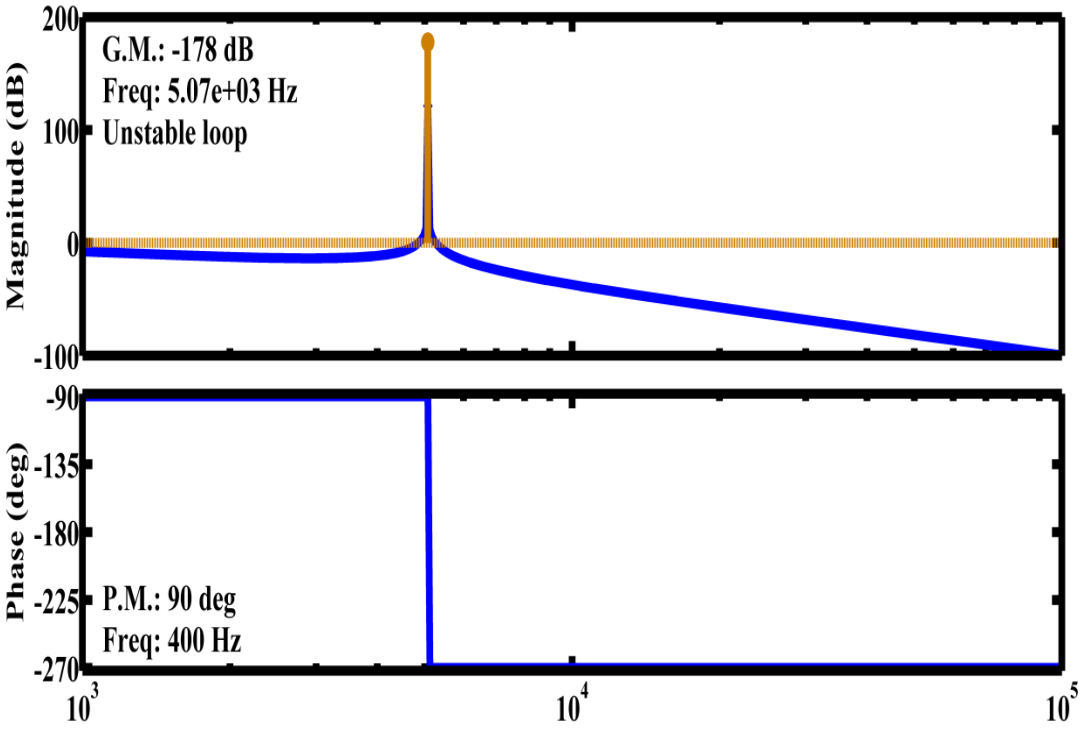

Figure 3.4. Open Loop Bode Plot of Plant Transfer Function

The open loop bode plots and root locus plots are given in figure 3.3 and figure 3.4 respectively. The plant transfer function is unstable and two poles lie in the left half plane. In order to make the plant transfer function stable some modification needs to be done. A feedback stabilizing loop is introduced having a transfer function of $A(s) = as^2$ as shown in figure 3.6.

The output current as obtained from figure 3.6 is given by the equation 3.25 which represents the output current.

$$Iu = \frac{K_{gain}}{(LgLuCs^3 + (Lg + Lu)s) + as^2 + K_{gain}} Iref - \frac{(Lgs^2C + 1)}{K_{gain} + as^2 + (LgLuCs^3 + (Lg + Lu)s)} Vutility \quad (3.25)$$

The double derivative term makes it non desirable. However, the expression of the capacitor current contains this double derivative and if it multiplied by the gain and feedback to the system, it can provide the necessary active damping that can make the system stable.

$$Ic = IuLuCs^2 + sIcVutility \quad (3.26)$$

The passive damping is achieved by multiplying the capacitor current with the gain k_b .Figure 3.7 shows the complete controller structure with the capacitor current included. The final controller structure with both the major and minor feedback loops is shown in figure 3.7.

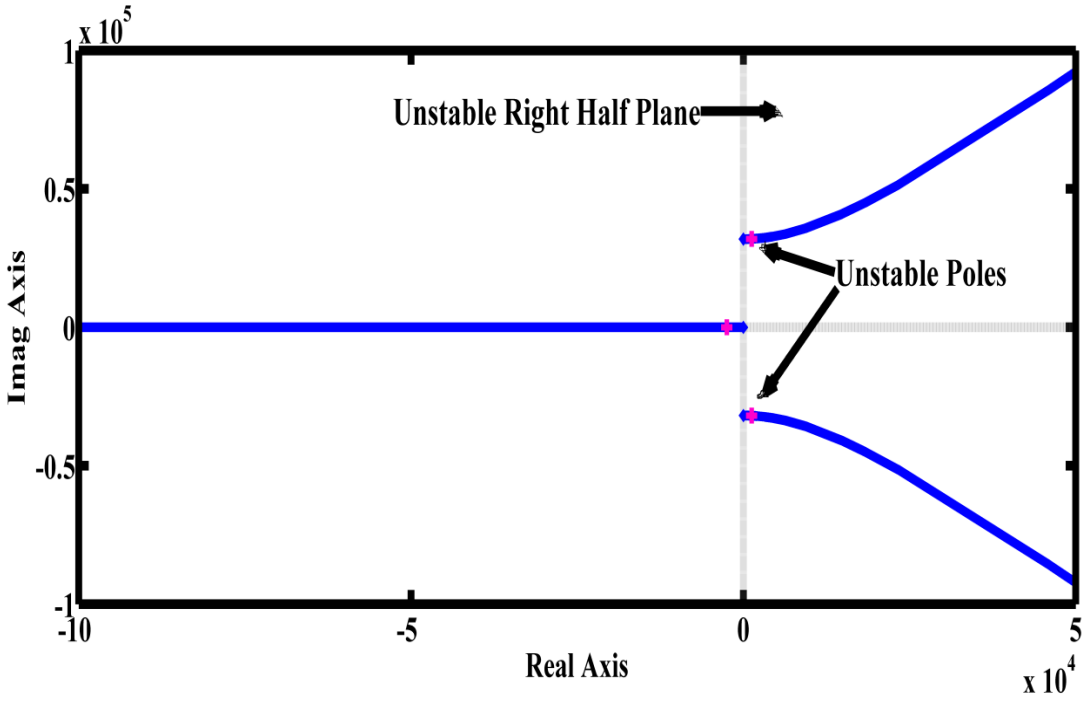

Figure 3.5. Open Loop Root Locus Plot of Plant Transfer Function

The block reduction techniques were applied and the simplified block diagram is shown in figure 3.8. The main advantage of the two loop feedback controller structure is that the inner loop gain given by k_b can alter both the plant transfer function as well as the disturbance transfer function. On the other hand, the main disadvantage is the inclusion of an extra current sensor as compared to the single feedback structure.

The open loop transfer function of the plant is given by the following equation

$$G_{plant(s)} = \frac{1}{CLgLus^3 + k_bLus^2 + (Lg + Lu)s} \quad (3.27)$$

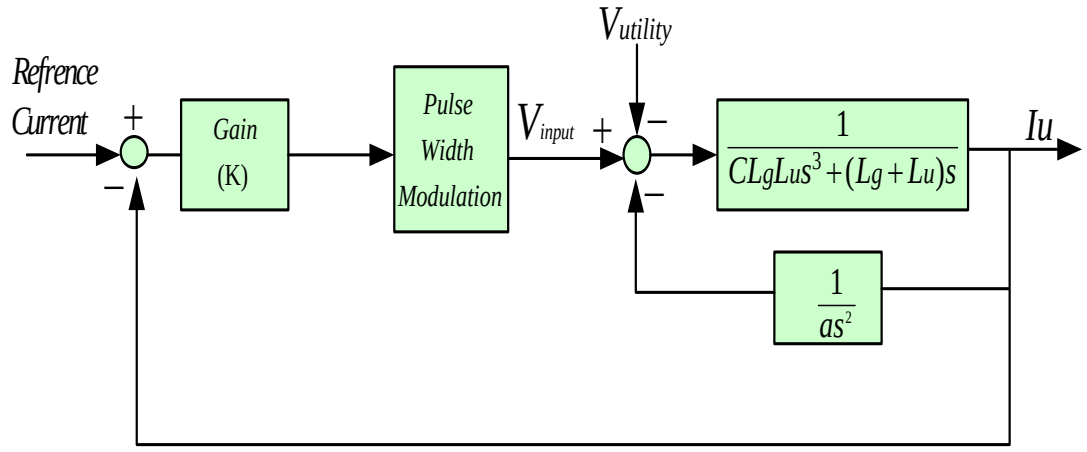

Figure 3.6. Stabilizing Feedback Loop

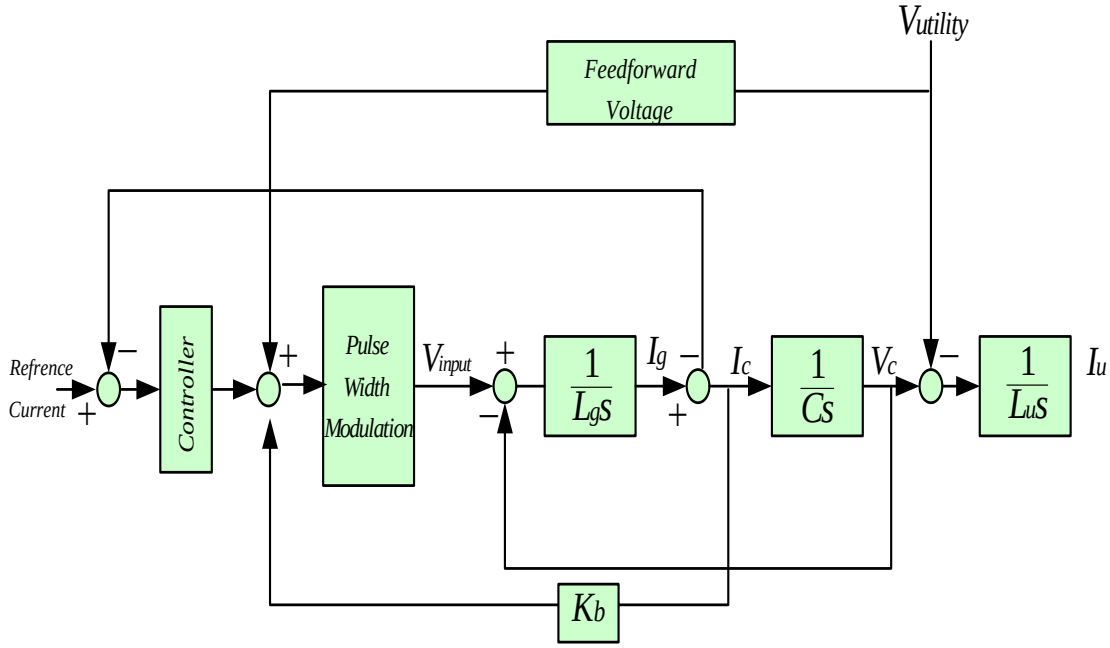

Figure 3.7. Controller Structure with Two Loop Feedbacks

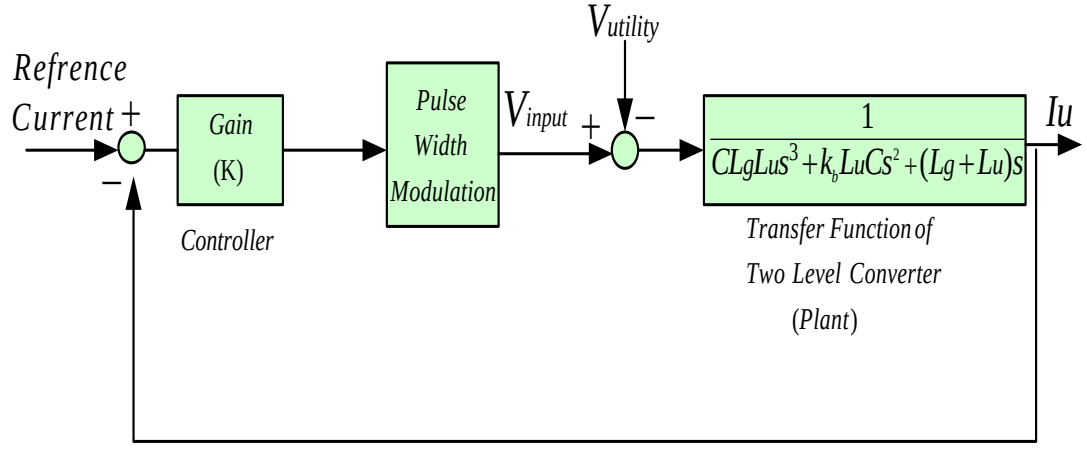

Figure 3.8. Simplified Block Diagram of Final Diagram

In order to include the disturbance effects of the grid a disturbance transfer function is derived which is given by the following equation

$$D_{ist(s)} = CLgs^2 + k_bCs + 1 \quad (3.28)$$

The output current after the inclusion of the disturbance is given by the following equation

$$Iu = \frac{K_{gain}G_{plant(s)}}{1+K_{gain}G_{plant(s)}} I_{ref} - \frac{G_{plant(s)}}{1+K_{gain}G_{plant(s)}} D_{ist(s)} V_{utility(s)} \quad (3.29)$$

The utility voltage forms the source of the disturbance which is rejected by the feed forward voltage [8] by having the same design as the utility voltage disturbance. However, it is difficult to implement practically because of the noise problems amplification.

3.2. Effect of Gain on Open Loop

The root locus and the bode plots help to identify the stability limits and the maximum gain that is achievable. In this regard two sets of LCL filter values are being investigated. These values help to identify the maximum gain k_b that is allowable without making the system unstable. Lu is taken as to be 50 micro H in both cases. In the first case however Lg is taken to be 250 micro H whereas in the second case it is taken as 230 micro H.

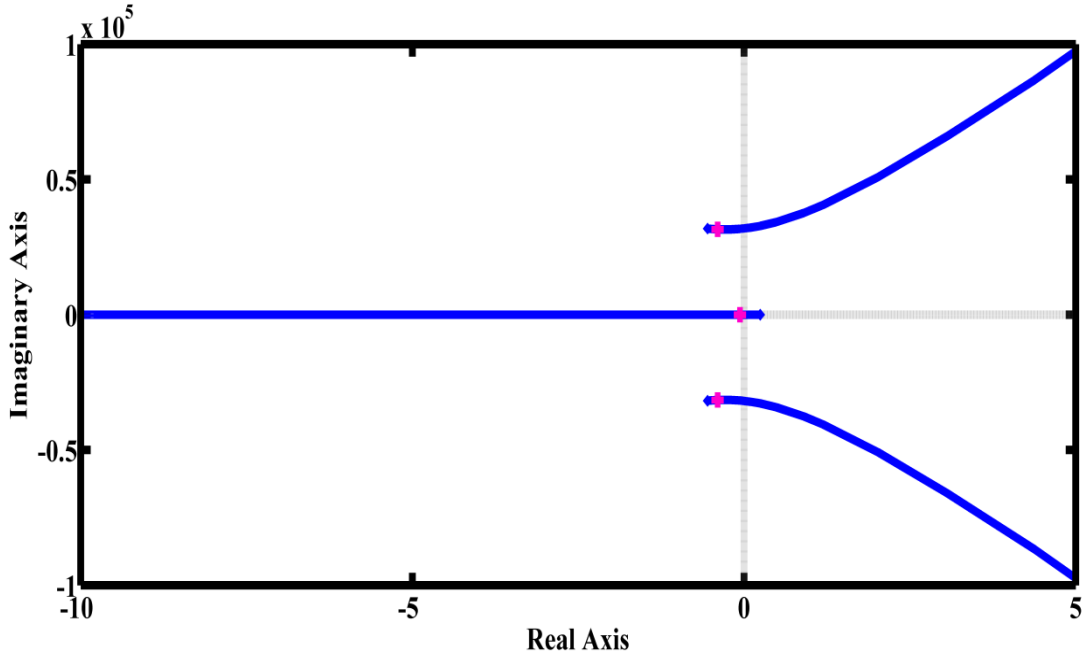

Figure 3.9. Root Locus of Open Loop with K_b=1

We know that the there is no oscillatory response when the roots of the equations are real. However, as shown in the figure 3.9. There are two imaginary roots and one real root. The bode plot of the open loop show that the gain margin is very low. In order to increase the gain margin the K_b is increased from 1 to 3 which gives the open loop root locus as shown in figure 3.10. It can be seen from the figure that as the gain is increased the imaginary poles move towards the right half plane. This trend is shown

in figure 3.13. It was found that the maximum gain that can be achieved without poles moving into the instability region is 3.

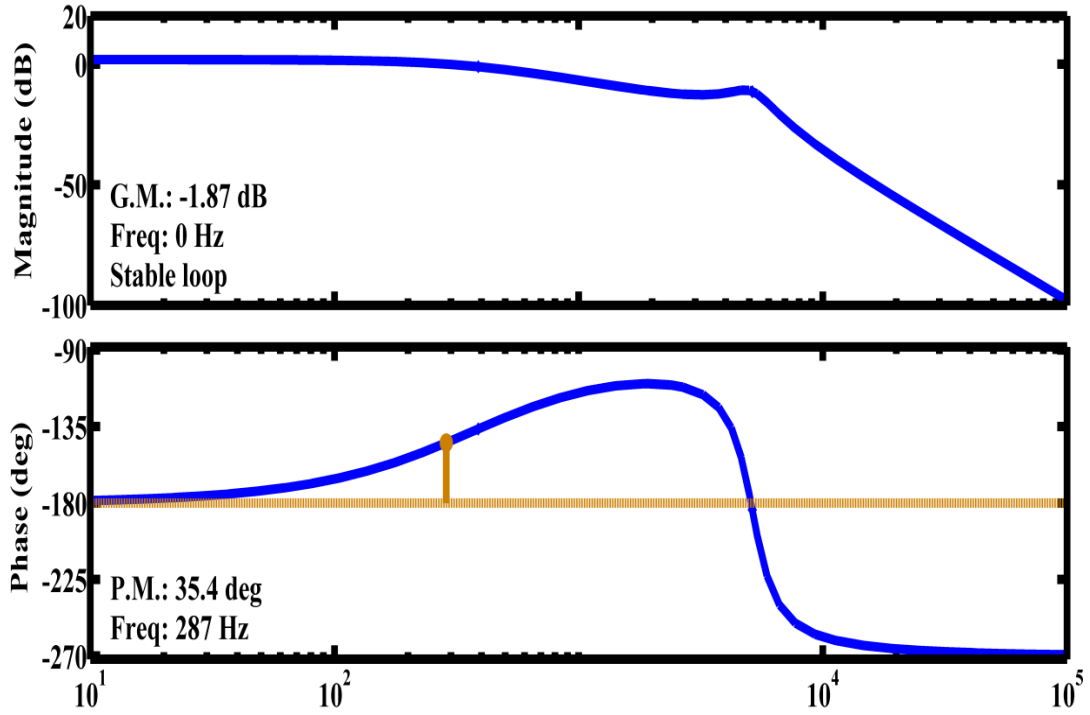

Figure 3.10. Open Loop Bode plot with K_b =1

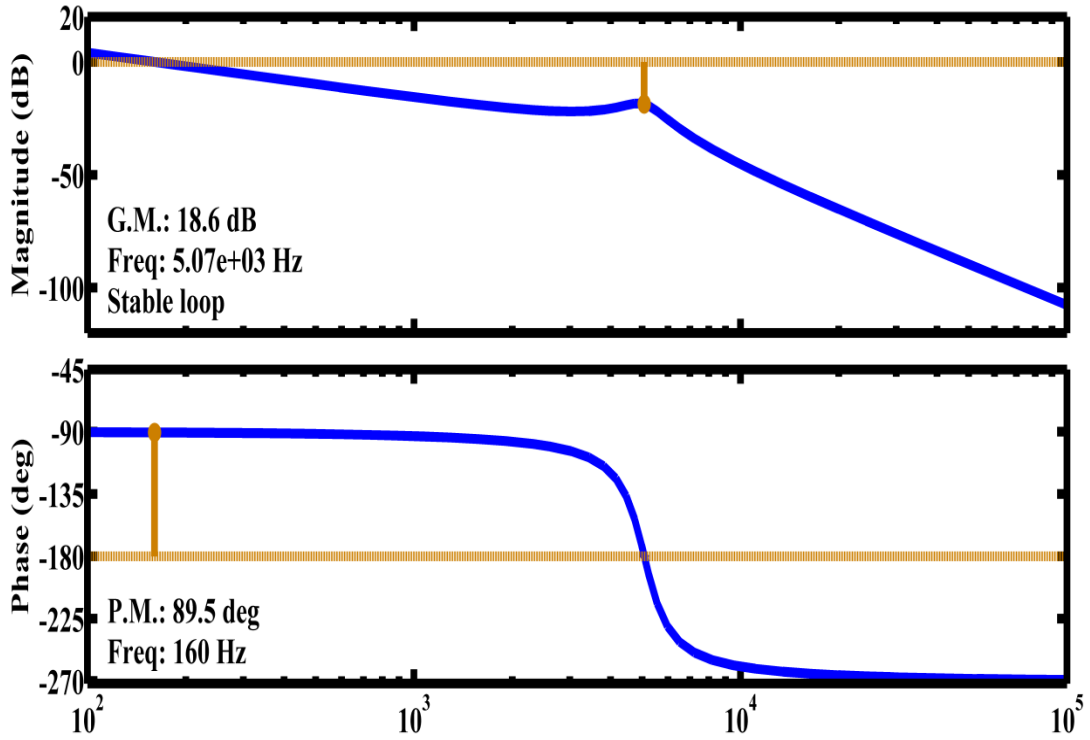

Figure 3.11. Open Loop Bode Plot of Open Loop with K_b=2

However, practicing the good control system design techniques a suitable value of the gain was chosen to be 2 which gives the enough safe margin to work with the system without moving into instability. By choosing the gain value of 2 the Phase margin (P.M.) is 89.5 degrees and Gain Margin (G.M.) is 18.6 dB.

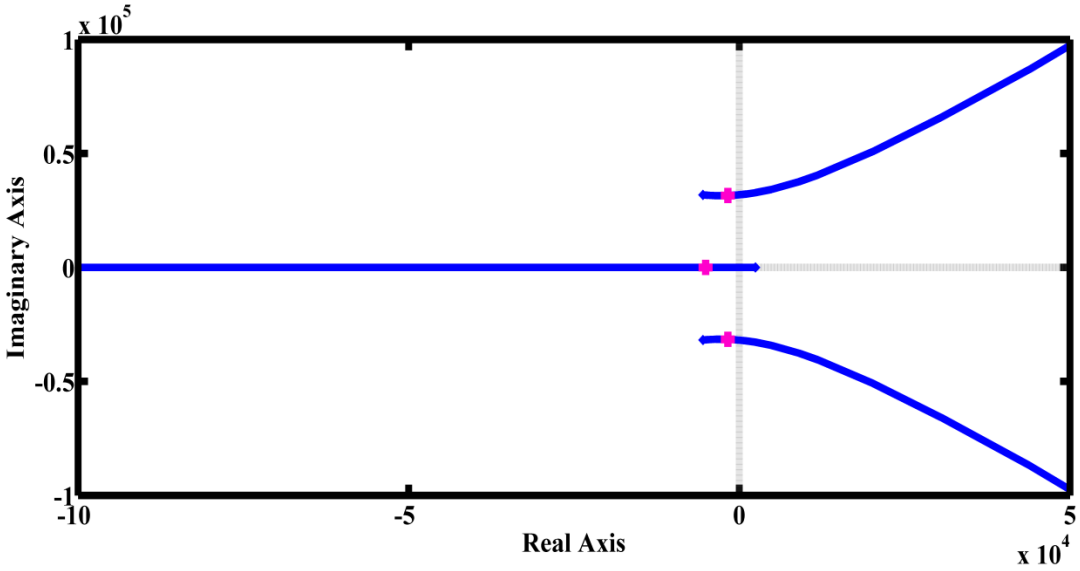

Figure 3.12. Root Locus of Open Loop with K_b =3

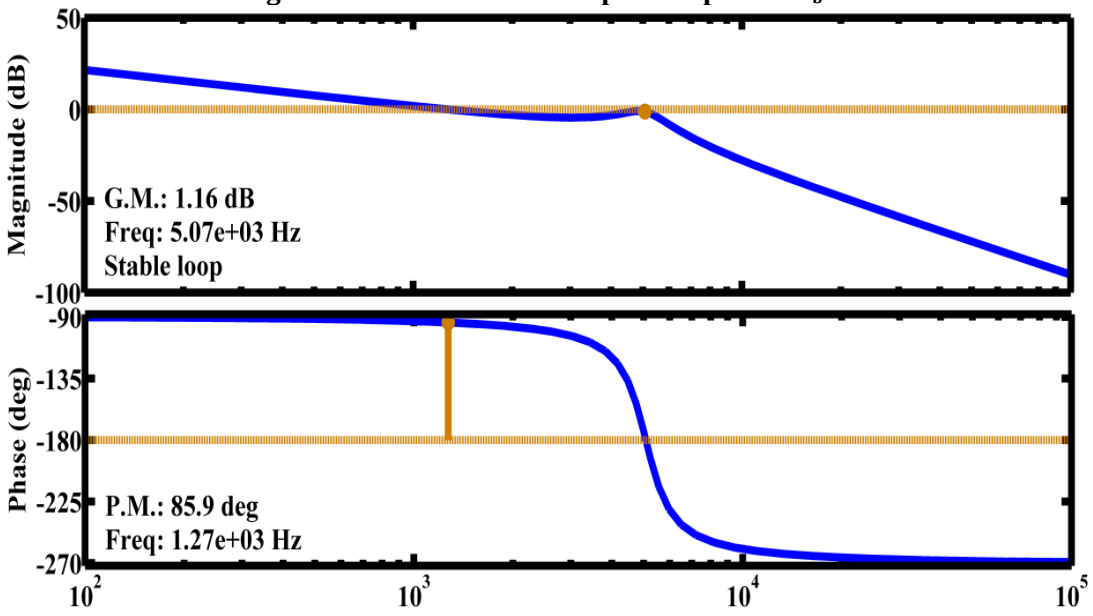

Figure 3.13. Open Loop Bode Plot of Open Loop with K_b=3

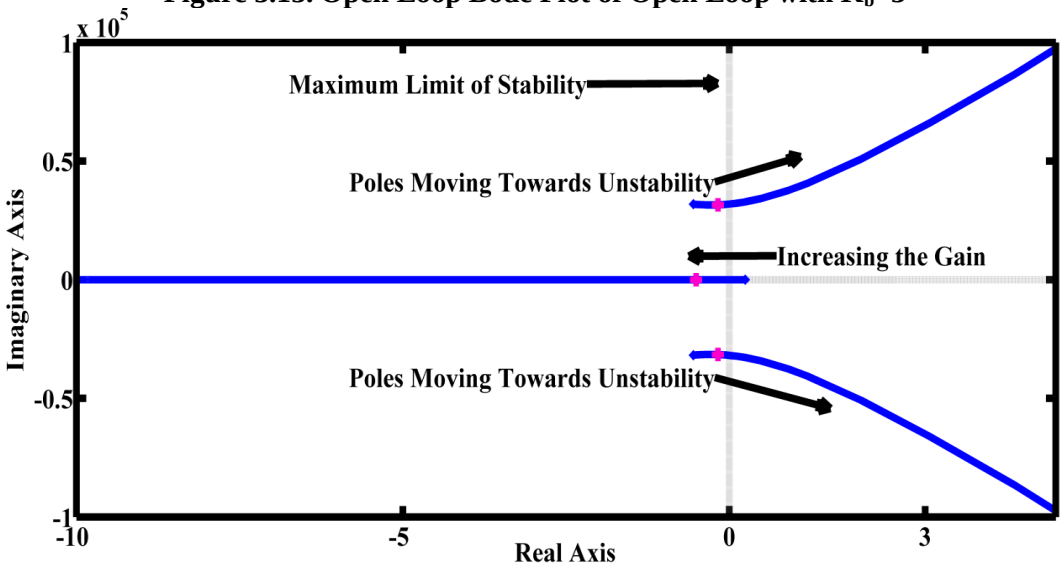

Figure 3.14. General Trends of Open Loop Root Locus Plot

3.3. Summary

In this chapter a single phase equivalent model of the grid connected LCL filter is developed. The effect of gain on open loop was being investigated by the help of root locus and the bode plots. These plots help to identify the stability limits and the maximum gain that is achievable without making the system unstable. In this regard two sets of LCL filter values were being investigated. These values were used to identify the maximum gain k_b that is allowable without making the system unstable.

References

[1] J. Dannehl, M. Liserre, S. Member, F. W. Fuchs, and S. Member, “Filter-Based Active Damping of Voltage Source Converters With LCL Filter,” vol. 58, no. 8, pp. 3623–3633, 2011.

[2] J. Dannehl, S. Member, F. W. Fuchs, S. Member, S. Hansen, P. B. Thøgersen, and S. Member, “Investigation of Active Damping Approaches for PI-Based Current Control of Grid-Connected Pulse Width Modulation Converters With LCL Filters,” vol. 46, no. 4, pp. 1509–1517, 2010.

[3] R. Beres, X. Wang, F. Blaabjerg, C. L. Bak, and M. Liserre, “A review of passive filters for grid-connected voltage source converters,” *2014 IEEE Appl. Power Electron. Conf. Expo. - APEC 2014*, pp. 2208–2215, Mar. 2014.

[4] C. C. Active-damping, C. Bao, X. Ruan, S. Member, X. Wang, W. Li, and S. Member, “Step-by-Step Controller Design for LCL -Type Grid-Connected Inverter with,” vol. 29, no. 3, pp. 1239–1253, 2014.

[5] S. G. Parker, B. P. McGrath, and D. G. Holmes, “Regions of active damping control for LCL filters,” *2012 IEEE Energy Convers. Congr. Expo.*, pp. 53–60, Sep. 2012.

[6] L. C. L. G. Inverter, D. Pan, S. Member, X. Ruan, S. Member, and C. Bao, “Capacitor-Current-Feedback Active Damping With Reduced Computation Delay for Improving,” vol. 29, no. 7, pp. 3414–3427, 2014.

[7] E. Twining, S. Member, and D. G. Holmes, “Grid Current Regulation of a Three-Phase Voltage Source Inverter With an LCL Input Filter,” vol. 18, no. 3, pp. 888–895, 2003.

[8] M. a. Abusara, M. Jamil, and S. M. Sharkh, “Repetitive current control of an interleaved grid-connected inverter,” *2012 3rd IEEE Int. Symp. Power Electron. Distrib. Gener. Syst.*, pp. 558–563, Jun. 2012.

Chapter 4

Design and Analysis of Classical Controllers

4.1. Testing the Robustness of the PI Controller

A strategy for testing the robustness of a PI controller is made by changing the LCL filter values. The filter values were tested for both increase as well as a decrease in the LCL filter parameter values for the three cases. In the first case the filter parameter values were changed to 5%. In the second case 10% of the filter parameter values were changed and in the final case the controller was tested when the filter parameter values were changed to 15 % . The step responses were studied as well as bode diagrams were being plotted for the various changes in the values.

4.1.1. Case 1 (5% Increase and Decrease in Impedance Values)

To test the robustness of a PI controller a 5 % increase and decrease in the impedance value was made. The corresponding step response from the PI controller with the changed parameter is shown in fig. 4.1. Table 4.2 summarizes the different characteristics of the PI controller for both cases. It is important to mention here that the values of the PI controller are kept same during all these cases with K_p=0.18 and K_i=14.67. It is evident from the step responses that the step responses remain same for both the cases. However, there is a slight change in the overshoot value which was 10.3% in the case of the 5% decrease in the impedance value and 11.1% for the 5 % increase in the impedance value. As in the previous cases there is zero steady state error and in both cases the final value is 1 because of the linear model of the grid connected inverter being used.

4.1.2. Case 2 (10% Increase and Decrease in Impedance Values)

The LCL filter parameters were changed to 10% and the PI controller was tested. The parameters of the PI controller were kept same as stated in case 1. It can be seen from the fig. 8 that the subsequent changes in the parameter values are not affecting the step responses from the PI controller.

However, there is a greater overshoot value of 11.5% was observed when there was a 10 increase in the impedance value. The settling value is achieved at 0.029 sec for a 10% decrease in the impedance value and 0.034 sec for a 10 % increase in the impedance values.

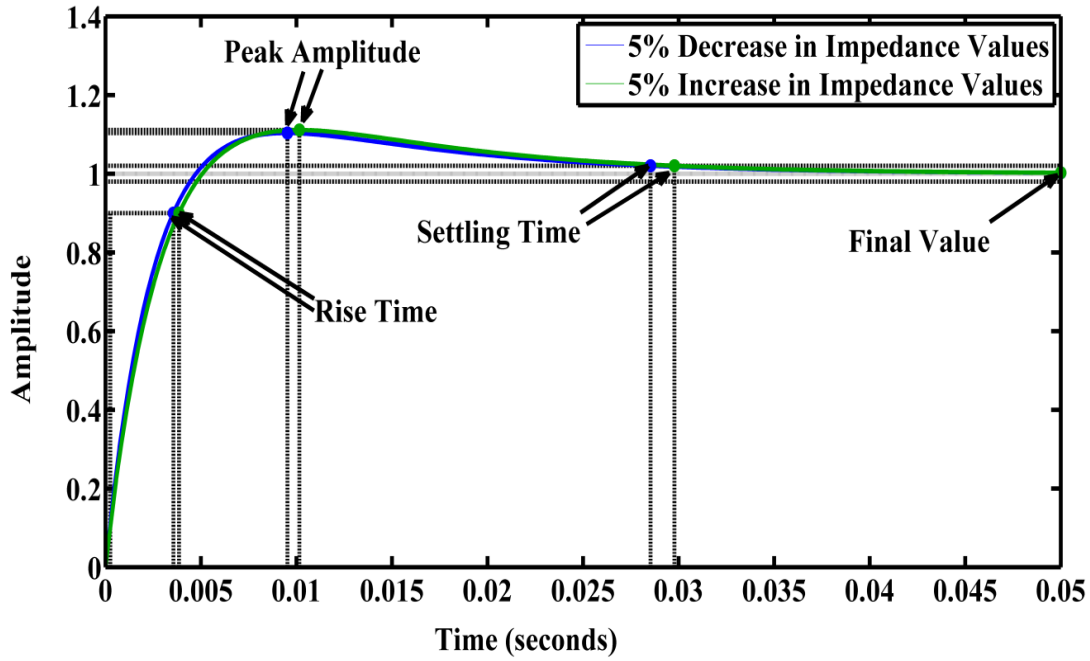

Figure 4.1. Step Response of a PI Controller for Case 1.

Table 4.1. Different Parameters of PI Controller for Case 1.

S.No.	Parameter	Response with 5% decrease	Response with 5% increase
1.	Peak Amplitude	1.09	1.1
2.	Overshoot	10.3 %	11.1%
3.	Rise Time	0.00332 Sec	0.00359 Sec
4.	Settling Time	0.00285 Sec	0.0298 Sec
5.	Final Value	1	1
6.	K_p	K_p =0.18	K_p =0.18
7.	K_i	K_i=14.67	K_i =14.67

4.1.3. Case 3 (15% Increase and Decrease in Impedance Values)

Fig. 4.3 shows the step responses from the PI controller when the impedance values are changed to 15%. The parameters are kept same as in case 1 and case 2. It can be seen from the figure that the step responses from the PI controller are smoother without any oscillations observed. There exists no steady state error and the final value is 1 in both the cases. Table 4.4 summarizes the parameters for both the step responses.

4.2. Bode Plots for the Variation In the LCL Filter Values

In order to ensure a reliable and robust operation of the grid connected inverter three cases are developed in which the LCL filter values are varied to 5% ,10% and 15 %. The bode plots are drawn to see if the system can handle these changes with sufficient gain margin and phase margins available. The bode plots for 5% changes in the LCL filters are shown in fig 4.4,4.5 and 4.6 respectively. It can be seen from these figures that irrespective of the changes in the LCL filter the gain margins and

phase margins exist, thus showing that the system can handle the variations in the filter parameters without being unstable.

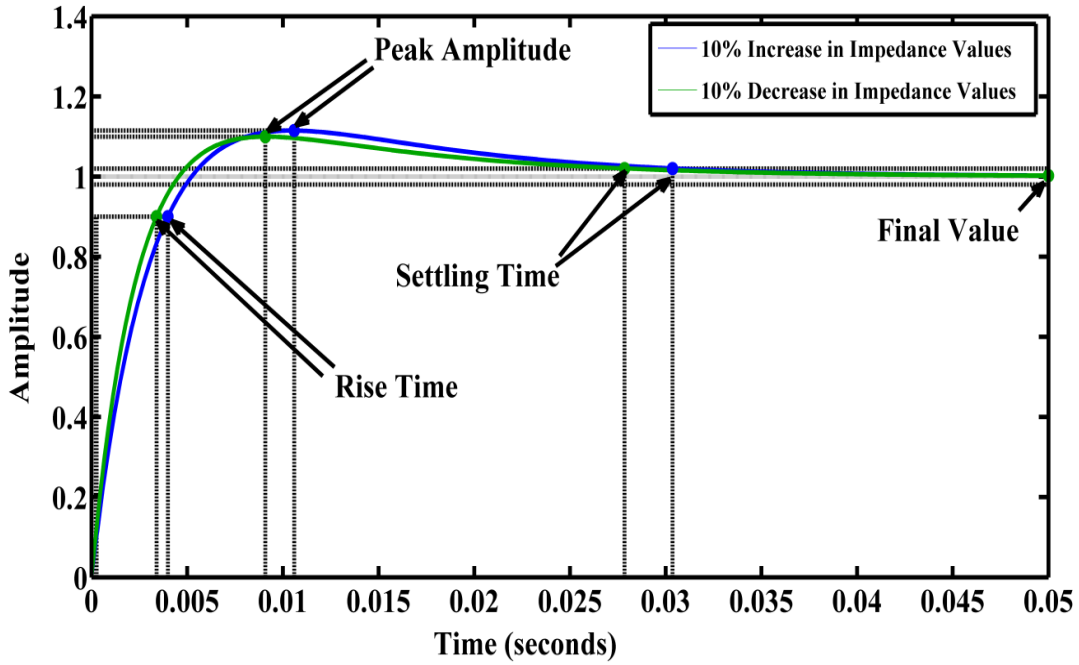

Figure 4.2. Step Response of a PI Controller for Case 2

Table 4.2. Different Parameters of PI Controller for Case 2

S.No.	Parameter	Response with 5% decrease	Response with 5% increase
1.	Peak Amplitude	1.09	1.11
2.	Overshoot	9.94%	11.5 %
3.	Rise Time	0.00318 sec	0.00373 sec
4.	Settling Time	0.0279 sec	0.0304 sec
5.	Final Value	1	1
6.	K_p	K_p =0.18	K_p =0.181
7.	K_i	K_i =14.67	K_i =14.67

4.3. Bode Plots for the Variation In the Grid Inductor Values

The grid inductor acts as a coupling point between the grid and the converter. Due to its major significance as a coupling point, the effects of the variations in behavior of the converter are of significant value. In addition to that the values of the inductor can vary significantly with the changes in the location where the converter needs to be installed.This results in the uncertainty in the behavior of the system which in turn can result to a degradation in the performance of the converters. In lieu of the above mentioned reason the grid inductor values were varied and the subsequent bode plots were drawn to investigate the effect of its variation in the behavior of the system. Fig. 4.7 shows the bode plots when the grid utility inductor is varied 25%.The bode plots show that there is not a significant change in the bode responses when the inductor values are varied.

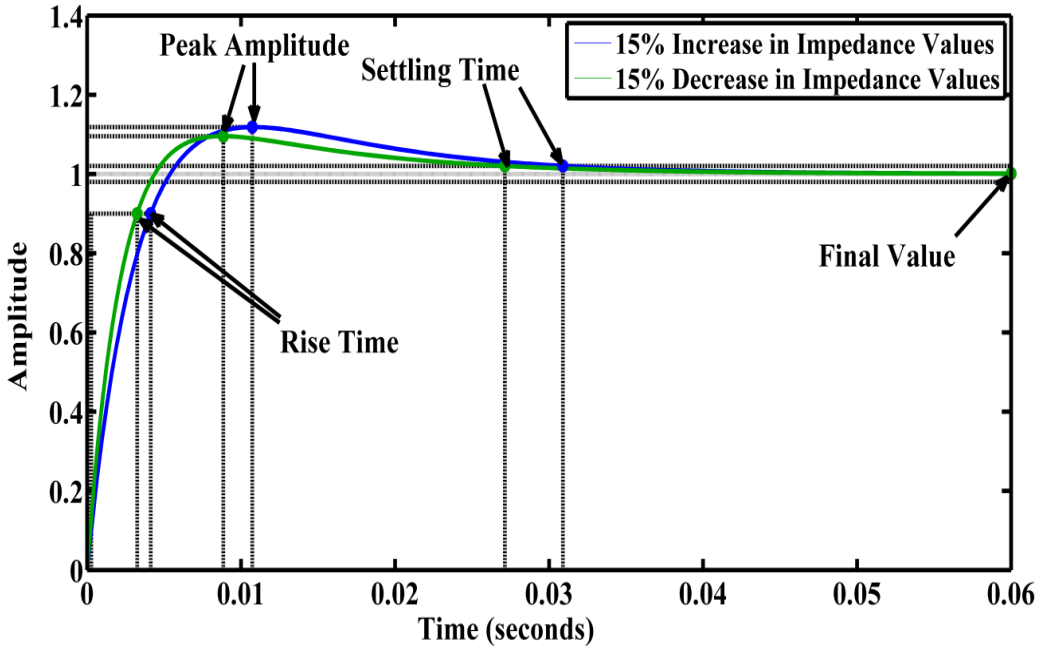

Figure 4.3. Step Response of a PI Controller for Case 3

Table 4.3. Different Parameters of PI Controller for Case 3

S.No.	Parameter	Response with 15% decrease	Response with 15% increase
1.	Peak Amplitude	1.05	1.12
2.	Overshoot	9.53%	11.8 %
3.	Rise Time	0.00304 Sec	0.00346 Sec
4.	Settling Time	0.0271 Sec	0.00386 Sec
5.	Final Value	1	1
6.	K_p	K_p =0.181	K_p =0.181
7.	K_i	K_i =14.67	K_i =14.67

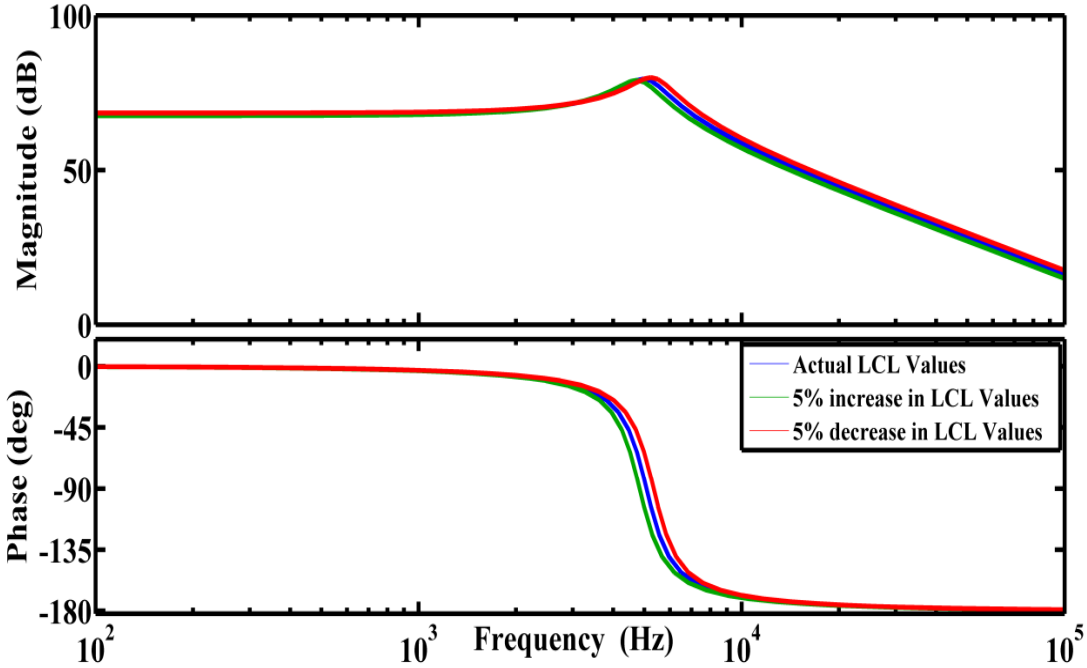

Figure 4.4. Bode Plots for the 5% variation in the LCL filter Parameters

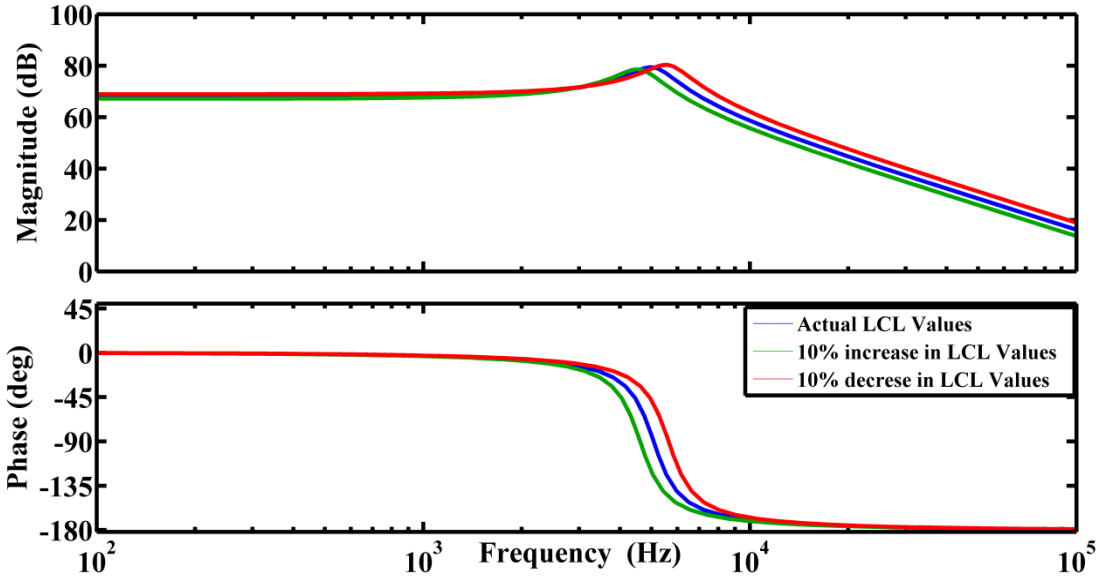

Figure 4.5. Bode Plots for the 15% variation in the LCL filter Parameters

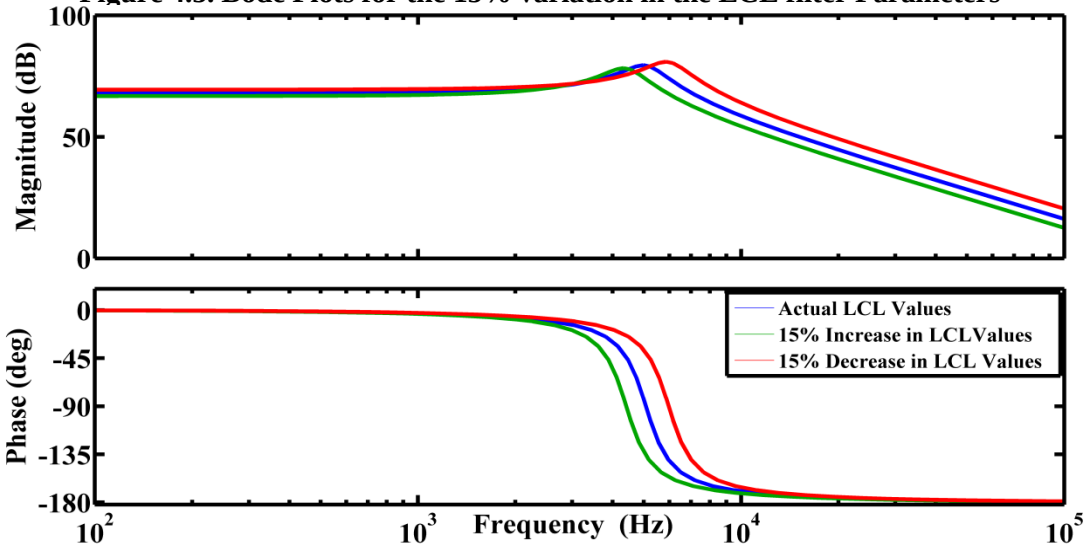

Figure 4.6. Bode Plots for the 15% variation in the LCL filter Parameters

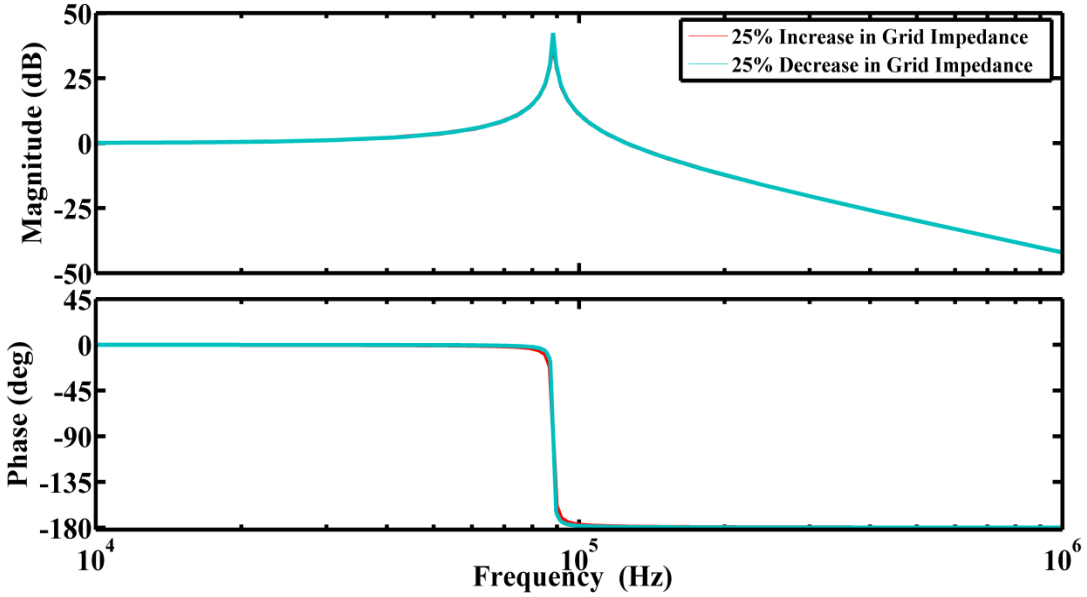

Figure 4.7. Bode Plots for the 25% variation in the Grid filter Parameters

The resonance peaks are consistent and the cutoff frequency is approximately around 10,000 Hz. The low frequencies are allowed to pass through the filter, whereas the higher frequencies are blocked as shown by the sharp decline after 10,000 Hz frequency. This also means that no frequencies greater than 10,000 Hz would be allowed to pass through. The steeper response around the cutoff frequencies is an indication of the effectiveness of the filtering action irrespective of the changes.

Fig.4.8. shows the bode plots when the utility inductor values are varied 50%. As compared to the earlier case when the inductor values were varied 25% the bode plots show an inconsistent response. There exists a frequency gap between the plots which also means that the frequencies around the cutoff frequencies would be varied resulting in an unpredictable performance of the system. The resonance peaks move towards higher frequencies as the value of the inductor is increased which is consistent with the circuit theory.However, this worst case scenario shows that the system could experience some difficulties if there exist a large increase or decrease in the utility inductor.

4.4. Bode Plots for the Variation In the Capacitor Values

One of the design limitations imposed when designing an LCL filter that the cutoff frequency of the filter must be at least 9-12 times greater than grid frequency. In addition to this it must also be half than the switching frequency of the inverter.Another design limitation is that the capacitor value should not be so large

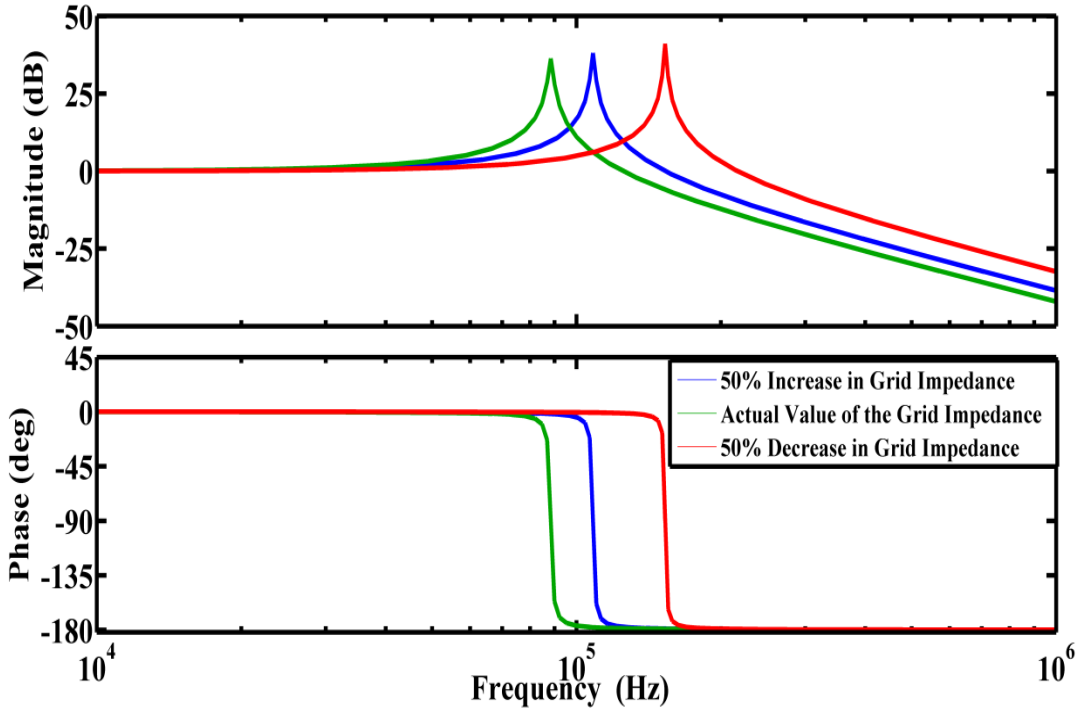

Figure 4.8. Bode Plots for the 50% variation in the Grid filter Parameters

that it causes the reduction of the power factor greater than 5%. These all design requirements arises the need to choose a capacitor value that has not only been consistent with the design requirements but would also ensure a good filtering action of an LCL filter.

The change in the capacitor values can affect the resonant frequency of the LCL filter. Thus a capacitor value can be selected according to the designed requirements of the resonant frequency. Another important aspect that affects the value of the selection of a capacitor value is the system bandwidth. However, this aspect is much more important for the design scenarios when a model predictive controller is employed as in the case of the repetitive controller[1]–[5].

Three values of the capacitances were selected and their subsequent bode plots were drawn. It can be seen from the figure that the lower the value of the capacitor, the higher is the resonant frequency. An interesting observation was made for the bode plot having the capacitor value of 80 micro Farads. The bode plot for this case is investigated further and shown separately in fig.4.9.

Fig.4.10 shows that the bode plot for the case when the capacitance has a value of a 80 micro farad. It can be seen in the figure that the phase margin is infinity as the magnitude is below zero degrees for all the frequencies.It also shows that it can lead to a problematic case when the system has to track the references. We can however make a slight modification in the system by introducing a gain in the system such that its magnitude plot shifts slightly above the current position. A dc gain is introduced in the system. The new bode plot with the dc gain added is shown in Fig. 4.11. The margin command was used to show the existence of the phase margin as the magnitude plot has shifted above the previous position of figure 4.10. Fig 4.12. shows the variation of the bode plots for the different values of the capacitors with dc gain added to the system.The bode plots show that for the capacitance value of 22 micro farads the plot is much steeper providing better attenuation as compared to the other two capacitor values.

4.5. Frequency Spectrum Analysis of Classical Controllers

Fig. 4.13 shows the frequency spectrum of an auto tuned P controller by using Fast Fourier Transform (FFT) feature of Matlab. The x axis represents the frequencies at which harmonics occur. The harmonics are predominant at the odd frequencies of 150 HZ (3^{rd} Harmonic), 250 Hz (5^{th} Harmonic), 350 Hz (7^{th} Harmonic), 450 Hz (9^{th} Harmonic), 550 Hz (11^{th} Harmonic), 650 Hz (13^{th} Harmonic) and low harmonics of

higher order at 750 Hz, 850 Hz and 950 Hz respectively. The y axis gives the magnitude of these harmonics in terms of percentage of fundamental frequency of 50 Hz.

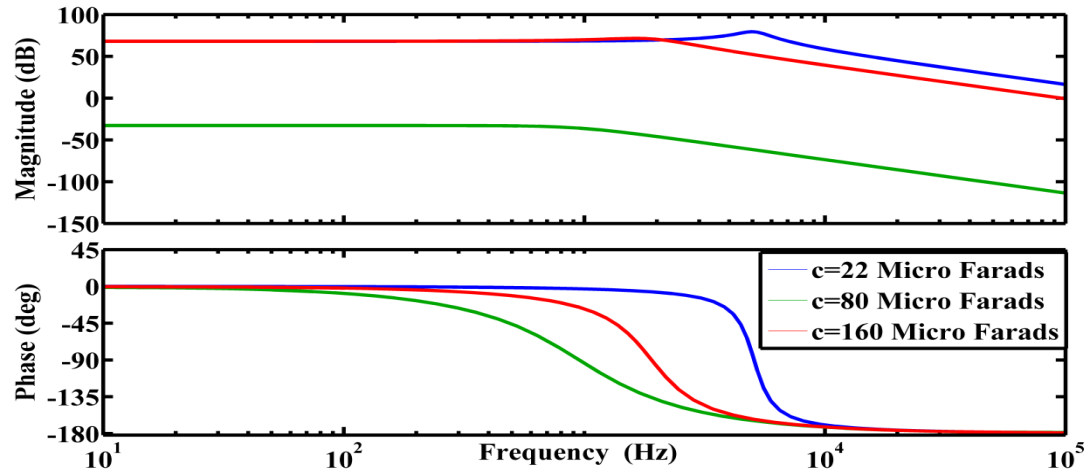

Figure 4.9. Bode Plots for the Variation in Capacitance Values

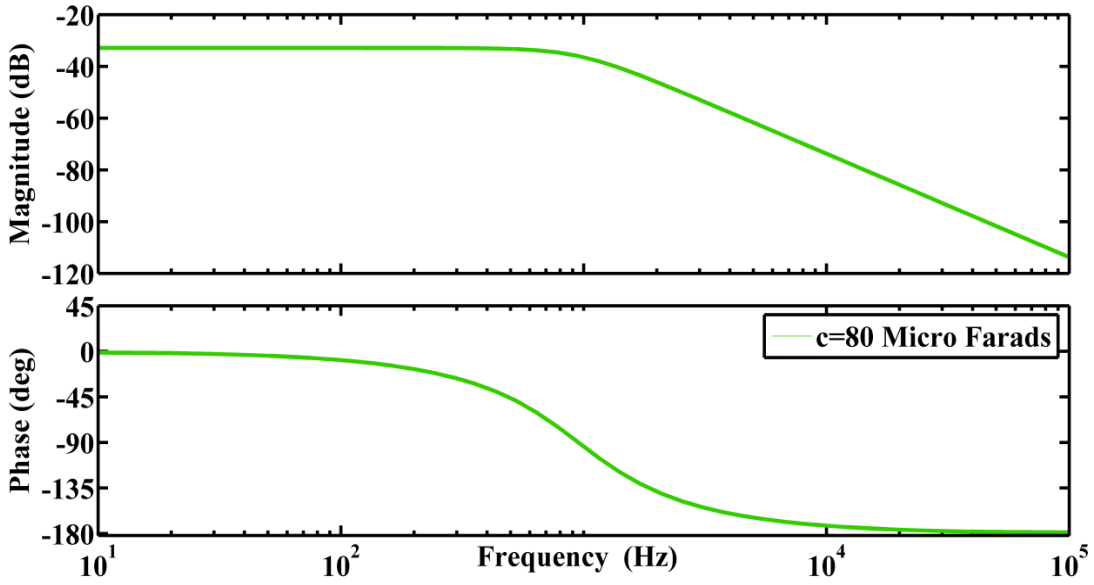

Figure 4.10. Bode Plot for the infinity Phase Margin for c=80 micro Farads

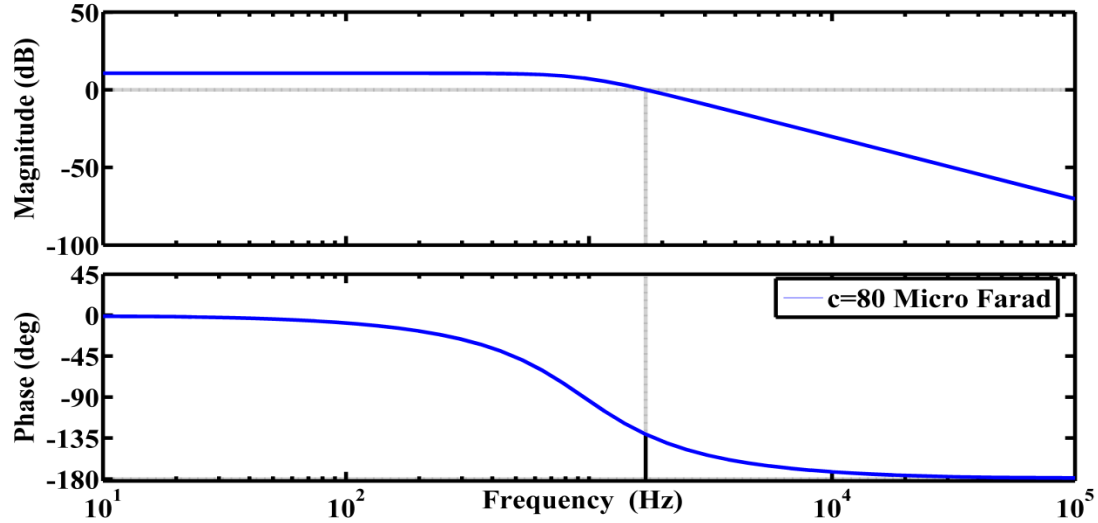

Figure 4.11. Bode Plot after addition of DC Gain for c=80 micro Farads

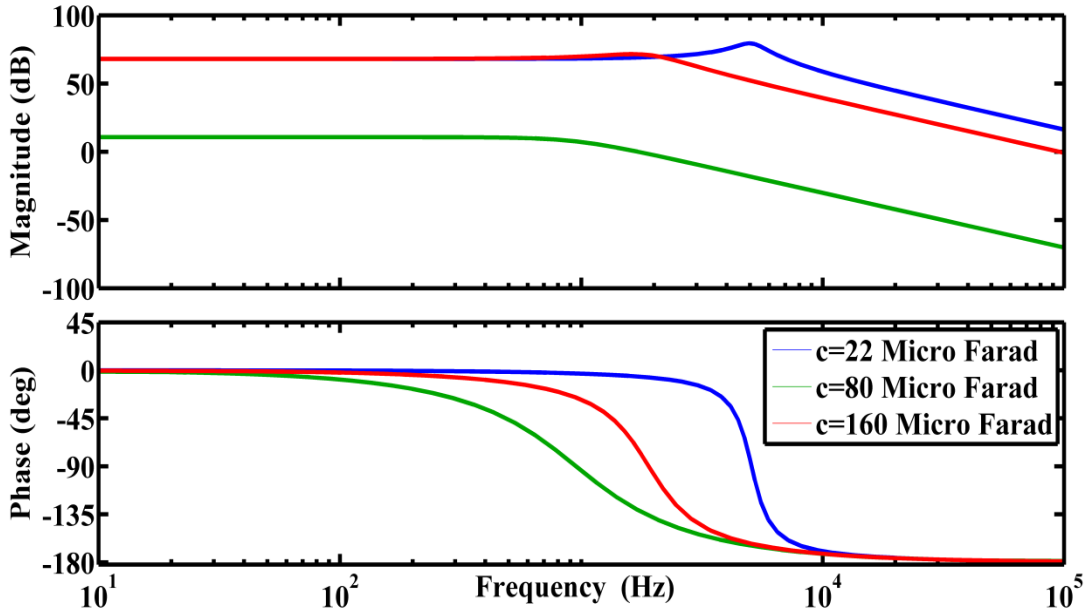

Figure 4.12. Bode Plot after addition of DC Gain for Various Capacitance Values

It is evident from the figure that the conventional P controller fails to satisfy the recommended ANSI-IEEE standards for the Total Harmonic Distortion (THD) values. In order to get a satisfactory performance and to suppress the harmonics, some intuitive designing is required.

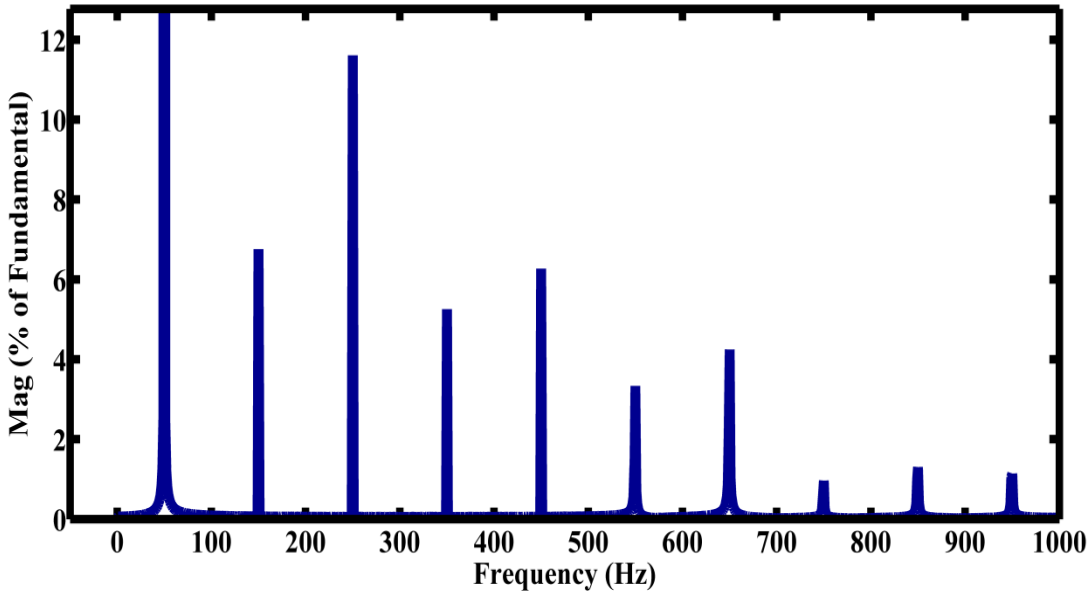

Figure 4.13. Frequency Spectrum for Auto Tuned P Controller having THD=17.54%

Fig.4.14. shows the output waveform from auto tuned P controller. It is evident from the figure that the output current was successively able to follow the reference current of 50 Amperes. However, the quality of the output current is distorted as which is clearly indicated by the distorted waveform of output current

The auto tuned P controller failed to suppress the harmonics. In order to further enhance the performance of the P controller the gain of the P controller was adjusted

to a value of P=0.243 as compared to the auto tuned value of P=0.92. This resulted in the decrease of the THD value of 17.54% to 10.03%. It is important to mention here that the decrease in the gain value of the P controller has decreased the THD value but at the cost of other characteristics of the current waveform which was evident in the form of a decrease in the percentage reference current error from 1.58% to 3%.

It also shows that the auto tuning feature focuses on the overall characteristic of the system. Since the design objective of the controller is to decrease the THD thus making the robust controller, which was achieved at the cost of an increase in the percentage reference current error of the controller. It also seconds the fact that there is always a trade off when achieving a certain performance criteria of the controller. Therefore, all the subsequent controllers would be designed intuitively with the prime focus kept on robustness provided that the other characteristics of the output also lie in an acceptable range.

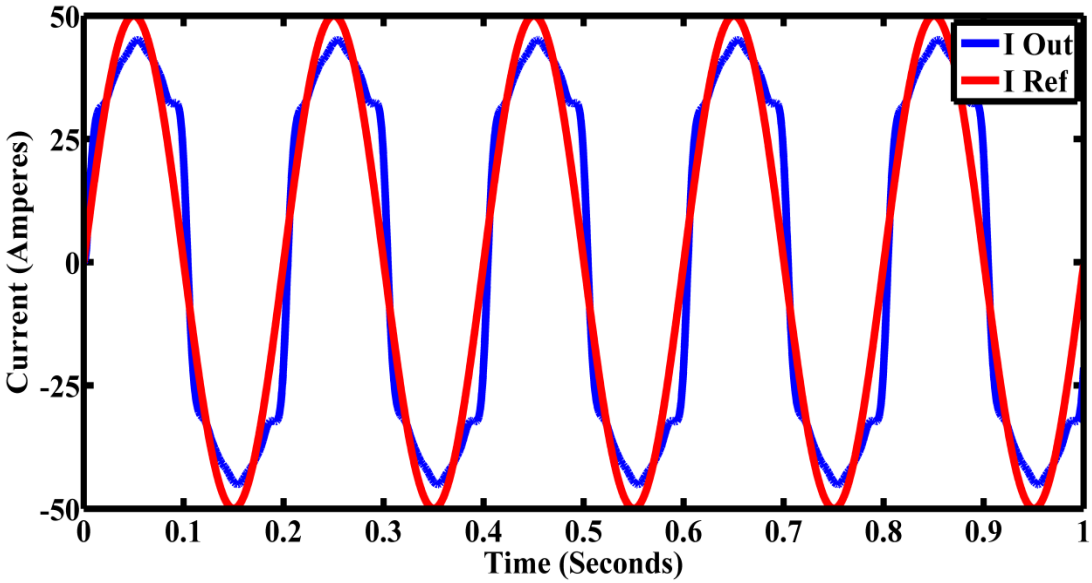

Figure 4.14. Output Waveform for Auto-Tuned P Controller

Fig.4.16. shows the output waveform from intuitively tuned P controller. It can be seen from the figure that the output waveform is less distorted as compared to the output waveform from P controller as shown in fig.4.14. However, the output waveform is less than the reference waveform which resulted in an increase of the percentage reference current error of 1.58% to 3%.

In order to further reduce the THD values to the applicable limits of ANSI-IEEE recommended values a PI Controller was designed. Fig. 4.15 shows the FFT analysis of the PI controller. The PI controller was able to suppress the THD values to 8.05% a 2 % decrease as compared to intuitively design P controller. It important to mention here that though the output waveform of PI controller is better as compared to P

controller then, when it comes to mitigation of harmonics the integral portion plays no role in the reduction of THD. Thus, for both P and PI controllers if the values of the P are kept same the output THD of the waveform would be same. However, there would be a difference in the shape of the output waveform from both controllers.

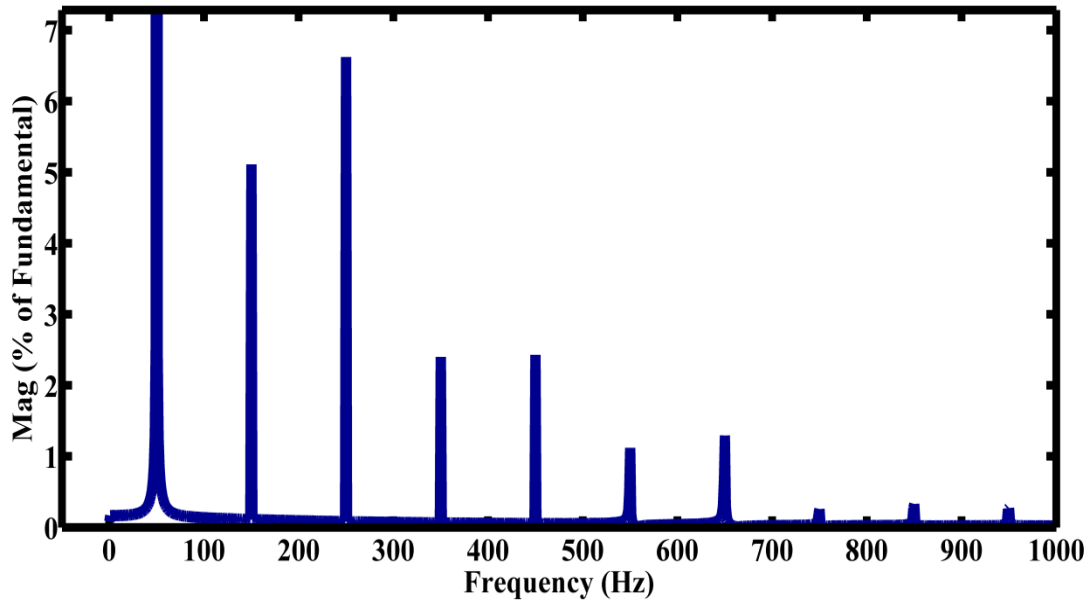

Figure 4.15. Frequency Spectrum for Manually Tuned P Controller having THD=10.03%

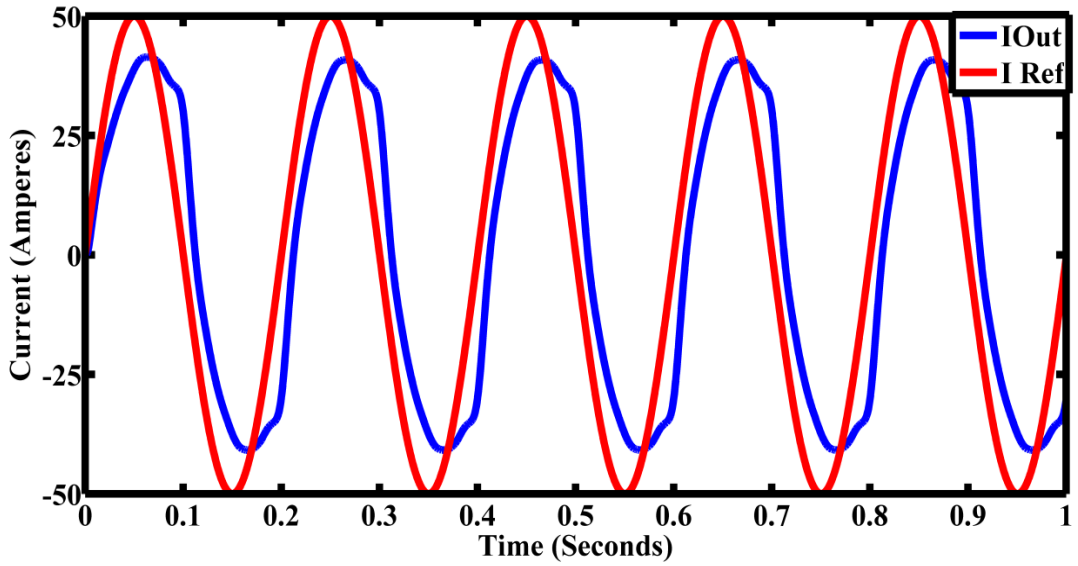

Figure 4.16. Output Waveform for Manually Tuned P Controller

The P of the PI was able to reduce the THD values, but it still failed the ANSI-IEEE recommended THD values. The odd harmonic at 250 Hz was the highest harmonic that the PI controller failed to suppress.

A Proportional Integral Derivative (PID) controller was designed in order to achieve the ANSI-IEEE standards. The PID controller not only failed to comply with the standards but its performance was also poorer as compared to the PI and intuitively tuned P controller.

It can be seen from the table that the PI controller was being able to reduce the THD to a minimum value of 8.05% among the conventional controllers. However, it produces a maximum overshoot of 10.07% as compared to other controllers. The Phase margins are more or less same for all the conventional controllers. However, a minimum gain margin was produced when using an auto tuned P controller, which was then increased to a value of 13.3 dB when it was manually tuned.

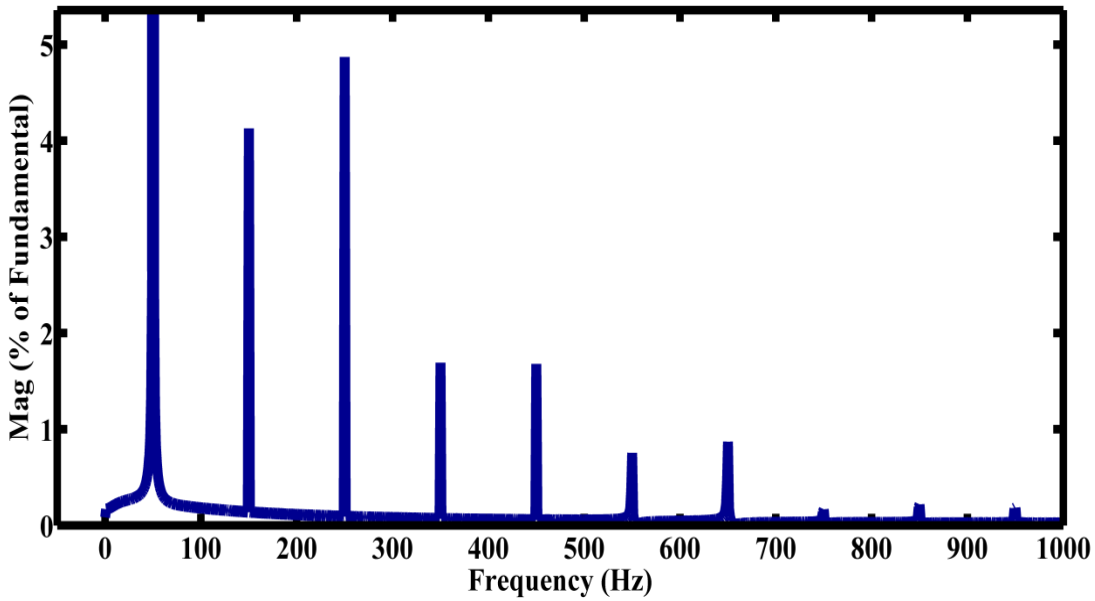

Figure 4.17. Frequency Spectrum for PI Controller having THD=8.05%

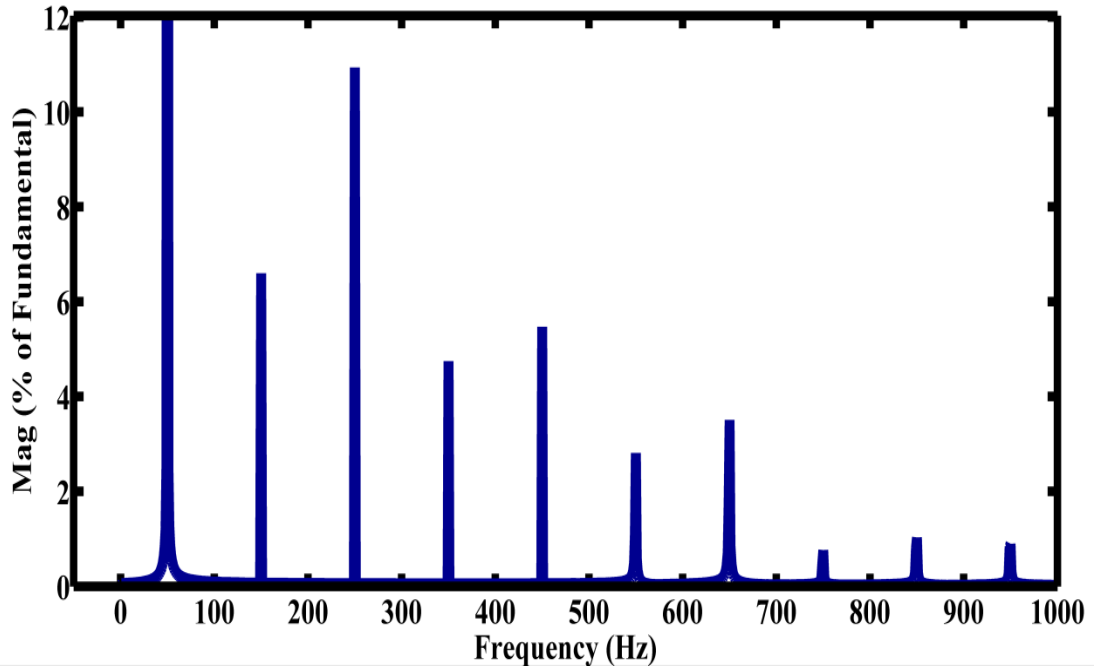

Figure 4.18. Frequency Spectrum for PID Controller having THD=16.13%

Thus the frequency spectrums of the conventional controllers show that a more advance controller is needed to be designed in order to satisfy the performance criteria of ANSI-IEEE standards of THD.

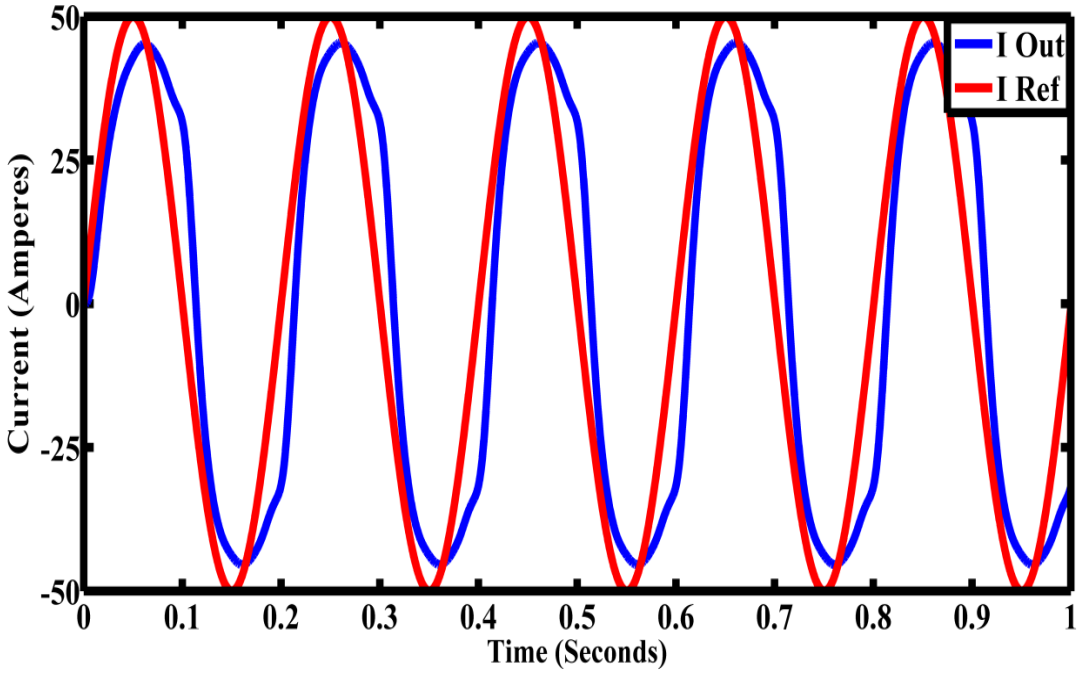

Figure 4.19. Output Waveform for PID Controller

Table 4.4. Characteristics of the Conventional Controller

S.No.	Parameters	P Controller (Auto Tuned) P=0.92	P Controller (Manually Tuned) P=0.243	PI Controller P=0.18 I=14.67	PID Controller P=0.861 I=-25.83 D=0.007
1.	Rise time	0.000831 Sec	0.003643 Sec	0.00346 Sec	0.000719 Sec
2.	Settling time	0.00448 Sec	0.00643 Sec	0.0292 Sec	0.0013 Sec
3.	Overshoot	3.31%	0%	10.7%	0.89%
4.	Peak	1.03	1	1.11	1.01
5.	Gain margin	1.88 dB @ 3.19e04 rad/sec	13.43 dB @ 3.19e04 rad/sec	16 dB @ 3.19e04 rad/sec	18.3 dB @ 1.77e04 rad/sec
6.	Phase margin	89.9 dB @ 2.31e03 rad/sec	89.9 dB 608 rad/sec	80 dB @ 482 rad/sec	87 dB @344e03 rad/sec
7.	Close loop	Stable	Stable	Stable	Stable
8.	Total Harmonic Distortion Values	17.54%	10.03%	8.05%	16.13%

4.6. Summary

In this chapter the robustness of the classical controllers was being investigated by varying the LCL filter values. The bode plots showed that the classical controllers were able to handle the slight variations. However, they failed to satisfy the ANSI-IEEE recommended THD values which show that a more advance controller is needed to be designed in order to satisfy the performance criteria of IEEE.

References

[1] M. Jamil, B. Hussain, R. J. Boltryk, and S. M. Sharkh, “Microgrid Power Electronic Converters : State of the Art and Future Challenges,” 2009.

[2] M. a. Abusara, M. Jamil, and S. M. Sharkh, “Repetitive current control of an interleaved grid-connected inverter,” *2012 3rd IEEE Int. Symp. Power Electron. Distrib. Gener. Syst.*, pp. 558–563, Jun. 2012.

[3] M. A. Abusara and S. M. Sharkh, “Design and control of a grid-connected interleaved inverter,” *IEEE Trans. Power Electron.*, vol. 28, pp. 748–764, 2013.

[4] D. Chen, J. Zhang, and Z. Qian, “An improved repetitive control scheme for grid-connected inverter with frequency-adaptive capability,” *IEEE Trans. Ind. Electron.*, vol. 60, pp. 814–823, 2013.

[5] S. Jiang and F. Z. Peng, “Repetitive control of grid-connected inverter using a high resonance frequency LCL filter,” in *2013 Twenty-Eighth Annual IEEE Applied Power Electronics Conference and Exposition (APEC)*, 2013, pp. 2781–2787.

Chapter 5

Optimal (LQR) and Proportional Resonant Controller

5.1. Frequency Response of Proportional Resonant Controller

The Proportional Resonant (PR) controller's behavior was studied by looking at the bode plots when changing each parameter. As seen from the figure the gain of the controller increases, whereas the bandwidth stays constant as *Ki* is changed from 10 to 10000. The value of *Kp* and ζ is taken as zero.

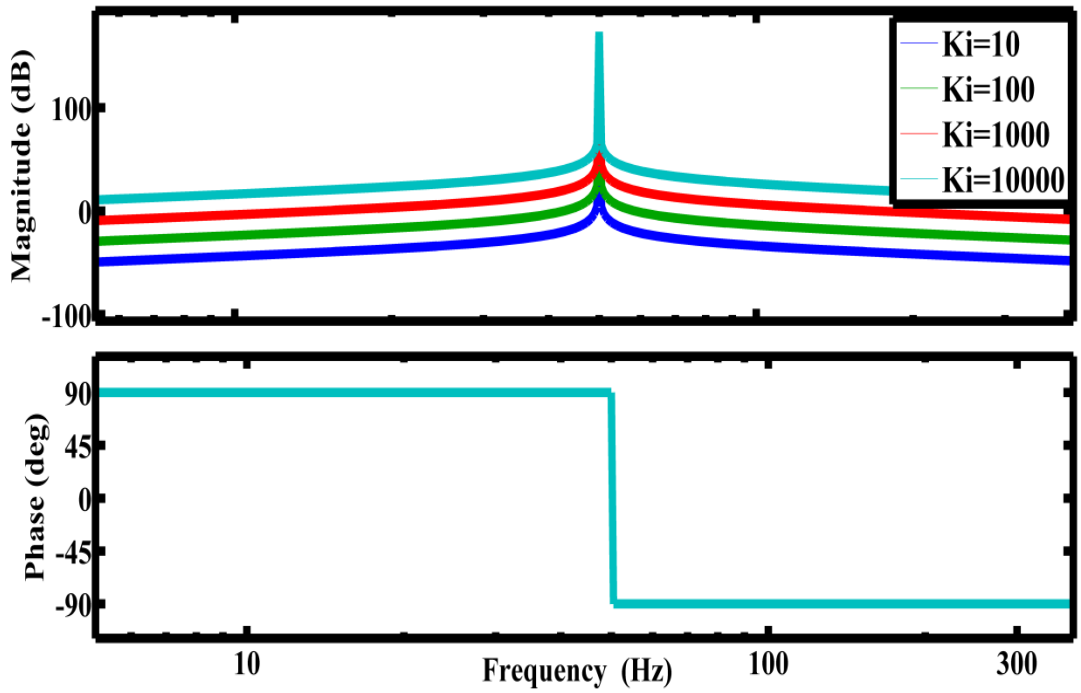

Figure 5.1. Frequency response of Proportional Resonant controller when ki Changes

The frequency response of the PR controller when K_p changes from 1 to 1000 is shown in the figure. It can be seen from the figure gain at all the frequencies tend to increase as the value of K_p is increased, but results in the decrease of the bandwidth along with the decrease in the amplitude of the phase.

The quality factor Q and the damping ratio ζ are given by;

$$\zeta = \frac{1}{2Q} \tag{5.1}$$

$$G_{PR}(s) = K_p + \frac{K_i \omega_0 s}{s^2 + \left(\frac{\omega_0}{Q}\right)s + \omega_0^2} \tag{5.2}$$

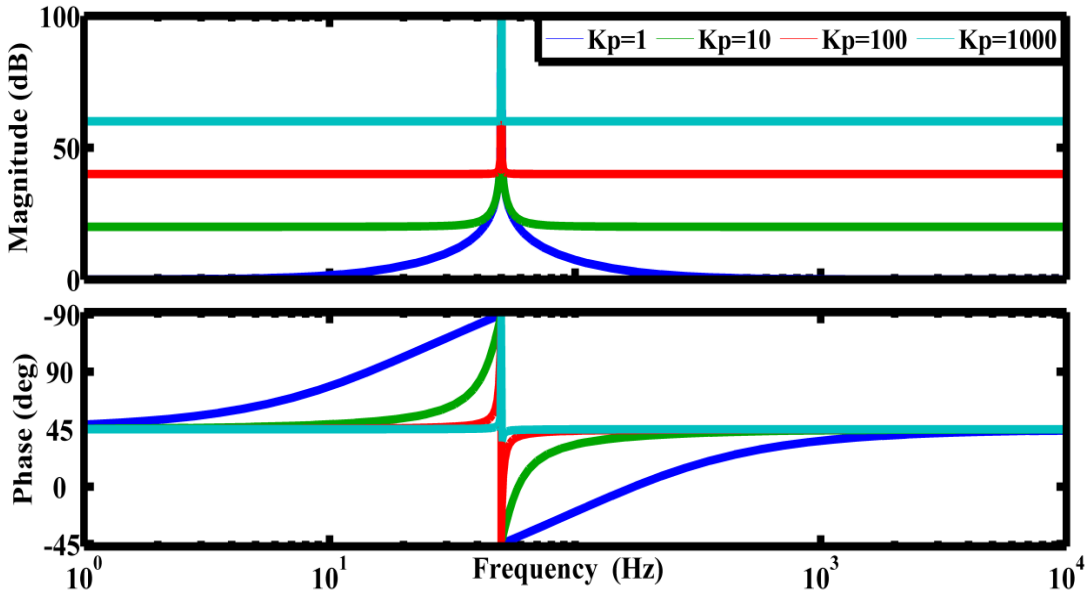

Figure 5.2. Frequency Response of Proportional Resonant Controller When K_p Changes

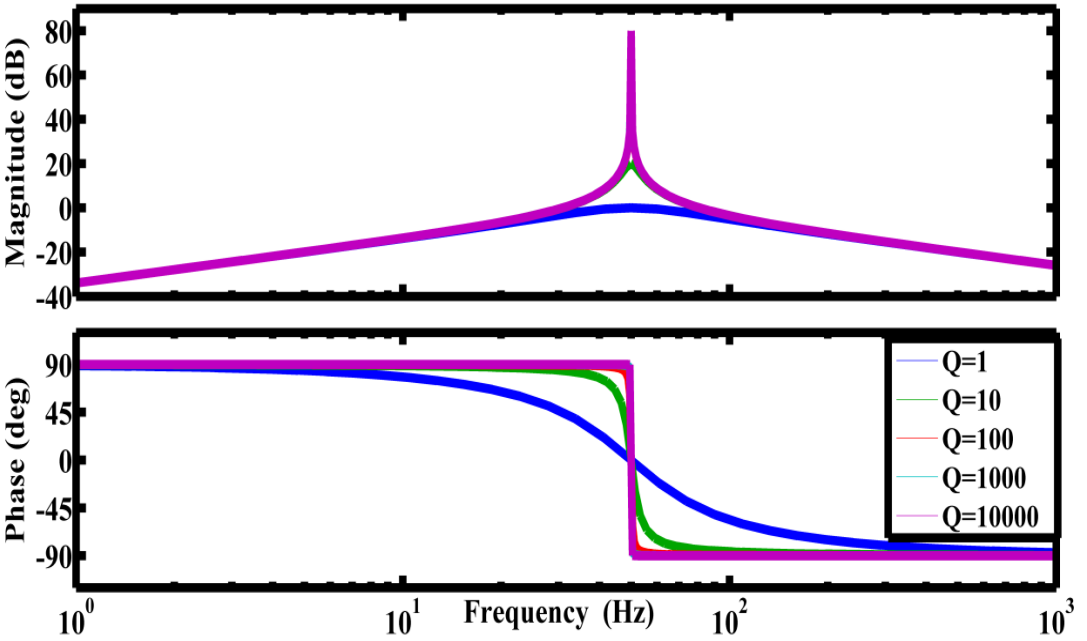

Figure 5.3. Frequency Response of Proportional Resonant Controller When Q Changes

As shown in the figure, with increase in Q, the peaking magnitude at the resonant frequency increases. In order words, greater the quality factor the more closely the PR behavior is to an ideal PR controller that provides an infinite gain at the resonant frequency. However, due to the stability issues the values of the quality factor are usually a tradeoff and therefore a suitable value of Q is selected that gives a satisfactory performance.

The infinite gain of the ideal Proportional Resonant (PR) controller gives rise to the stability problems. Also, it leads to an ideal quality of the GCI which is non-

realizable in real time situations. For this purpose a modified PR controller is used whose gain is a finite value thus mitigating the stability problems[1][2][3][4][5].

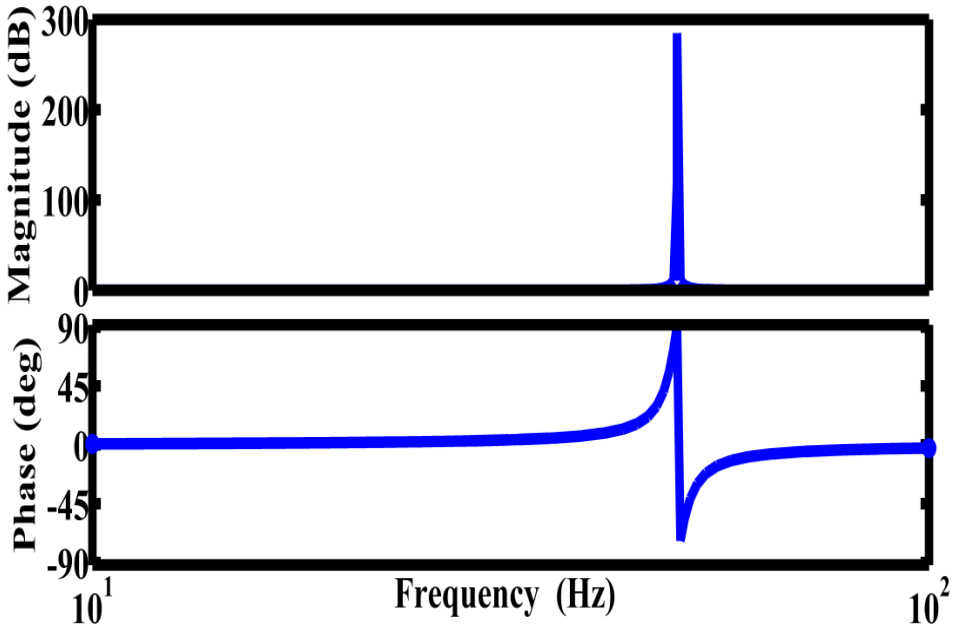

Figure 5.4. Bode diagram of the Ideal Proportional Resonant Controller with K_i =1 ζ =10 ws =314 rad sec^{-1}

The modified PR controller can also be adjusted to make it less susceptible to the frequency changes in the utility. The transfer function of the modified PR controller is given by

$$G_{PR(\text{modified})}(s) = K_p + \frac{K_i s}{s^2 + 2\zeta ws + w^2} \tag{5.3}$$

The inclusion of damping term has two benefits. It decreases the infinite gain at the fundamental frequency to a realizable finite value and also improves the bandwidth of the modified PR controller. The bode plot for the modified PR controller is shown in Fig. 5.5.

5.2. Linear Quadratic Regulator

The situation where a set of linear differential equations get involved in order to define a dynamic system along with the quadratic function to tackle with the cost is known as Linear Quadratic problem. This implies that the controller settings overseeing a system are considered by utilizing a mathematical calculation that reduces the value of the cost function with the help of weighting variables delivered by an engineer. The cost function is regularly characterized as an aggregate of the deviations of key estimations from their coveted qualities. Basically**,** this calculation Essentially, the LQR calculations deal with the monotonous work done by engineers.

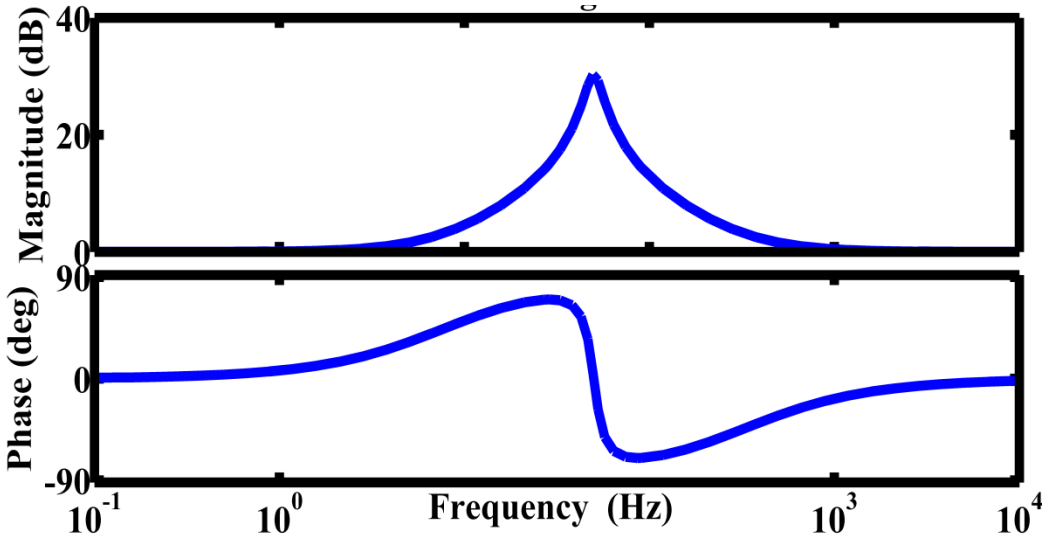

Figure 5.5. Bode diagram of the Modified Proportional Resonant Controller K_i =10 ζ =0.01 *ws* =10 rad sec^{-1} *w* =314 rad sec^{-1}

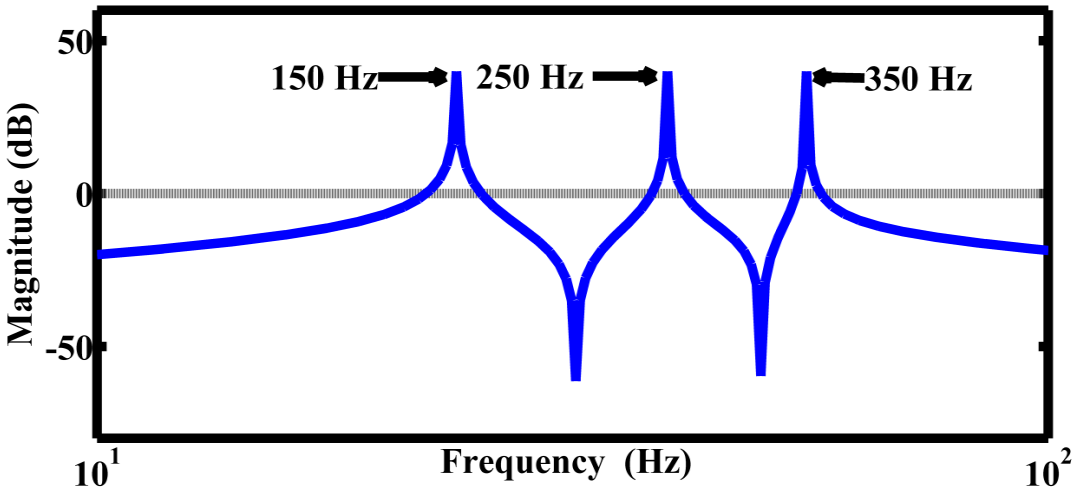

Figure 5.6. Proportional Resonant Controller Gains at Harmonic Frequencies K_i =10 ζ =0.01 *ws* =10 rad sec^{-1} *w* =314 rad sec^{-1}

Notwithstanding, there is still a need to determine the weighting factors and then comparing the outcomes with required objectives. This implies that this algorithm will in any case be an iterative methodology where the engineer determines the generated "optimal" controllers by taking advantage of simulations and after that modifies the weighting components to get a controller increasingly in accordance with the specified outline objectives. Thus, LQR calculation is, at its center, simply a mechanized method for uncovering a proper state-feedback controller. A basic flow chart for the LQR controller is shown in the given figure. Several new optimizing methods to optimize LQR have also been applied recently[6][7][8].

LQR approach is helpful in weighing factor of performance index in accordance with the designer's desires and constraints. For state space LQR controller design, equations and state variables are established in equations respectively.

5.3. Frequency Spectrum Analysis of Optimal Controllers

5.3.1. Frequency Spectrum Analysis of Proportional Resonant Controller

A novel Proportional Resonant (PR) controller was designed using Harmonic Compensators (HC) for higher order harmonics. The frequency spectrum analysis was obtained as shown in Figure 5.8.

As shown in the Figure that the PR controller was able to achieve the prescribed limits of ANSI-IEEE of 5% of THD. The highest harmonic was observed at 250 Hz (5th Harmonic) with the magnitude of 3.4% of the fundamental frequency. By using the PR controller THD is 0.4 % less than the prescribed limits of recommended THD values. As it was stated earlier the increase in the performance of the controller was achieved at the cost of the increased complexity at the same time.

5.3.2. Frequency Spectrum Analysis of Linear Quadratic Regulator (LQR)

The frequency spectrum analysis of the conventional controllers showed that they were unable to meet the operating requirements. In order to reduce the THD to the acceptable limits a Linear Quadratic Regulator (LQR) was designed. The state space model was achieved by using the state space block of Matlab. The values of the gain are given by

Q=[0.5 0 0; 0 135 0; 0 0 10000000]

R=0.3

Fig. 5.9. shows the frequency spectrum of a LQR. The LQR though successively reduced the THD to 4.51%. It is important to note that adjusting the gains of a LQR controller is an iterative process and there is no hard fast rule that states how they should be adjusted. After a trial and error process the LQR controller was being adjusted so that it can reduce the THD to 4.51% as compared to 8.05% of a PI controller.

A further adjustment in the gains may have reduced the THD limits further, but it results in the severe performance degradation of the LQR. Therefore, the gain of an LQR was being kept such that it achieves a THD of 4.51%.

Fig.5.11 summarizes the THD values for the different current controllers that were designed. It can be seen from the figure that the allowed IEEE THD values is 5% and the only controllers that are able to keep the THD values under this limit are optimal controllers PR and LQR. Therefore in the presence of the utility harmonics the classical controllers failed to satisfy the IEEE limits.

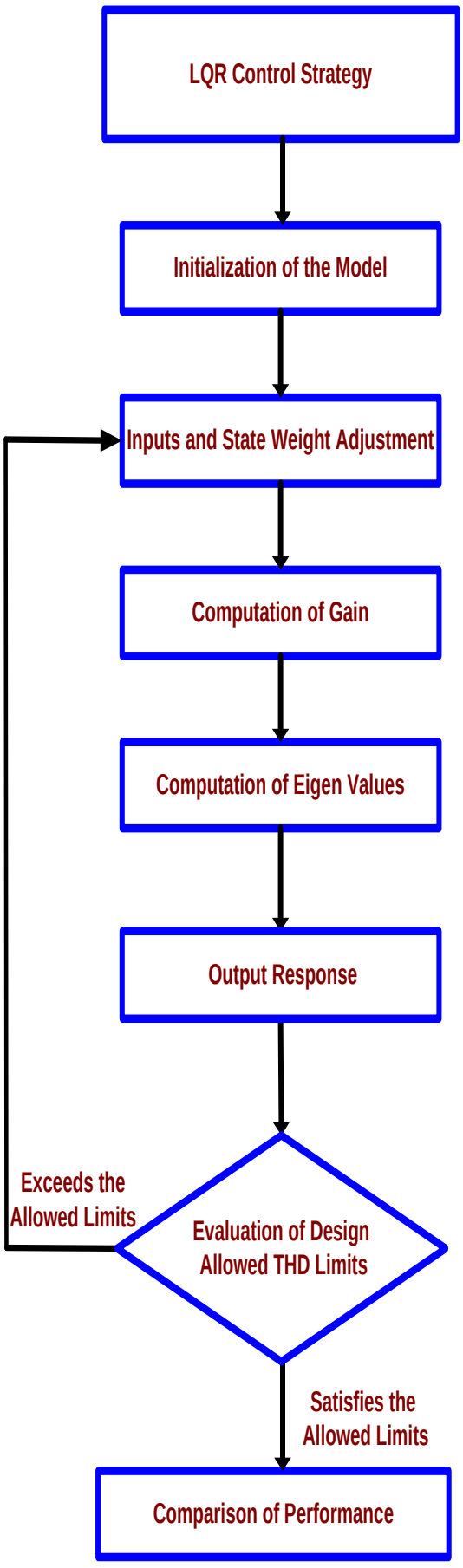

Figure 5.7. Flow Chart for the LQR Algorithm

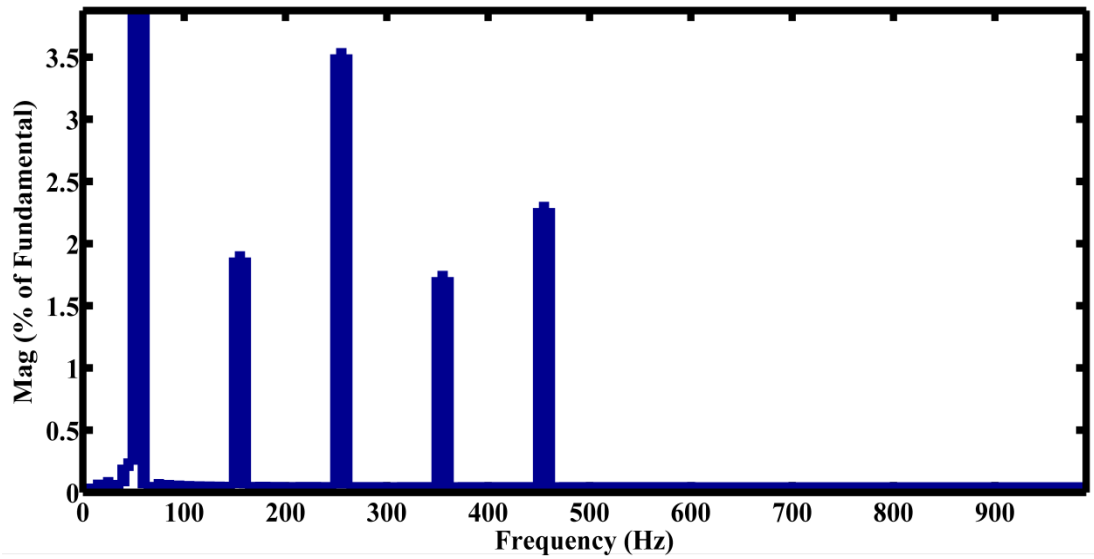

Figure 5.8. Frequency Spectrum for Proportional Resonant Controller having THD 4.96%

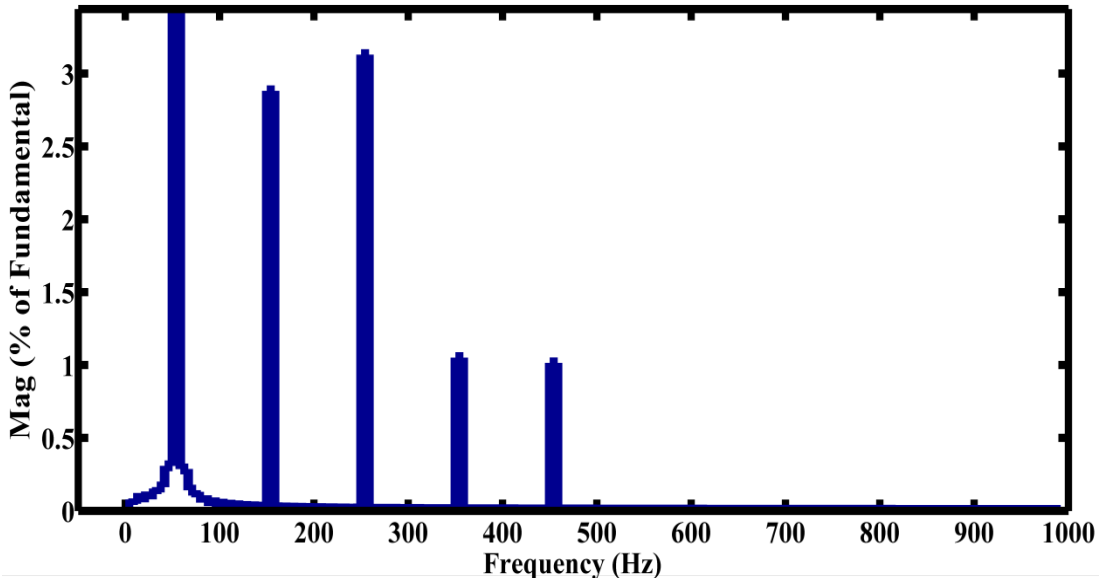

Figure 5.9. Frequency Spectrum for LQR having THD 4.51%

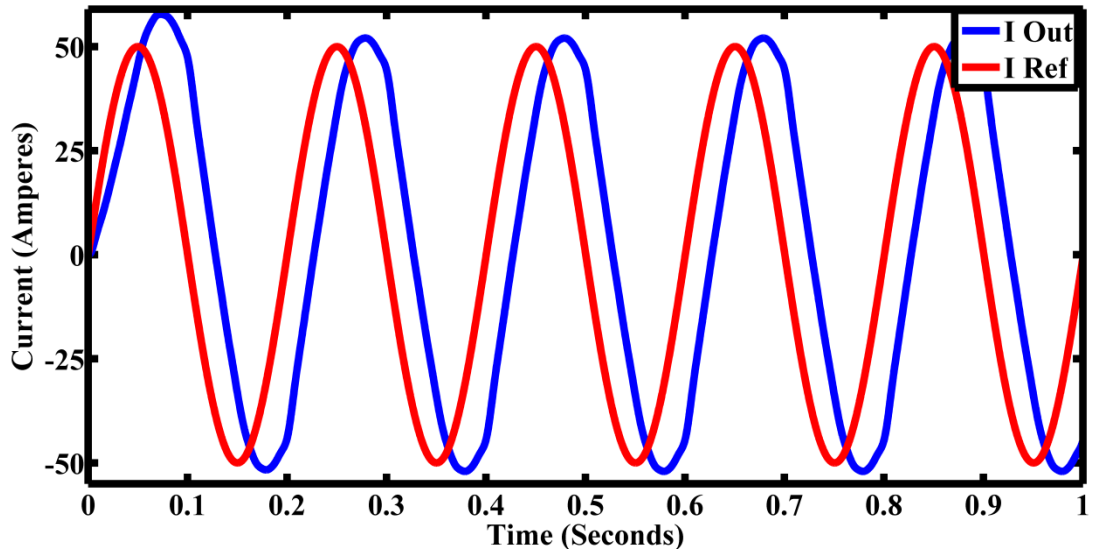

Figure 5.10. Output Waveform of LQR Controller

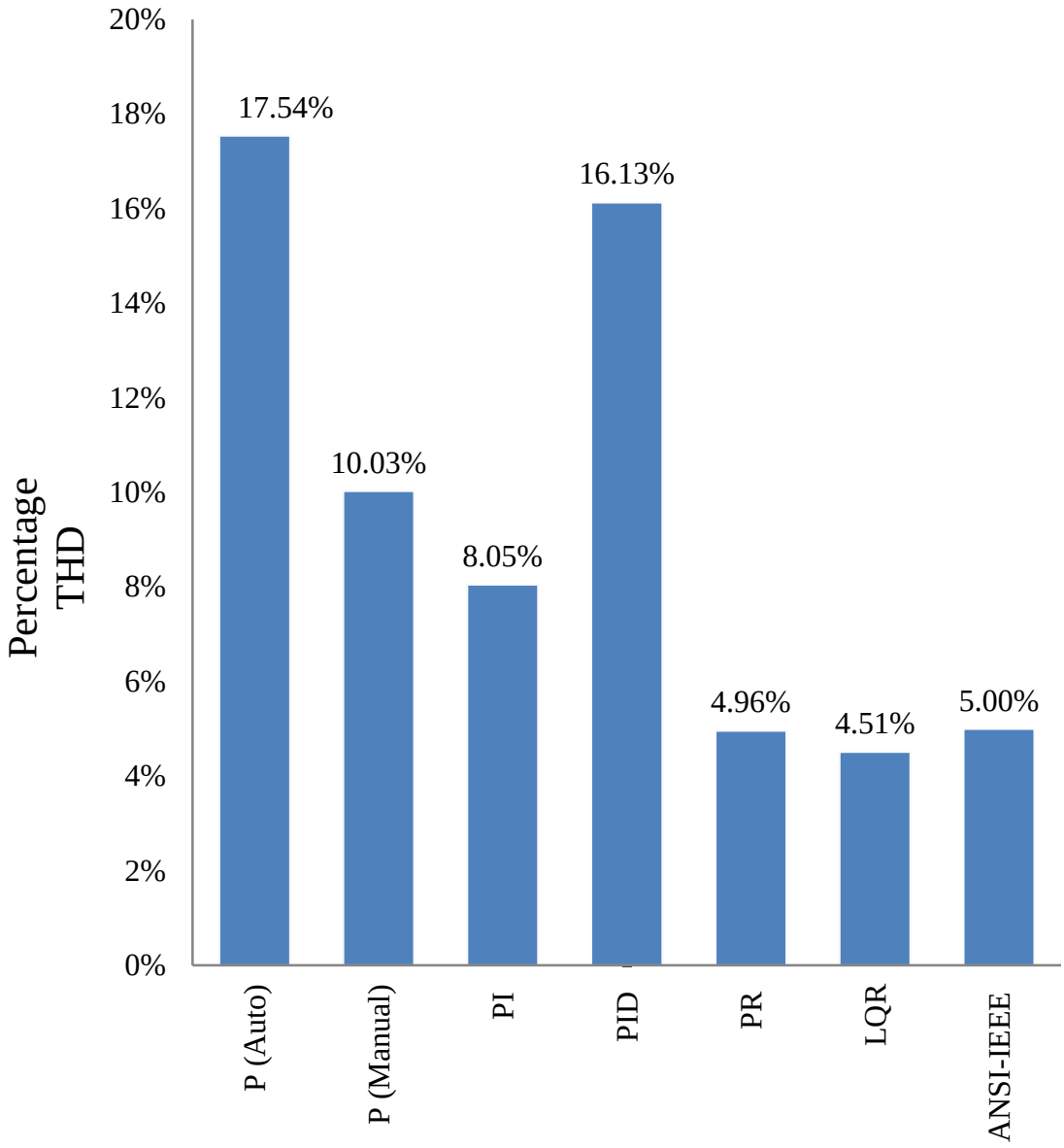

Figure 5.11. THD Values for the Designed Current Controllers

5.4. Conclusions

- The overall aim of this research has been to investigate the performance of current controllers of utility connected two-level Pulse Width Modulated LCL filter based grid connected inverters.
- Effect of gain on open loop root locus plot was being studied and the value of the inner loop gain was selected to produce a stable response.
- Classical controllers were being stimulated and the simulation results reveal that it is difficult to produce an output current according to the standards of IEEE as the gain at the harmonic frequency of interest is not high enough. Thus, it was concluded that the classical controllers fail to suppress the utility

harmonics and advance controllers are needed to suppress the utility harmonics.

- Proportional Resonant controllers were being investigated and two types of PR were being simulated. It was found that the ideal proportional resonant controller tends to produce higher gains at the desired frequencies. However, these values of gains are very high and they tend to make the system unstable. In addition to that a sharp ideal cut off frequency also tend to produce difficulties during practical implementation.
- In order to address the issues of ideal PR a modified PR was used to mitigate the harmonics at the desired frequencies. The results showed that the gains produced at the desired frequencies were able to effectively mitigate the utility harmonics.
- The Frequency response of both Optimal Controllers (PR and LQR) showed that both controllers were being able to satisfy the IEEE standards in the output current.

5.5. Suggestions for future work:

- In this thesis optimal controllers were being investigated separately. However, a hybrid controller employing a combination of controllers can also be an exciting area to carry out research.
- The results of this research can be further extended in the form of investigation on the performance of designed controllers in the presence of noise and random perturbations.
- The application of optimal controllers for other topologies such as multilevel utility connected inverters could be another interesting area for further research.
- The application of genetic algorithms to the LQR controllers can also be an exciting area to carry research on.

References

[1] K. Zhou, Y. Yang, F. Blaabjerg, W. Lu, and D. Wang, “Selective Harmonic Control for Power Converters,” no. 2, pp. 4–8, 2014.

[2] J. Kwon, X. Wang, and F. Blaabjerg, “Impedance Based Analysis and Design of Harmonic Resonant Controller for a Wide Range of Grid Impedance,” 2014.

[3] Y. Yang and S. Member, “Benchmarking of Grid Fault Modes in Single-Phase Grid-Connected Photovoltaic Systems Frede Blaabjerg.”2015

[4] X. Wang and P. C. Loh, “Design-Oriented Analysis of Resonance Damping and Harmonic Compensation for LCL-Filtered Voltage Source Converters,” pp. 216–223, 2014.

[5] X. Wang, M. Liserre, H. S. H. Chung, W. Wu, Y. Sun, M. Huang, H. Wang, and F. Blaabjerg, “A Robust Passive Damping Method for LLCL -Filter-Based Grid-Tied Inverters to Minimize,” vol. 29, no. 7, pp. 3279–3289, 2014.

[6] C. Olalla, R. Leyva, A. El Aroudi, and I. Queinnec, “Robust LQR control for PWM converters: An LMI approach,” *IEEE Trans. Ind. Electron.*, vol. 56, pp. 2548–2558, 2012.

[7] D. Karaboga and B. Basturk, “On the performance of artificial bee colony (ABC) algorithm,” *Appl. Soft Comput.*, vol. 8, no. 1, pp. 687–697, Jan. 2012.

[8] K. Hassani and W. Lee, “Optimal Tuning of Linear Quadratic Regulators Using Quantum Particle Swarm Optimization,” no. 59, pp. 1–8, 2014.

Submitted in "2015 International Conference on Alternative Energy in Developing Countries and Emerging Economies (2015 AEDCEE)", May 28-29, 2015, Bangkok, Thailand

Annexure I

Issues Challenges and Solutions for the Energy Crisis of Pakistan

[a)] Gussan Maaz Mufti[1] [b)] Dr. Mohsin Jamil [2] [a)] Dr. Adeel Waqas [1]

[1] Center for Energy Systems Engineering (CES) NUST, Address; NUST H-12 Islamabad, Pakistan

[2] School of Mechanical and Manufacturing Engineering (SMME) NUST, Address; NUST H-12 Islamabad, Pakistan

Abstract: Pakistan is an energy deficient country and the current power crisis of Pakistan is hampering its economic development. This article investigates the main causes that have led to the current power shortage of Pakistan. An overview is given to the major causes such as ineffective power policies, ineffective distribution system and tariff system that have led to the current power shortage in Pakistan. Additionally, the possible measures that can help to address these issues and help Pakistan overcome its power crisis are also presented.

Keywords: Energy, Power crisis, Generation Companies, Distribution Companies, Power Policy.

1. Introduction:

In the modern world, the industrial development plays an important role in the development of every country. The industrial development in turn depends on a reliable electricity supply[1]. The increasing worldwide demand for energy increased the concerns of the different countries regarding their energy security. Due to this, the focus is now shifting on the diversification, generation and efficient allocation of the energy sources. These problems can be addressed by achieving optimal energy mix through changes in fuel consumption, by promoting energy efficiency and an effective integration of the renewable energy sources. For a developing economy like Pakistan, with a high population growth rate, it is important to maintain a balance

Author to whom correspondence should be addressed. Electronic mail: 12gussanmufti@ces.nust.edu.pk

between energy supply and demand as energy consumption is directly linked to the economic growth of a country. In recent years, economists have worked on finding the relationship between the two entities[2][3].The studies[4][5] noted that Gross Domestic Product (GDP) of Pakistan is directly linked to energy in the country which was found to be thirty percent. In their findings, they recommended to increase the generation capacity based on the growing needs of the industrial sector, agricultural sector and domestic sector in order to achieve sustainable economic growth.

Fig. No. 1. shows a relationship in which it is seen that Per capita energy consumption in developed countries and their Gross National Product (GNP) is much higher than in countries with low incomes[6]. A sharp fall from fifteen to ten percent of the investment in the GDP ratio for Pakistan between 2008 and 2013 was observed as contrary to other South Asian countries.

All these reports and figures further strengthen the notion that the energy crisis of Pakistan is the main cause in the declination of the exports as well as hampering the economic development of the country. A deep investigation into its root causes and practical implementation of their solutions both for small as well as large scale is essential for the economic growth of Pakistan.

2. Issues and Challenges for the Energy Sector of Pakistan:

Fig. No. 2. shows the power hierarchy of Pakistan. The current power crisis of Pakistan is not only due to the mismanagement and negligence in the past ten to fifteen years only. In fact, it is the lack of foresightedness, short term solutions and non-coherent power policies which extend along over a quarter of a century. It is likely that power shortage will increase to 8000 MW by 2017 and rise to over 13,000 MW in 2020[7].

I. Short Sighted Power Policies:

A policy decision was made in 1987 that banned Water and Power Development Authority (WAPDA) from investing in thermal generation plants. The policy, though novel in its approach resulted in the shortages of power. Thus, this change in policy was reflected in the form of power deficiency that had already begun to create serious problems in the early 90s, when the power shortages were experienced. WAPDA and Karachi Electric Supply Corporation (KESCO) were responsible for

the power supply of the whole country and they were suffering from large losses due to corruption, inefficiency and bad governance of these entities. On the other hand, the government was not able to invest in new projects in its capacity building due to the financial constraints. Even the up gradation and modernization of existing plants was not possible. Therefore, in order to reform the energy sector, the government turned to the private entities. It was the fore seed that a competition from the introduction of the private firms would result in the better performance of the public sector energy entities. The power policy of 1994 provided generous incentives for

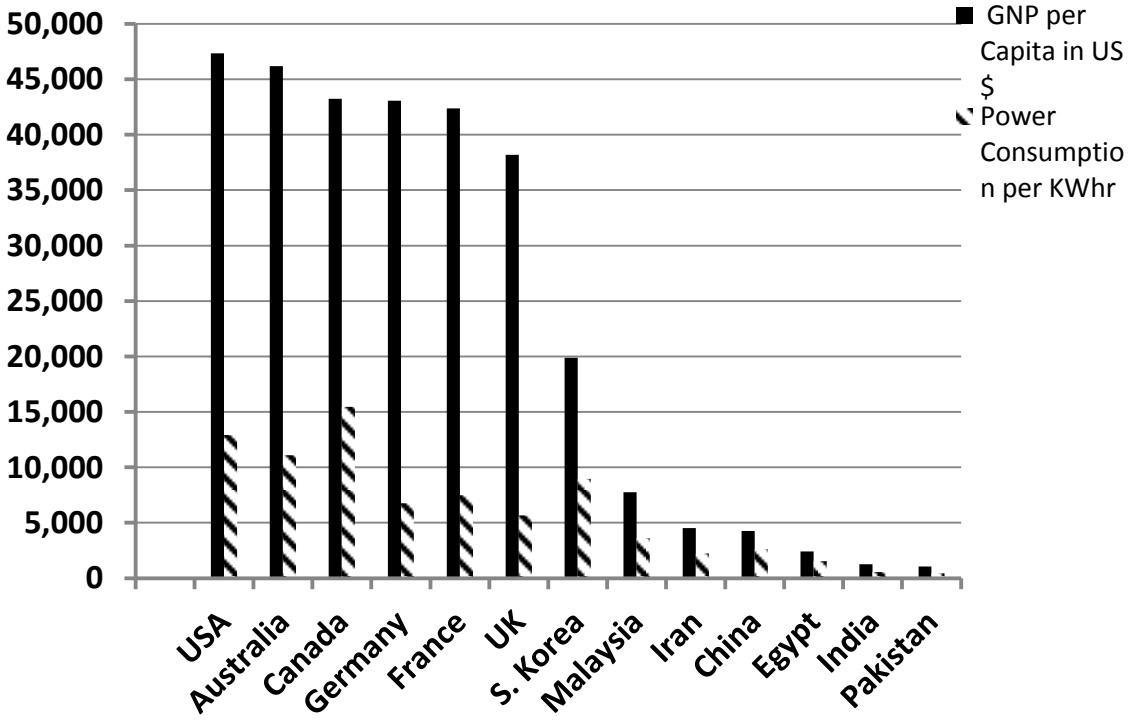

Fig. No. 1 Per Capita Energy Consumption and Gross National Product of Different Countries

Independent Power Plants (IPP) that resulted in the attraction of investments and increasing the production capacity of the system[8].

However, the power policy in 1994 was based on a more expensive generation mix mostly from oil. The oil based generated power was more costly and the increase in tariffs were not the true reflection of the cost that WAPDA had to bear. This resulted in adversing the WAPDA's finances. The energy policy of 2002 like that of 1994 continued these policies without any preference given to the source used for energy

production. This resulted in the private sector happily relying on the thermal power plants that used exported and expensive furnace oil along with natural gas. A major flaw in both the energy policies was that in spite of the incentives given to the IPPPs there was no concern shown by the government about the efficiency at which they were operating. It was the major factor that the power plants continued to run without having any check or balance on the efficiency under which they were operational.

In short, the energy policies formulated and followed during the last two decades have led to the current crisis, because of the high costs and an unsustainable energy production, resulting from a thermal based generation fuel mix.

II. Inefficient Distribution System:

WAPDA was disintegrated into eight distribution companies (DISCOs) under the reforms of 1992 policy to improve distribution services and to improve the recovery of their debts to strengthen its financial position. It was expected that independently operating generation companies having professionally qualified executives will guarantee better results and lower losses than bureaucratically run WAPDA. Unfortunately, these targets were not met. In Pakistan the values for the transmission and distribution losses are higher as compared to other countries as shown in Table No. 1[9]. Electricity theft commonly called as administrative losses, has reached new heights in the recent times[10]. Many of the DISCOs as shown in Table No. 2 continue to show distribution losses from 20% to 40%, which are very high as compared to other well performing (DISCOs[10]).

III. Tariffs:

The National Electric Power Regulatory Authority (NEPRA) is the regulatory body that determines the tariffs of each DISCO, which is forwarded to the government that notifies a unified tariff. Due to a high generation cost and losses there is a difference between the tariffs determined by the NEPRA and the tariffs that are announced by the government to be charged from consumers. This difference is paid by the government in the form of the subsidy. Despite substantial tariff increases over the last four years, this gap continues to increase. The inability of the government to pay the differential cost to the DISCOs results in the form of the circular debt.

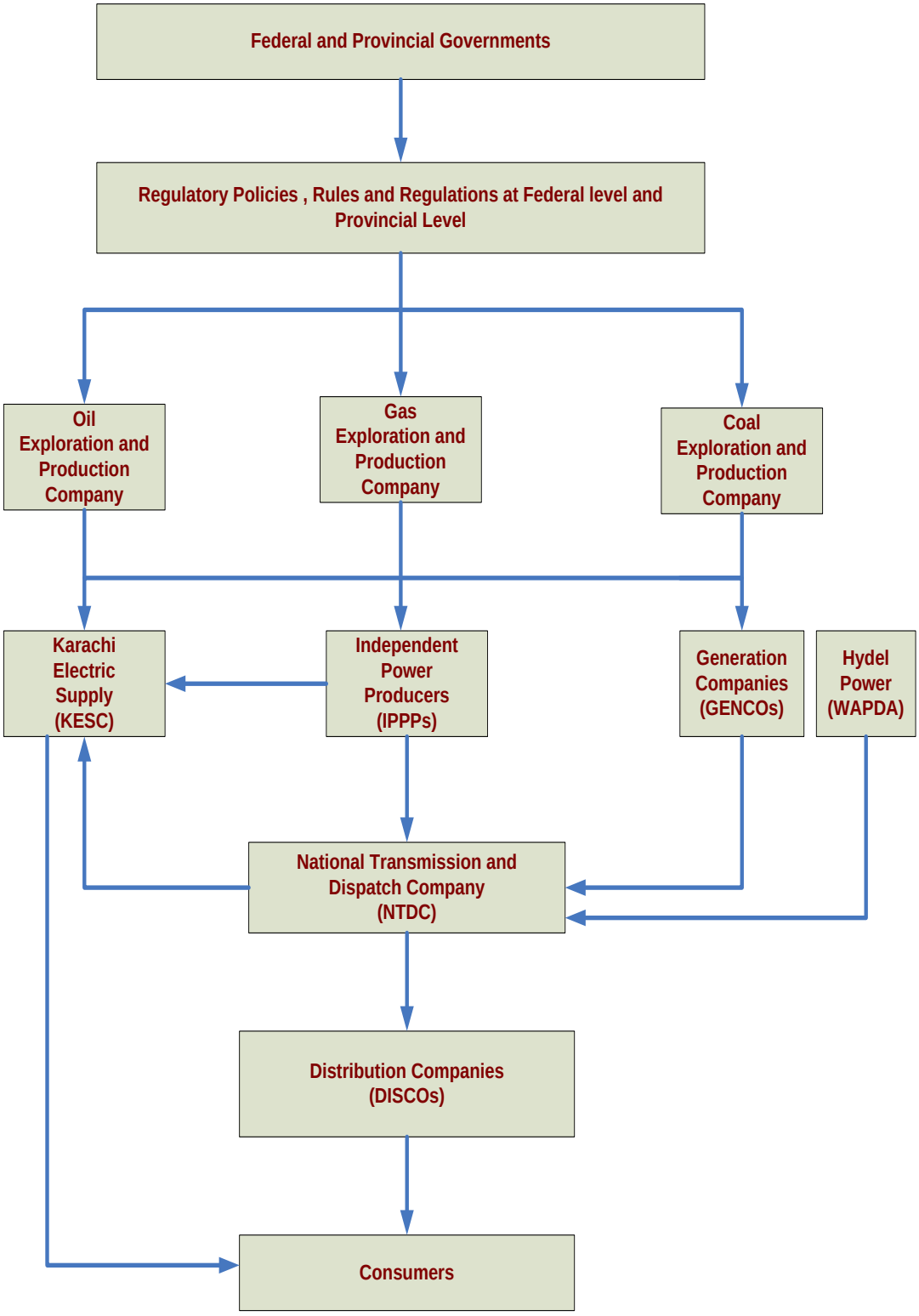

Fig. No. 2 Power Structure of Pakistan

Table No: 1 Transmission and distribution Losses of Different Countries

S.NO.	Country Name	Transmission and Distribution Losses as Percentages of the Total Output Power
1.	Germany	4.3 Percent
2.	Australia	5.3 Percent
3.	United States	6 Percent
4.	Malaysia	6.4 Percent
5.	United Kingdom	7.6 Percent
6.	Saudi Arabia	9.4 Percent
7.	Russia Federation	10 Percent
8.	Bangladesh	10.3 Percent
9.	Iran	14.6 Percent
10.	Pakistan	16.9 Percent
11.	India	21.1 Percent
12.	Developing Countries (UN Classification)	16.1 Percent
13.	Average Value of the World	8.1 Percent

Over the past few years, the government has given millions of dollars in order to reduce this circular debt, but it continues to grow with the passage of time[12]. This circular debt has resulted in a number of the negative effects such as underutilization of the generation capacity, a higher cost of the electricity generation due to the low plant capacity factors and a lack of trust for the future foreign investments in the power and energy sector of Pakistan. There is no short cut to reduce this circular debt. The consumer end tariff rationalization that truly reflects the cost of the energy production and measures taken in order to reduce the theft of electricity can help to reduce this debt.

Table No: 2 Transmission and Distribution Losses of Distribution Companies (DISCO's) of Pakistan

S.No.	Name of the Distribution Company	Year 2011-2012		Year 2012-2013
		Target for the Percentage Transmission and distribution losses set by NEPRA	Actual Percentage of Transmission and Distribution Losses incurred in DISCO's	Target for the Percentage Transmission and distribution losses set by NEPRA
1.	Islamabad Electric Supply Company Limited (IESCO)	9.50	9.52	9.50
2.	Lahore Electric Supply Company Limited (LESCO)	12	13.5	12
3.	Gujranwala Electric Power Company Limited (GEPCO)	10.50	11.22	10.50
4.	Faisalabad Electric Supply Company Limited (FESCO)	10.83	10.90	10.83
5.	Multan Electric Power Company Limited (MEPCO)	15	17.91	15
6.	Peshawar Electric Supply Company Limited (PESCO)	28	35.98	28
7.	Hyderabad Electric Supply Company Limited (HESCO)	22	27.73	22
8.	Quetta Electric Supply Company Limited (QESCO)	18	20.56	18

3. Solutions:

Energy is essential to economic and social development and improved quality of life. The current energy situation in Pakistan is due to the reasons explained in the foregoing section. The complexity and serious consequences due to the energy crisis in Pakistan, requires that swift and serious actions are taken that would result in an uninterrupted supply of electricity to our industrial, agricultural and domestic

consumers. The following measures could be taken in an effort to resolve the current crisis.

I. Altering the Generation Mix:

There is a need to change the current and expensive energy mix of Pakistan[13]–[21] and energy production from fossil fuels is also resulting in high greenhouse gas emissions.. This can be achieved by placing a ban on future generation plants that are based on oil. Priority should be given to power plants that are based on a cheaper source of energy such as hydro power plants[22]. In this regard, several measures have already been taken by the government by installing hydro power plants that could help in reducing the gap between demand and supply. A list of the future hydro power plants is given in Table No. 3[22])

Table No. 3. Upcoming Independent Power Producer's Hydro Power Projects

S.No.	Project	Location	Capacity (MW)	Projected Completion Year
1.	Patrind Hydropower Project	Kunhar River,Khyber Pakhtunkha/Azad Jammu and Kashmir	147	2017
2.	Gulpur Hydropower Project	Poonch River, Gulpur, Azad Jammu and Kashmir	100	2018
3.	Sehra Hydropower Project	Poonch River, Azad Jammu and Kashmir	130	2018
4.	Suki kinari Hydropower project	Kunhar River, Mansehra, Khyber Pakhtunkha	870	2020
5.	Karot Hydropower Project	Jehlum River, District Rawalpindi, Punjab	720	2020
6.	Azad Pattan Hydropower Project	Jehlum River,Sudhnoti, Azad Jammu and Kashmir	640	2020
7.	Chakothi-Hattian Hydropower Project	Muzaffarabad, Azad Jammu and Kashmir	500	2020

II. Power Theft and Tariff Rationalization:

In addition to an expensive energy mix, another important reason for the rising cost of electricity has been excessive transmission and distribution losses. Stringent measures to check theft of electricity, with strict regulations and their practical implementation with the help of law enforcement agencies will be necessary in order to reduce these losses.

Another problem is that consumers of effectively functioning DISCOs have to pay for the corruption, theft and inefficiency of poorly functioning DISCOs. Its major cause is the unified tariff system. The real purpose for the establishment of DISCO's was that NEPRA would determine different tariffs for each DISCO that would have been based on its performance. Unfortunately, this aim was never met. The current system of uniform prices with subsidies provided by the government provides no incentives for these DISCOs to improve their performance. It is imperative to introduce a performance based pricing system for each DISCO as determined by NEPRA. The poor performance should be addressed immediately and must be resolved in a given time frame otherwise penalized in the form of a higher tariff.

III. Capacity Building of Public Sector Plants:

The power plants run by the government urgently need investment in order to restore their productivity. Improving the efficiency of these power plants can help to decrease the gap between demand and supply. This investment would not only increase the generation capacity of these power plants, but would also help to improve the plant capacity factor thus reducing the cost of the unit of the electricity that is produced and sold to the consumers. Theft of oil is another issue that needs to be resolved in these publicly operating generating units. A strict control and audit by a neutral party can help to check this pilferage but would also ensure that the oil provided to these entities meets the required standards.

IV. Energy Conservation and Demand Side Management:

Fig. No. 3 shows the energy consumption pattern for the last five years which shows that the major sector for the energy consumption in Pakistan is domestic sector (Pakistan Energy Year Book 2013"© Hydrocarbon Development Institute of

Pakistan"). The gap between the demand and supply of electrical power can also be reduced by improving the consumption of electricity, especially during peak hours with the help of time metering method[25]. Similarly, the energy consumption can also be reduced on the demand side by adopting energy efficient measures such as use of energy efficient devices and appliances in households and industry. An awareness campaign should be started on a national level that creates awareness among the masses to avoid wastage of electricity.

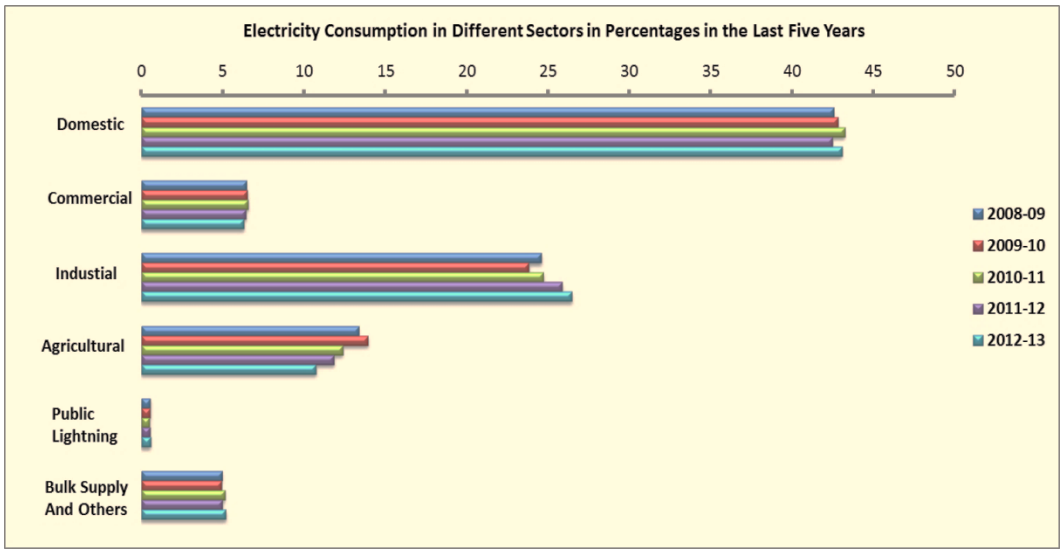

4. Conclusion:

This article highlights the major issues for the power crises of Pakistan. It is the need of the hour that coherent and foresighted national level policies are formulated that have national consent to set up future power generating plants by employing local resources, such as water, coal, nuclear and renewable energy sources to solve the present energy crises of Pakistan. Additionally, by improving the infrastructure and improving the managerial issues of the power distribution hierarchy, the power crises of Pakistan can be reduced by a significant amount.

References:

[1] M. A. Abusara and S. M. Sharkh, "Design and control of a grid-connected interleaved inverter," *IEEE Trans. Power Electron.*, vol. 28, pp. 748–764, 2013.

[2] I. Ozturk, "A literature survey on energy–growth nexus," *Energy Policy*, vol. 38, no. 1, pp. 340–349, Jan. 2010.

[3] N. Bowden and J. E. Payne, "Sectoral Analysis of the Causal Relationship Between Renewable and Non-Renewable Energy Consumption and Real Output in the US," *Energy Sources, Part B Econ. Planning, Policy*, vol. 5, no. 4, pp. 400–408, Sep. 2010.

[4] A. Aqeel, "The Relationship Between Energy Consumption," vol. 8, no. 2, pp. 101–110, 2001.

[5] J. Asafu-adjaye, "The relationship between energy consumption , energy prices and economic growth : time series evidence from Asian developing countries ☙," pp. 615–625, 2000.

[6] "World Development Indicators | Data." [Online]. Available: http://data.worldbank.org/data-catalog/world-development-indicators. [Accessed: 17-Jul-2014].

[7] S. Muhammad and M. Shahbaz, "Mp r a," no. 35588, 2011.

[8] J. M. Fraser, "Lessons from the Independent Private Power Experience in Pakistan," 2005.

[9] "World Development Indicators | The World Bank." [Online]. Available: http://wdi.worldbank.org/table/5.11. [Accessed: 17-Jul-2014].

[10] S. A. Qureshi and F. Mahmood, "Evaluation by Implementation of Distribution System Planning for Energy Loss Reduction," vol. 4, pp. 43–55, 2009.

[11] "www.nepra.govt.pk." [Online]. Available: http://www.nepra.org.pk/. [Accessed: 17-Jul-2014].

[12] M. Analysis, "Mp r a," no. 55929, 2014.

[13] W. Ajaz, "C omparing Economic Feasibility of Domestic Solar Water Heater Installation in Major Cities of Pakistan," vol. 1, no. 1, pp. 35–42, 2014.

[14] M. K. Farooq, S. Kumar, and R. M. Shrestha, "Energy, environmental and economic effects of Renewable Portfolio Standards (RPS) in a Developing Country," *Energy Policy*, vol. 62, pp. 989–1001, Nov. 2013.

[15] M. Amer and T. U. Daim, "Selection of renewable energy technologies for a developing county: A case of Pakistan," *Energy Sustain. Dev.*, vol. 15, no. 4, pp. 420–435, Dec. 2011.

[16] A. B. Awan and Z. A. Khan, "Recent progress in renewable energy – Remedy of energy crisis in Pakistan," *Renew. Sustain. Energy Rev.*, vol. 33, pp. 236–253, May 2014.

[17] M. H. Sahir and A. H. Qureshi, "Assessment of new and renewable energy resources potential and identification of barriers to their significant utilization in Pakistan," *Renew. Sustain. Energy Rev.*, vol. 12, no. 1, pp. 290–298, Jan. 2008.

[18] U. K. Mirza, N. Ahmad, K. Harijan, and T. Majeed, "Identifying and addressing barriers to renewable energy development in Pakistan," *Renew. Sustain. Energy Rev.*, vol. 13, no. 4, pp. 927–931, May 2009.

[19] S. S. Amjid, M. Q. Bilal, M. S. Nazir, and A. Hussain, "Biogas, renewable energy resource for Pakistan," *Renew. Sustain. Energy Rev.*, vol. 15, no. 6, pp. 2833–2837, Aug. 2011.

[20] A. Demirbas, "Global Renewable Energy Projections," *Energy Sources, Part B Econ. Planning, Policy*, vol. 4, no. 2, pp. 212–224, Oct. 2009.

[21] H. Aras, O. Balli, and A. Hepbasli, "Global Solar Radiation Potential, Part 1: Model Development," *Energy Sources, Part B Econ. Planning, Policy*, vol. 1, no. 3, pp. 303–315, Sep. 2006.

[22] I. Yüksel, "Dams and Hydropower for Sustainable Development," *Energy Sources, Part B Econ. Planning, Policy*, vol. 4, no. 1, pp. 100–110, Jan. 2009.

[23] "Private Power & Infrastructure Board." [Online]. Available: http://www.ppib.gov.pk/N_upcoming_hydel.htm. [Accessed: 17-Jul-2014].

[24] "© Hydrocarbon Development Institute of Pakistan."

[25] I. Global, P. Republic, and W. Oil, "How Pakistan Is Coping with the Challenge of High Oil Prices," no. Winter, pp. 551–574, 2007.

Submitted in "2015 International Conference on Alternative Energy in Developing Countries and Emerging Economies (2015 AEDCEE)", May 28-29, 2015, Bangkok, Thailand

Annexure II

Two Level Voltage Source Grid Connected Inverter for Solar Photovoltaic System

[a)] Gussan Maaz Mufti[1] [b)] Dr. Mohsin Jamil [2] [a)] Dr. Adeel Waqas [1]

[1] Center for Energy Systems Engineering (CES) NUST, Address; NUST H-12 Islamabad, Pakistan

[2] School of Mechanical and Manufacturing Engineering (SMME) NUST, Address; NUST H-12 Islamabad, Pakistan

Abstract: In the recent years, the demand for the grid connected inverters has increased immensely as they act as an interface between the photo voltaic systems and the utility. The focus of this research article is to model and analyze the design characteristics of a two level, pulse width modulated, grid connected inverter using Matlab. The Proportional Integral and Proportional Resonant controller are being investigated and the performance of these controllers under different parameter variations and grid impedance changes are being discussed. These simulations result show that the proper tuning of the controllers result in a satisfactory controller performance parameters.

Keywords:Grid Connected Inverter, Current Control, Renewable Energy Systems, LCL filter, Photo Voltic Systems.

Introduction:

In the modern world, the industrial development plays an important role in the development of every country. The industrial development in turn depends on a reliable electricity supply. The increasing worldwide demand for energy increased the concerns of the different countries regarding their energy security. Due to this, the focus is now shifting on the diversification, generation and efficient allocation of the energy sources. Solar Photo Voltaic (PV) has been a major portion in the energy mix of European nations for over a decade. Italy, Greece and Germany meets more than 5 percent of the annual electricity generated by solar PV but most of the European countries have reached their peaks for the production of the solar PV. Asian countries on the other hand have started investing in solar PV. A total of 36.9 GW of solar capacity of the whole world was added in 2013 in which china's share

was 31 percent[1].

The current quality fed to the utility from the Photo Voltaic Systems (PVS) mainly depends upon the Current Controller employed in the Grid Connected Iinverters (GCIs). Therefore; it is essential that output current is free from any harmonics and distortions from the Current Controller. The two commonly used CCs that are used in PVS are Proportional Integral (PI) controller and Proportional Resonant (PR) controller. A comparison between the PI controllers and PR controllers has been done comprehensively in [2]**.** The aim of using all these control techniques and structures is to ensure better disturbance rejection and to raise outer loop gain. But drawback of using these controllers is that they offer low loop gain at the fundamental frequency and its harmonics. Furthermore, their disturbance rejection capability is also poor due to which THD of output current is also poor and contradicts with standards and limits. So there is a need of a suitable controller which is able to provide high gain at fundamental and other frequencies of choice. To gain high loop gain and better harmonic rejection at fundamental and other harmonics

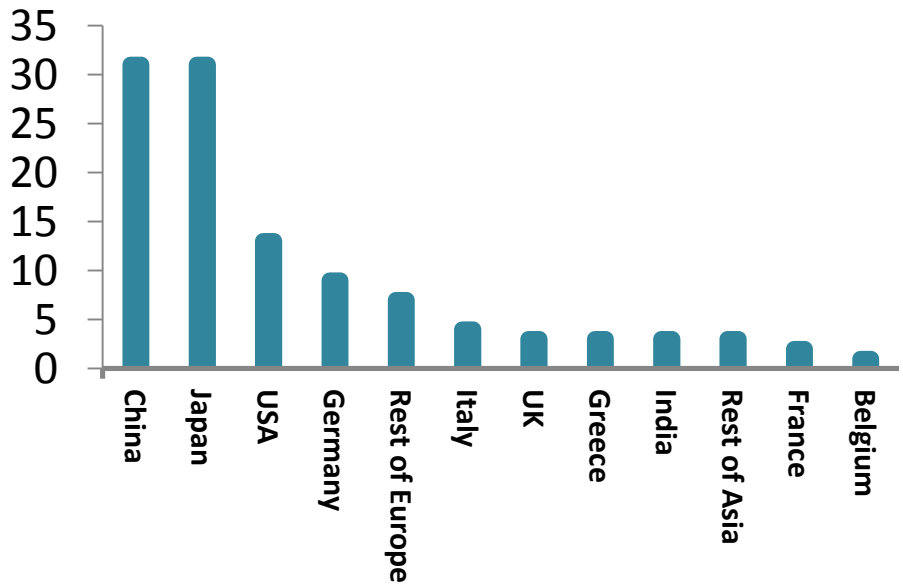

Fig. 1 PV Shares of the World

The main objective of this article is to design a grid connected PVS and investigates the performance of PI Current Controller and PR Current Controller by simulating the linearized single phase system in *Matlab*. The performance of both Current Controllers is analyzed and compared using the axioms of control theory.

The system values that are used for the Matlab simulation are given in the following table

Sr. No.	Electrical Parameter	Symbol	Value
1	Peak Voltage of the Grid	V_{peak}	230 *V (rms)*
2	DC link voltage	V_{dc}	800*Vdc*
3	Grid inductor	L_g	350μH
4	Utility inductor	L_u	50μH
5	Capacitor	C_s	22.5μF
6	Switching frequency	f_s	10*kHz*
7	Grid Frequency	f_g	50*Hz*
8	Output Current	I_{out}	50*A*

The control system forms an integral part of the PVS[3]-[6]. The control of the renewable energy system has two main parts. The grid side control and the input power control. The grid side control mainly handles the power flow and its control from the grid side. It may include control of active and reactive power, synchronizing the grid and quality of the power. The input power control ensures that maximum power is extracted from the renewable energy systems, keeping in view the safety and reliability of the whole system.

The control scheme that is applied to control the converter of the grid side in the renewable energy systems has two interlinked control loop. The inner current loop has a faster response and it controls the grid current. It is the main loop for the quality of power that is fed to the utility. It also ensures the protection of the equipment by controlling the current. The external voltage loop is responsible for controlling the voltage across the capacitor that serves as the D.C. link. Inherently system will be unstable if the output grid current of an LCL filter is directly feed backed, so to stabilize the system, there must be an additional feedback loop. Additional feedback can be provided either by the main inductor current or by capacitor current[7].

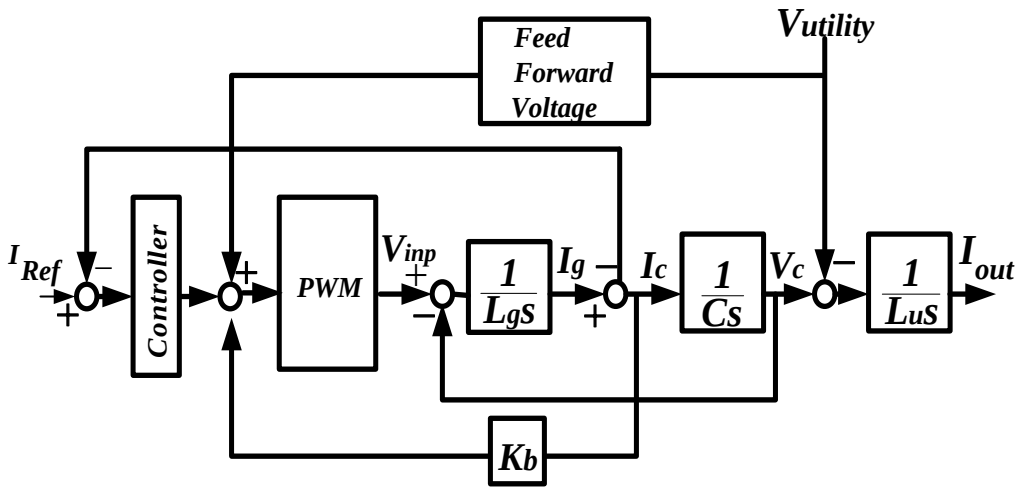

Fig. 2 Control Structure of the Grid Connected Inverter

If gain for PWM block is assumed to be unity then the relationship between output current and reference input current is given by the following transfer function;

$$I_{out} = \frac{Gz(s)}{1+Gz(s)} I_{ref} - \frac{G_{plant}(s)}{1+Gz(s)} \text{Vutility} \quad (1)$$

$$Gz(s) = G_{plant}(s) * G_{controller}(s) \quad (2)$$

$$G_{plant}(s) = \frac{1}{(LgL_uCs)s^3 + (K_bL_uCs)s^2 + (L_g + L_u)s} \quad (3)$$

To make the system more realizable and closer to real time scenarios a disturbance function can be introduced which is given by the following equation as

$$\text{Disturbance}(s) = V_{utility}(L_gCs^2 + K_CCs + 0.5) \quad (4)$$

Filter design

The main aim of the filter in GCI connected on the utility side is to protect the components of the inverter due to the disturbances coming from the utility. It also prevents unwanted harmonics and distortions from entering the utility.

There are different filters that can be used in GCI. The most common configurations are L type filter, LC type filter, LCL type filter and LCCL type filter [8]–[13]The selection criteria depends upon the topology configuration, the purpose of the inverter and the system performance requirements. Each type of filter has its own advantages and disadvantages associated with it for example, L type filters are bulky due to heavier inductor used in them and they are costly too.LC is another type of filter which is also commonly used. It is more compact in size as compared to the L filter. However, the impedance mismatching of LC filter causes degradation in its performance resulting in its inability to remove the harmonics along with the stability

issues.

The LCL filter addresses the issues due to the LC filter and provides flexibility along with better results in robust conditions. It is therefore critically important to design and select the proper type of filter. The resonant frequency of the LCL filter is given by the following equation

$$w_{resonant} = \sqrt{\frac{L_g + L_u}{L_g L_u C}} \quad (5)$$

where

L_g = Inductor connected on the PV side

L_u =Inductor connected on the utility side

C = the capacitor of the filter

To reduce the resonance damping can be accomplished by either active means or passive means. Mostly, a resistor is connected in series with the capacitor that accomplishes the damping and also increases the stability of the system**.**

An active damping system is used for the control system as shown in Fig. 3**.** The current of the capacitor along with the loop gain (inner) K_b provides the necessary damping and stability to the system.

Proportional integral controllers are used with the *dq* control as they have shown good performance in these systems. The transfer function of the proportional integral controllers for a three phase system is given by

$$G_{PI}(s) = \begin{pmatrix} K_p + \frac{K_i}{s} & 0 \\ 0 & K_p + \frac{K_i}{s} \end{pmatrix} \quad (6)$$

Where

K_p = Proportional Gain of the PI Controller

K_i =Integral Gain of the PI Controller

The implementation of Proportional Resonant controller becomes easier because it is in stationary frame and it could be implemented by three controllers. Only two controllers are required if the three phase circuit has an isolated neutral. The complexity of the controller is much less as compared to PI controllers. The transfer function of the Proportional Resonant controller for the three phase system is given

$$G_{PR}(s) = \begin{pmatrix} K_p + \frac{K_i s}{s^2 + w^2} & 0 & 0 \\ 0 & K_p + \frac{K_i s}{s^2 + w^2} & 0 \\ 0 & 0 & K_p + \frac{K_i s}{s^2 + w^2} \end{pmatrix} \quad (7)$$

Where

K_p = Proportional Gain of the PI Controller

K_i =Integral Gain of the PI Controller

w = Resonant frequency

The ideal resonant controller has no phase shift and gives an infinite gain at the resonant frequency as shown in the bode plot of ideal proportional resonant controller in Fig. 4. This gain helps to nullify the steady state error. The proportional gain determines the phase margin, gain margin and dynamics of the systems.The infinite gain of the ideal Proportional Resonant (PR) controller gives rise to the stability problems. Also, it leads to an ideal quality of the GCI which is non-realizable in real time situations. For this purpose a modified PR controller is used whose gain is a finite value thus mitigating the stability problems.

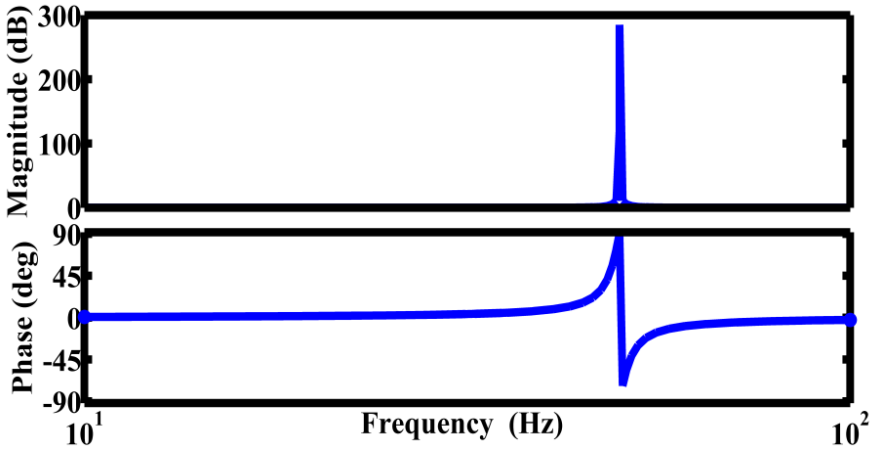

Fig. 3 Bode diagram of the Ideal Proportional Resonant Controller with K_p =1 K_i =10 w =314 rad sec^{-1}

The modified PR controller can also be adjusted to make it less susceptible to the frequency changes in the utility. The transfer function of the modified PR controller

is given by

$$G_{PR(modified)}(s) = K_p + \frac{K_i s}{s^2 + 2\zeta ws + w^2} \qquad (8)$$

The inclusion of damping term has two benefits. It decreases the infinite gain at the fundamental frequency to a realizable finite value and also improves the bandwidth of the modified PR controller. The bode plot for the modified PR controller is shown in Fig. 5.

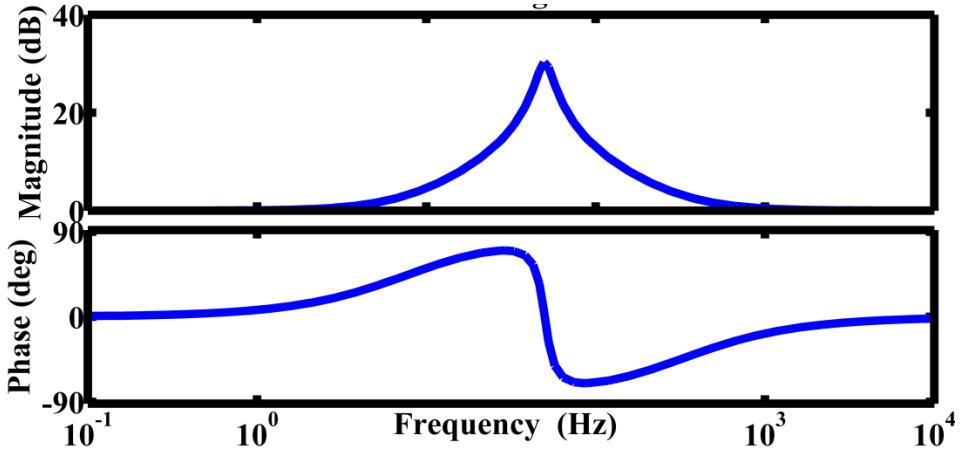

Fig. 5 Bode diagram of the Modified Proportional Resonant Controller K_i =10 ζ =0.01 ws =10 rad sec^{-1} w =314 rad sec^{-1}

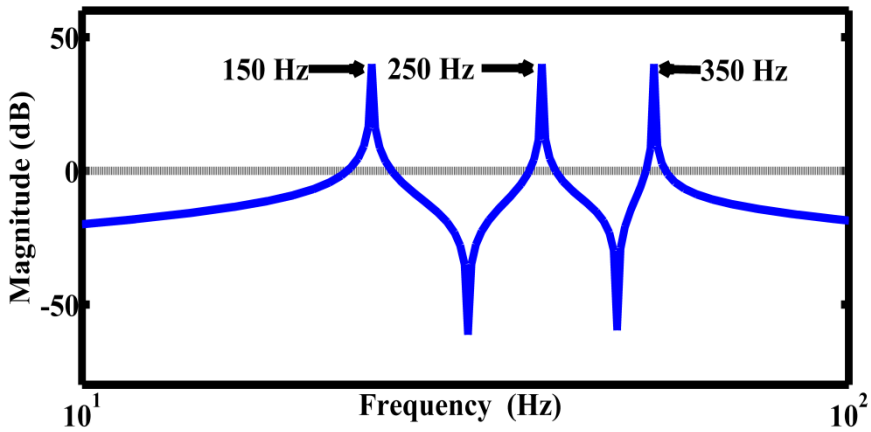

Fig. 4 Proportional Resonant Controller Gains at Harmonic Frequencies K_i =10 ζ =0.01 ws =10 rad sec^{-1} w =314 rad sec^{-1}

Simulations were carried using Matlab/Simulink. The LCL filter was designed using the procedures of [14][7] such that the maximum ripple current and the reactive power produced are within the acceptable limits.

The PI controller was designed using Matlab/Simulink. Fig. 7 shows the Fast Fourier Transform (FFT) analysis of the PI controller when the THD of 2.74% was introduced in the utility voltage. The THD values in the output were found to be

8.05%. Though it was able to reduce the THD values, but it failed the ANSI-IEEE recommended THD values which is 5 %. The odd harmonic at 250 Hz was the highest harmonic that the PI controller failed to suppress. The THD value of the PI controller is 8.05 %.

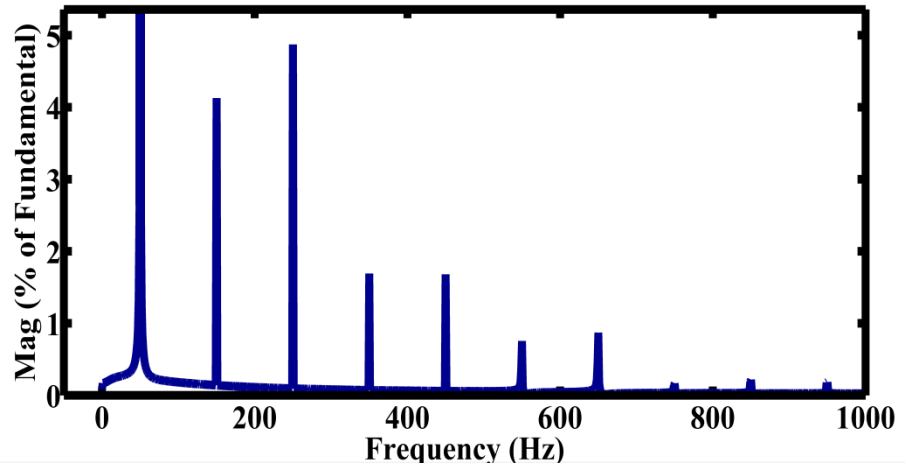

Fig. 6 Fast Fourier Transform Analysis from PI Controller

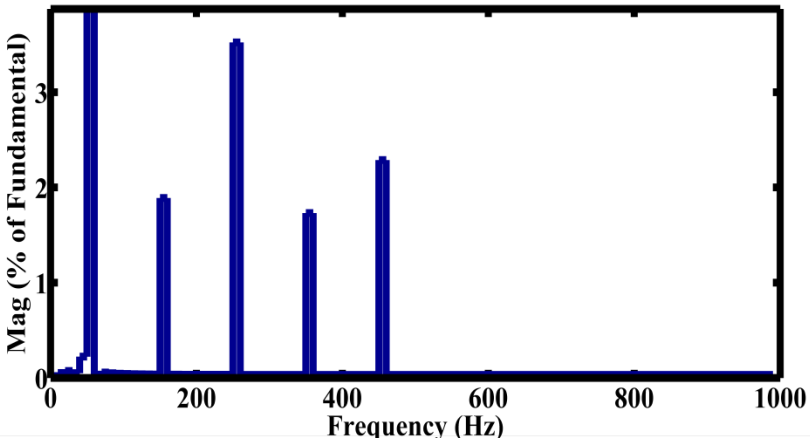

Fig.7 Fast Fourier Transform Analysis from Proportional Resonant Controller

The 3rd, 5th and 7th harmonics of a PR controller is less than the PI controller. The THD value of PR was 4.96%. The 3rd harmonic was 1.7 %, whereas 5th and 7th harmonic values were 3.5 % and 1.6 % respectively. These simulation results were encouraging and additional harmonic compensation could be used to produce better results.

Conclusions

This paper presents a comparison between PI controller and PR current controllers for Utility connected PV systems. These results show that the PR controller is able to meet the IEEE standards as compared to PI controller under harmonics. However,

additional harmonic compensation can be used to produce more promising results with the PR controller. In the future, further investigation of both controllers on Real Time Digital Simulator (RTDS) would be done to verify the results obtained from Matlab

Acknowledgements

The author would like to thank the reviewers for their valued comments and suggestions.

References

[1] M. Brower, D. Green, R. Hinrichs-rahlwes, S. Sawyer, M. Sander, R. Taylor, I.Giner-reichl, S. Teske, H. Lehmann, M. Alers, and D. Hales, 2014. 2014.

[2] R. Teodorescu and F. Blaabjerg, "A New Control Structure for Grid-Connected LCL PV Inverters with Zero Steady-State Error and Selective Harmonic Compensation," vol. 00, no. C, pp. 580–586, 2004.

[3] M. Trifkovic, M. Sheikhzadeh, K. Nigim, and P. Daoutidis, "Modeling and Control of a Renewable Hybrid Energy System With Hydrogen Storage," IEEE Trans. Control Syst. Technol., vol. 22, no. 1, pp. 169–179, Jan. 2014.

[4] A. Chauhan and R. P. Saini, "A review on Integrated Renewable Energy System based power generation for stand-alone applications: Configurations, storage options, sizing methodologies and control," Renew. Sustain. Energy Rev., vol. 38, pp. 99–120, Oct. 2014.

[5] Y. Hong, R. Waters, C. Boström, M. Eriksson, J. Engström, and M. Leijon, "Review on electrical control strategies for wave energy converting systems," Renew. Sustain. Energy Rev., vol. 31, pp. 329–342, Mar. 2014.

[6] M. A. Abusara, M. Jamil, and S. M. Sharkh, "Repetitive current control of an interleaved grid-connected inverter," 2012 3rd IEEE Int. Symp. Power Electron. Distrib. Gener. Syst., pp. 558–563, Jun. 2012.

[7] D. N. Zmood, S. Member, and D. G. Holmes, "Stationary Frame Current Regulation of PWM Inverters With Zero Steady-State Error," vol. 18, no. 3, pp. 814–822, 2003.

[8] M. Jamil, B. Hussain, R. J. Boltryk, and S. M. Sharkh, "Microgrid Power Electronic Converters : State of the Art and Future Challenges," 2009.

[9] M. Liserre and P. Bari, "Design and Control of an LCL-filter based Three-phase Active Rectifier," vol. 00, no. C, pp. 299–307, 2001.

[10] S. G. P. Inverter, H. Cha, and T. Vu, "Comparative Analysis of Low-pass Output Filter for," pp. 1659–1665, 2010.

[11] T. Liu, X. Hao, X. Yang, M. Zhao, and L. Xiong, "A novel grid voltage feed forward control strategy for three-phase grid-connected VSI with LCCL filter," 2012 IEEE Int. Symp. Ind. Electron., pp. 86–91, May 2012.

[12] J. Lettl, J. Bauer, and L. Linhart, "Comparison of Different Filter Types for Grid Connected Inverter," pp. 1426–1429, 2011.

[13] T. C. Y. Wang, "Output filter design for a grid-interconnected three-phase inverter," IEEE 34th Annu. Conf. Power Electron. Spec. 2003. PESC '03., vol. 2, pp. 779–784.

[14] "Wiley: Grid Converters for Photovoltaic and Wind Power Systems -Remus Teodorescu, Marco Liserre, Pedro Rodríguez."